The Influence of the Tensile Material Properties of Single Annulus Fibrosus Lamellae and the Interlamellar Matrix Strength on Disc Herniation and Progression

by

Diane Elizabeth Gregory

A thesis
presented to the University of Waterloo
in fulfillment of the
thesis requirement for the degree of
Doctor of Philosophy
in
Kinesiology

Waterloo, Ontario, Canada, 2009

© Diane Elizabeth Gregory 2009

I hereby declare that I am the sole author of this thesis. This is a true copy of the thesis including any required final revisions, as accepted by my examiners.

I understand that my thesis may be made electronically available to the public.

Diane Elizabeth Gregory

Abstract

Low back pain is highly prevalent in the developed world, with 80% of the population being affected at some point in their lives. Herniation, a common injury to the intervertebral disc, is characterized as the posterior migration of the nucleus pulposus through the layers of the annulus fibrosus. Various risk factors have been associated with the development of disc herniation, but the mechanisms are largely not understood. For example, exposure to vibration has been linked to the occurrence of herniation, yet our understanding of this association is not clear. It is hypothesized that vibration cyclically loads the tissues of the intervertebral disc until failure occurs as a result of fatigue. Tissues at risk of fatigue failure may include the intra-lamellar matrix, the connective tissue found between collagen fibres within a single lamella, and the inter-lamellar matrix, the connective tissue found between adjacent lamellae. In order to determine the mechanistic link between vibration and herniation, a firm understanding of the properties of the intervertebral disc as well as the intra and inter-lamellar matrices are of utmost importance. Further, it is important to determine these properties under physiological loading scenarios. This thesis consists of five studies, which have each provided a unique piece to the intervertebral disc herniation puzzle in order to better understand this mechanistic link. First, it was discovered that annular tissue is subject to significantly higher stresses and is stiffer under biaxial strain as compared to uniaxial strain. Biaxial strain is more representative of the *in vivo* loading scenario and provides more accurate information regarding scenarios that the annulus can tolerate and those that can result in injury. It was also revealed that, when strained at physiological strain rates (up to 4%/sec), these mechanical properties do not change such that they are independent of

strain rate. Therefore, when strained at varying rates akin to voluntary movement, the annulus is not subject to higher stresses or altered stiffness. Second, the effect of vibration, an acknowledged risk factor for herniation, was examined on the mechanical properties of the intra and inter-lamellar matrices. It was discovered that vibration altered these matrices such that they were more extensible and strained to greater magnitudes, yet did not reach higher stresses before failing. It was hypothesized that this increased extensibility was due to damage to elastin, as elastin assists in minimizing tissue deformation and helps tissues recover from tensile strain. The final study assessed the effect of exposure to vibration on the development of disc herniation. The initiation of herniation was observed in a significantly greater number of intervertebral discs exposed to vibration as compared to a control condition. Although epidemiological studies had documented a correlation between exposure to vibration and herniation, this was the first study to conclude that exposure to vibration is in fact a mechanical risk factor for the development of herniation and increases the incidence of herniation. Further, based on the findings of the mechanical properties of the intra and inter-lamellar matrices, and in particular the observed 15-20 times greater failure strength of the intra as compared to inter-lamellar matrix, it would appear that the inter-lamellar matrix, and thus delamination, may be the weakest link in the herniation pathway.

This thesis has uncovered new information regarding physiological mechanical properties of the annulus. Further, new information regarding the intra and inter-lamellar matrices was obtained, improving our understanding of the healthy disc. Last, by subjecting the disc to a known risk factor for herniation, hypotheses were generated

regarding the initiation and progression of disc herniation, specifically related to the roles of the intra and inter-lamellar matrices.

Acknowledgements

First and foremost, I wish to thank my supervisor, Dr Jack Callaghan, who has supported me during my years at Waterloo. You always allowed me to explore my interests even as they migrated towards ramblings of various proteins! You provided me with countless opportunities, and have helped prepare me for my career.

I wish to also thank my committee members, Dr Stuart McGill, Dr Clark Dickerson, and Dr Wayne Brodland, for their interest and even excitement in my thesis. Your questions and suggestions made this thesis stronger, which I appreciate very much. Also, I would like to thank Dr Ron Zernicke for serving as my external committee examiner and taking the time to help me improve my work.

Thank you very much to Caleb Horst and Jim Veldhuis for assistance with the BioTester 5000 and listening to my thoughts about the system and my thesis.

I have spent the last six years at Waterloo, and during my Masters and PhD, I have met the most wonderful people. You've all made it so much fun to be here (especially outside the lab) and it's you that makes leaving as hard as it is. Jennie, you especially made Waterloo feel like home. For the rest of my life I wish I could have you as my spokesperson! I'm hard pressed to think anyone believes in me as much as you.

Thank you so much to my sisters, Sharon and Sam. Having you guys as roommates through all of this was pretty cool and you were both so good at helping me through the stressful days. You two really are the most wonderful ladies in the world! And Mom and Dad, thank you for everything, especially the panicked phone calls home – I know they increased near the end of this thesis! I love you all very much.

Last, and most importantly, I would like to thank Steve Brown. I can't believe how endless your support and excitement in my research has been, including reading everything I've ever written, listening to every presentation I've ever given, and asking about every test I've ever conducted in the lab. But thank you even more for all the support and love you've given me in every other aspect of my life, and thank you for being my best friend.

Table of Contents

List of Tables xi

List of Figures xii

Chapter 1 – Thesis Introduction 1

1.1 General Introduction 2
1.2 Specific Purpose of Thesis 7
1.3 General Hypotheses 9

Chapter 2 – Review of Literature 10

2.1 Review of Anatomy 11
2.1.1 General Anatomy 11
2.1.2 Intervertebral Disc 14
2.1.2.1 Nucleus Pulposus 14
2.1.2.2 Annulus Fibrosus 15
2.1.2.3 Lamellar Anatomy 17
2.1.2.4 Interlamellar Cells 19
2.2 Material Properties of the IVD 22
2.2.1 Lamellae Mechanics 22
2.2.1.1 Traditionally Examined Material Properties of the Annulus Fibrosus 22
2.2.1.2 Tensile Loading 23
2.2.1.3 Biaxial Tensile Testing 27
2.2.1.4 Interlamellar Shear Strength 27
2.3 Intervertebral Disc Herniation 30
2.3.1 Stages of Herniation 30
2.3.2 Risks Factors 34
2.3.2.1 Whole Body Vibration 34
2.4 Summary 36

Chapter 3 – A comparison of uniaxial and biaxial mechanical properties of the annulus fibrosus: A porcine model 37

Chapter synopsis 38
3.1 Introduction 40
3.2 Methods 41
3.2.1 Tissue Preparation 41
3.2.2 Tissue Testing Protocol 43
3.2.3 Data Analysis 48
3.2.4 Statistical Analysis 51
3.3 Results 52

3.3.1 Tissue Characteristics **52**
3.3.2 Tensile Tests **52**
3.4 Discussion **56**
3.5 Conclusion **60**

Chapter 4 – An examination of the effect of strain rate on the tensile mechanical properties of the annulus fibrosus **61**

Chapter synopsis **62**
4.1 Introduction **63**
4.2 Methods **65**
4.2.1 Tissue Dissection and Preparation **65**
4.2.2 Tissue Mounting and Testing **66**
4.2.3 Data Analysis **71**
4.2.4 Statistical Analysis **71**
4.3 Results **72**
4.4 Discussion **78**
4.5 Conclusion **84**

Chapter 5 – Mechanical properties of the annulus fibrosus and the consequence of vibration: An examination of the intralamellar matrix **85**

Chapter synopsis **86**
5.1 Introduction **87**
5.2 Methodology **89**
5.2.1 Pre-loading and Compressive-loading Protocol **89**
5.2.2 Single Layer Specimen Dissection and Preparation **91**
5.2.3 Data Analysis **96**
5.2.3.1 Toe Region **98**
5.2.3.2 Linear Region **98**
5.2.3.3 Initial Failure **98**
5.2.3.4 Tensile Strength and Failure Strain **99**
5.2.3.5 Material Toughness **99**
5.2.4 Statistical Analysis **99**
5.3 Results **100**
5.3.1 Effect of Vibration **100**
5.3.2 Effect of tissue site extraction **100**
5.4 Discussion **103**
5.5 Conclusion **107**
Chapter 6 – Examining the mechanical properties of the inter-lamellar matrix and the effect of vibration exposure **109**

Chapter synopsis **110**
6.1 Introduction **111**
6.2 Methods **113**

6.2.1 Specimen Preparation **113**
6.2.2 Mechanical Testing **113**
6.2.3 Annular Dissection and Preparation **114**
6.2.4 Mechanical Testing of Tissue Samples **114**
6.2.5 Data Analysis **115**
6.2.6 Statistical Analysis **115**
6.3 Results **118**
6.3.1 The Effect of Vibration **118**
6.3.2 The Effect of Tissue Location Extraction **118**
6.4 Discussion **120**
6.5 Conclusion **123**

Chapter 7 – Does vibration influence the initiation of intervertebral disc herniation? An in-vitro analysis to determine a causal relationship **124**

Chapter synopsis **125**
7.1 Introduction **126**
7.2 Methods **127**
7.2.1 Specimen Preparation **127**
7.2.2 Experiment 1 - Spinal Unit Mechanical Testing: Data Collection **128**
7.2.3 Experiment 1 - Spinal Unit Mechanical Testing: Data Analysis **130**
7.2.4 Experiment 2 - Post-collection Specimen Dissection **131**
7.2.5 Experiment 2 - Annular Tissue Mechanical Testing: Data Collection **132**
7.2.6 Study 2 - Annular Tissue Mechanical Testing: Data Analysis **132**
7.2.6.1 Toe Region **132**
7.2.6.2 Linear Region **133**
7.2.6.3 Initial Failure and Ultimate Strength **133**
7.2.6.4 Material Toughness **133**
7.2.7 Statistical Analysis **134**
7.3 Results **136**
7.3.1 Number of Herniated Discs and Extent of Herniation **136**
7.3.2 Study 1 - Spinal Unit Mechanical Testing **136**
7.3.3 Study 2 - Annular Tissue Mechanical Testing **138**
7.3.4 X-ray Images **138**
7.4 Discussion **142**
7.5 Conclusion **145**

Chapter 8 – Thesis Summary **146**

8.1 Thesis Summary **147**
8.2 Revisiting the Hypotheses **149**
8.3 Herniation Initiation and Progression as a Result of Vibration **150**
8.4 Limitations **156**

8.5 Future Directions **156**

Appendix **158**

References **162**

List of Tables

Table 3.1	Mean and standard deviation values for the elastic modulus and maximal stress reached at 20% true strain for all tissues, as well as for each tissue location.	**55**
Table 3.2	Mean and standard deviation values for the elastic modulus and maximal stress reached at 20% uniaxial strain, 20% constrained uniaxial strain, and 20% biaxial strain.	**55**
Table 5.1	Average (standard deviation) values for each of the variables examined collapsed across tissue harvest location for control tissues (n = 16) and vibrated tissues (n = 16). All variables, with the exception of the strain at the end of the toe region (identified with asterisk, p = 0.027) were not significantly different between the control and vibrated tissues (p>0.05).	**101**
Table 5.2	Average (standard deviation) values for each of the variables examined collapsed across exposure (control versus vibrated) for each tissue harvest location (n=8 for each location). No significant main effect was observed for any variable (p>0.05).	**101**
Table 6.1	Mean (standard deviation) for each mechanical property as an effect of vibration. Each condition (control/vibration) had a sample size of 12. Italicized p value indicates significance. Units are as follows: τ_T and τ_F: kPa, s_T and s_F; mm, g: N/m^3.	**119**
Table 6.2	Mean (standard deviation) for each mechanical property as an effect of location. Each location (anterior/posterior) had a sample size of 12. Units are as follows: τ_T and τ_F: kPa, s_T and s_F; mm, g: N/m^3.	**119**
Table 7.1	Mean (standard deviation) values for tissue samples obtained from the control and vibrated discs.	**140**
Table 7.2	Mean (standard deviation) values for tissue samples obtained from the non-herniated and herniated discs.	**141**

List of Figures

Figure 1.1	Pictorial representation of the annulus. The red sections represent connective tissue between adjacent lamellae, namely the inter-lamellar matrix, and the green sections represent connective tissue between adjacent collagen bundles within each lamellae, namely the intra-lamellar matrix. Relative size of each component is not to scale.	**4**
Figure 1.2	Flowchart of the contribution of each study to the understanding of disc herniation. Double tailed arrow between exposure to vibration and herniation represents a correlation rather than a causal relationship.	**8**
Figure 2.1	Sagittal view of the lumbar spine. Note the ligament attachment sites on the posterior boney elements. ISL – interspinous ligament, SSL – supraspinous ligament, LF – ligamentum flavum, PPL – posterior longitudinal ligament, ALL – anterior longitudinal ligament. Image from Adams et al., 2006, *The biomechanics of back pain*, pg 21.	**12**
Figure 2.2	Sagittal view of the intervertebral disc including the nucleus pulpous (NP), annulus fibrosus (AF), and endplates. Image from Adams et al., 2006, *The biomechanics of back pain*.	**13**
Figure 2.3	Annulus fibrosus fibre orientation in the intervertebral disc. Note the alternating fibre direction in adjacent lamellae. Image from Adams et al., 2006, *The biomechanics of back pain*, pg 15	**18**
Figure 2.4	Annulus fibrosus from ox tail following tensile strain. Note the formation of a cleft (W) in the superior lamella, which reveals the underlying lamella and intricate arrangement of collagen fibres. Image from Pezowicz et al., 2005.	**21**
Figure 2.5	Schematic representation of each of the examined directions of tension in the literature. A) Shows location of extracted annulus tissue B) extracted annulus tissue and arrows indicating direction of previously researched tension.	**24**
Figure 2.6	Magnified view of porcine outer anterior annulus fibrosus lamellae. Areas noted with arrows are potential weak locations in individual lamellae due to the visible collagen bundle segregations.	**32**

Figure 2.7 Dissection of the annulus fibrosus tissue following the initiation of disc herniation. The more outer lamellae do not show nuclear material (a and b), but the more inner lamellae (c and d) show that the nucleus pulposus has begun to penetrate the annulus fibrosus through formed clefts in the lamellae. Figure reproduced from Tampier et al., 2007. **33**

Figure 3.1 a) Depiction of dissection procedures to obtain annulus fibrosus tissue samples with only two adjacent lamellae. b) Direction of axial and circumferential tension. Axial tension is in the direction of spinal compression, while circumferential tension is perpendicular to the compressive axis. **45**

Figure 3.2 BioTester 5000 biaxial material testing apparatus. **46**

Figure 3.3 a) Biaxial tensile testing apparatus. Four rakes secure the tissue during biaxial tension, and two rakes are used for uniaxial tension. b) Biaxial configuration with four rakes inserted into the tissue, and c) Uniaxial configuration with two rakes inserted into the tissue. **47**

Figure 3.4 Graphical user interface for LabJoy 5.80. Graphs on right hand side display real-time force-time, displacement-time and force-displacement graphs. **49**

Figure 3.5 Cross-sectional area of each tissue sample was calculated in order to determine the stress in the circumferential direction. This was calculated by multiplying the tissue thickness (as measured with displacement measurement sensor) by the tissue width (as measured via calibrated image digitization). **50**

Figure 3.6 Representative stress-strain curve in the circumferential direction. Tissues were strained to 20% true strain, or 23% engineering strain. The elastic modulus (E) was determined by taking the slope of the linear portion of the stress-strain curve. This linear portion, on average, started at 82.5% of the final strain magnitude (γf). **54**

Figure 4.1 a) Biaxial testing apparatus set-up. Four rakes that are in series with actuators secure the tissue in place, which apply the strain. b) Image of a two-layered sample of the annulus fibrosus mounted in the testing apparatus. Strain was applied in the axial and circumferential directions. **68**

Figure 4.2 Data collection time line. Strain rates “A”, “B”, and “C” represent the three strain rates examined. The particular strain rate which was represented by each of the letters “A”, “B”, and “C” was randomized across the 20 tissues tested. The first 20% strain test within each block was excluded from analysis to yield three repeats at each of the three strain rates examined. **70**

Figure 4.3 Mean maximal stress collapsed across all tissue samples for slow (20% strain/20 sec), medium (20% strain/10 sec) and fast (20% strain/5 sec) strain rates in the axial and circumferential directions. Error bars denote 1 standard deviation. **75**

Figure 4.4 Mean elastic moduli collapsed across all tissue samples for slow (20% strain/20 sec), medium (20% strain/10 sec) and fast (20% strain/5 sec) strain rates in the axial and circumferential directions. Error bars denote 1 standard deviation. **76**

Figure 4.5 Stress-strain profiles of a two-layered annular tissue sample obtained from the superficial layers of the posterior annulus during each of the three rates of strain: slow (20% strain/20 sec), medium (20% strain/10 sec) and fast (20% strain/5 sec). **77**

Figure 5.1 A) Schematic representation of tissue harvest. Single layers of the annulus from the anterior and posterior-lateral region, and from both superficial and deep sections were obtained. B) Tissues (approximately 4x4 mm) were cut such that the orientation of the collagen fibres ran vertically and tension was applied perpendicular to the orientation (shown by arrows). **93**

Figure 5.2 Displacement measurement sensor. A calibrated laser beam (indicated by arrow) is projected onto the surface of the tissue in order to determine the tissue thickness. **94**

Figure 5.3 A) Single layer annular tissue mounted via rakes in the strain-controlled testing apparatus. Note the vertically aligned collagen fibres. White horizontal bar represents 10 mm. B) Sample tissue and dime for relative size comparison **95**

Figure 5.4 Representative stress-strain curve identifying variables of interest. A) Stress at the end of toe region (MPa) ; B) strain at the end of the toe region (% strain); C) Elastic modulus (MPa); D) stress at initial failure (MPa); E) strain at initial failure (% strain); F) tensile strength (MPa); G) Failure strain (% strain); H) usable material toughness. **97**

Figure 5.5 Interaction between tissue harvest location (anterior versus posterior/lateral) and depth (superficial versus deep) for A) strain at the end of toe region (% strain) (p=0.027) and B) Poisson's ratio (p=0.026). **102**

Figure 6.1 $A_{(1)}$: pictorial representation of the tissue sample dissection. $A_{(2)}$: Actual image of tissue at zero displacement. Dotted lines represent junction between single and bi-layered sections of the sample. Thus, each rake pierced only a single layer. B-D: Increasing displacement of tissue sample. Dotted lines represented original displacement. E: Shear stress-displacement curve identifying each mechanical property of interest as well as the location on the curve for each image ($A_{(2)}$-D). **116**

Figure 6.2 Schematic representation of shear strain. Grey portion represents each lamellae and the diagonal lines connect each lamellae represent the inter-lamellar matrix. Thickness of the inter-lamellar matrix (h) was assumed to be zero, thus displacement (Δx) was of interest rather than shear strain. Arrows indict direction of displacement. **117**

Figure 7.1 Example of a passive range of motion test (3 full flexion/extension cycles) for a functional spine unit. Dotted lines represent the end of the neutral zone in flexion and extension. These angles were set as the target flexion and extension angles in the herniation protocol. Solid lines indicate torque values at either end of the neutral zone. These values were used to calculate FSU stiffness. **129**

Figure 7.2 Example of a herniated disc. Upper left hand corner shows pictorial representation of how the disc was cut transversely in order to expose the inside of the disc and to assess the damage. Dye was injected into the nucleus prior to testing for visual tracking purposes. Scale is in cm. **135**

Figure 7.3 Significant interaction observed between condition (control/vibration) and injury (no herniation/herniation) for loss in disc height. **137**

Figure 8.1 Pictorial representation of herniation progression through the annulus. Note the stress riser occurring between two lamellae (left side) resulting in a hydraulic fissure or delamination. Once delamination has occurred, nuclear material is free to occupy the newly open space. **154**

Figure 8.2 Artist representation of the annulus. Light and dark green solid connections represent type IV collagen and light and dark green coils represent elastin in the intra-lamella matrix. Brown solid connections represent type IV collagen connecting adjacent lamellae, and brown coils represent elastin in the inter-lamellar matrix. The elastin (coils) assist in tensile recovery when either the intra or inter-lamellar matrix is strained. **155**

Figure A.1 Sample X-rays from Chapter 7. A) X-ray image at the start of collection before herniation protocol. B) X-ray taken after 6000 flexion/extension cycles. Radiopaque shows evidence of herniation. C) Dissection of segment confirms herniation. **160**

Figure A.2 Sample X-rays from Chapter 7. A) X-ray image at the start of collection before herniation protocol. B) X-ray taken after 6000 flexion/extension cycles. Radiopaque does not show sufficient evidence of herniation. C) Dissection of segment confirms herniation. **161**

Chapter 1

Introduction

1.1 General Introduction

Low back pain is very common, with 80% of the developed population being affected at some point in their lives (Leavitt et al., 1971). The etiology of low back pain is diverse, as are the physiological structures involved; however, debilitating pain is often the outcome. One of these structures, the intervertebral disc (IVD), is designed to allow spinal motion and dissipate shock, and is certainly not safe from injury. Intervertebral disc herniation and its initial stages is one of the most common injuries to the disc (Adams et al., 2006; Dammers & Koehler, 2002), with as high as 50% prevalence among individuals with low back pain (Dammers & Koehler, 2002). IVD occurrence is largely dependent upon the inter-relation among applied load, motion, and the mechanical properties of the disc components, namely the nucleus pulpous and the annulus fibrosus. A firm understanding of the properties of the disc is of utmost importance for our understanding of herniation initiation and progression.

For decades, the mechanical properties of the spinal joints as a structure have been extensively studied. Researchers have examined functional spine units (two adjacent vertebral bodies and the intervening disc) in their entirety (for example Adams, 1995; Adams et al., 1993; Adams et al., 1994; Adams & Dolan, 1996; Brown et al., 2002; Brown et al., 2008; Gunning et al., 2001; Mimura et al., 1994; Oxland et al., 1992; Panjabi et al., 1984; Panjabi et al., 1985; Shea et al., 1991) as well as multilayered slices of the annulus fibrosus (Ebara et al., 1996; Fujita et al., 1997). Further, the mechanical properties of single lamella in the annulus have also been examined (Holzapfel et al., 2005; Skaggs et al., 1994). While these latter studies conducted on the annulus have provided us with important information pertaining to the various properties of the IVD,

this knowledge has not been linked to the initiation and propagation of IVD injury nor has it been consistently realistic to *in vivo* conditions. Whether or not IVD tissue will become injured is highly dependent upon its mechanical properties.

The annulus of the disc is comprised of various components including the intra and inter-lamellar matrices. The intra-lamellar matrix is the connective tissue found between adjacent collagen bundles within each layer of the annulus. It functions to keep collagen fibres tightly bound together. It contains type VI collagen fibres (Melrose et al., 2008; Schollum et al., 2008), proteoglycans (Adams & Green, 1993), and elastin (Yu et al., 2002; Yu et al., 2005). The inter-lamellar matrix is comprised of similar components but is located between adjacent layers of the annulus, and helps to prevent delamination between the layers (Figure 1.1).

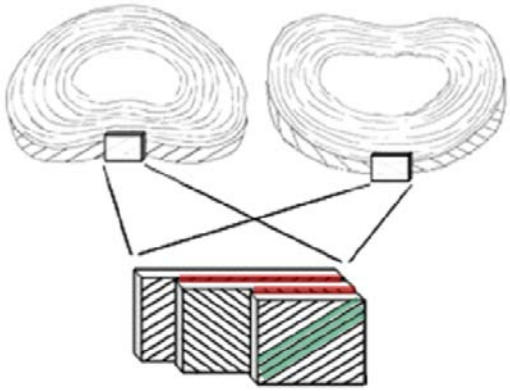

Figure 1.1: Pictorial representation of the annulus. The red sections represent connective tissue between adjacent lamellae, namely the inter-lamellar matrix, and the green sections represent connective tissue between adjacent collagen bundles within each lamellae, namely the intra-lamellar matrix. Relative size of each component is not to scale.

As mentioned, one of the most frequent injuries to the IVD is herniation (Dammers & Koehler, 2002), and its occurrence is dependent on the state of the IVD tissue. While previous work has suggested that disc herniation most readily occurs in a dehydrated disc when compressive stress concentrations are higher on the annulus (in particular in the posterior region) as compared to the nucleus (Adams et al., 2000), more recent work has suggested an alternate explanation. This explanation states that for herniation to occur, the nucleus must be well hydrated for there to be a relatively high hydrostatic pressure within the disc (Simunic et al., 2001), which creates stresses on the inner annulus. Wherever the highest stress lies, or where the weakest collagen bond exists, is where the nucleus will penetrate the lamellae. However, the collagen fibre bundles and the fibres themselves do not tear, but rather spread laterally to form a cleft, through which the nucleus will breach (Tampier et al., 2007). If loading conditions remain favourable for herniation propagation, for example repetitive flexion-extension (Callaghan & McGill, 2001), the nucleus will continue to push through clefts formed in each lamellar layer, at the weakest bond and/or highest stress location, and will progress from the inner annular layers through to the outer layers. A recent study by Pezowicz et al. (2005) in ox tail annular samples noted similar clefts in the annulus following the application of transverse tension (tension applied perpendicular to the orientation of the collagen fibre bundles), further supporting the notion that disc herniation initiation and propagation is influenced by the mechanical properties of the annulus, such as intra-lamellar and inter-lamellar strength and stiffness.

Exposure to whole body vibration is highly associated with both a high prevalence and incidence of low back pain (Bovenzi & Hulshof, 1999; Lis et al., 2007;

Robb & Mansfield, 2007) and disc herniation (Viikari-Juntura, 1997; Virtanen et al., 2007). However, these studies were not able to determine a causal relationship. Further, no attempt to understand the mechanism of disc herniation as a result of exposure to vibration has been documented. One possible mechanism is that vibration, given its repetitive nature, may decrease the strength, and thus tolerance, of the annulus over time since cyclic loading has been shown to have a similar negative effect on the fatigue life of many engineering materials (Dowling, 1993; Hertzberg, 1996; Hertzberg & Manson, 1980) including thermoplastics as documented by Riddell et al. (1966). Similar effects have been observed in biological tissues such as functional spinal units (Parkinson & Callaghan, 2007) and ligaments (Weisman et al., 1980). It is hypothesized, as a part of this thesis, that vibration may alter the mechanical properties of both the intra and inter-lamellar matrices making the annulus more susceptible to cleft formation and delamination.

Herniation can result in debilitating back pain and loss in quality of life. It is therefore very important to not only understand how exposures such as vibration affect the integrity of the disc, but to also be able to apply this information toward preventative measures. The following purposes of this thesis address the mechanical properties of the disc, specifically related to their role in disc herniation, and how they become altered following exposure to vibration. Further, this thesis also aims to identify the causal relationship between vibration and herniation, as currently only epidemiological studies have been able to provide a correlative relationship.

1.2 Specific Purpose of Thesis

The purpose of this thesis is five-fold:

1) To determine the mechanical properties of two-layered samples of the annulus lamellae:
    i) under uniaxial and biaxial tensile loading states
    ii) at various physiological strain rates
2) To determine the mechanical properties of the intra-lamellar matrix
3) To determine the mechanical properties of the inter-lamellar matrix
4) To assess the mechanical effect of exposure to axial vibration on the intra and inter-lamellar matrices
5) To determine the effect of vibration on intervertebral disc herniation initiation and propagation

This thesis consists of five studies, which have addressed the aforementioned purposes. Figure 1.2 displays a flow chart linking each of the studies in the effort to further our understanding of intervertebral disc herniation.

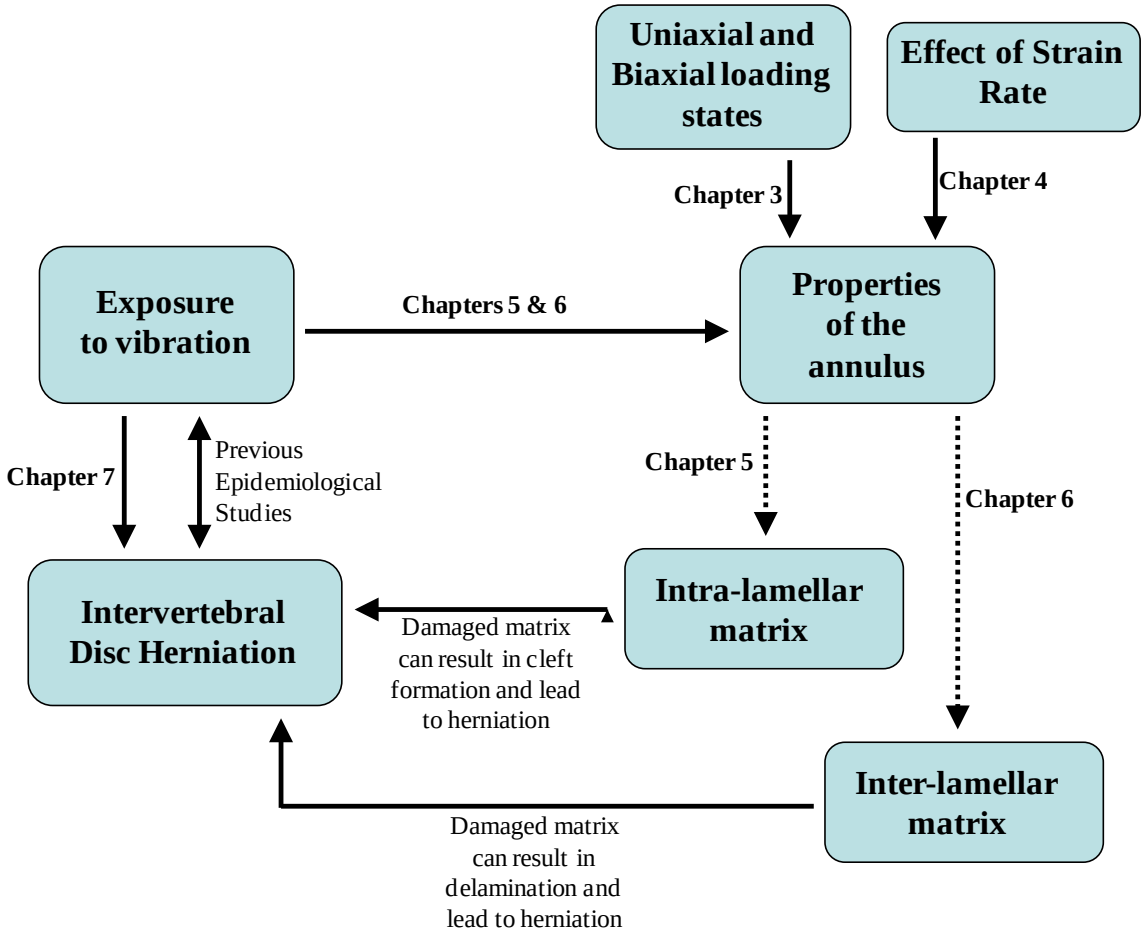

Figure 1.2: Flowchart of the contribution of each study to the understanding of disc herniation. Double tailed arrow between exposure to vibration and herniation represents a correlation rather than a causal relationship.

1.3 General Hypotheses

The overriding general hypothesis for this thesis was that exposure to vibration will alter the material properties of lamella of the annulus and accelerate *in vitro* induced IVD herniation. Specifically, it was hypothesized that:

1. Exposure to 5 Hz axial vibration will decrease the tensile strength and modulus of the intra-lamellar matrix due to material weakening often observed in materials following vibration (Hertzberg, 1980).
2. Exposure to 5 Hz axial vibration will also decrease the shear strength and modulus of the inter-lamellar matrix as it is hypothesized that vibration will accelerate delamination of the annulus.
3. A greater number of discs exposed to 5 Hz axial vibration in conjunction with repetitive flexion/extension will herniate as compared to control discs, which have not been exposed to vibration.

Five individual studies were conducted in order to address these aforementioned hypotheses. Chapters 3 through 7 address individual hypotheses and Chapter 8 addresses the more general hypotheses.

Chapter 2

Review of Literature

2.1 Review of Anatomy

2.1.1 General Anatomy

The human spine, not including the sacrum and coccyx, is typically comprised of 24 vertebrae: 7 cervical, 12 thoracic, and 5 lumbar. It is a flexible column capable of flexion/extension, lateral bend, and axial twist motions, while maintaining the ability to resist shear loads and high compressive loads. Each vertebra consists of lateral and posterior boney elements, with similarities existing in each of the three subdivisions of the spine: cervical, thoracic, and lumbar. These bony elements provide attachment surfaces for ligaments and muscle tendons (Figure 2.1). The most superior and inferior surfaces of the vertebrae are cartilaginous structures termed endplates. The endplates form the junction between the vertebral body and the intervertebral disc found between each adjacent vertebra (Figure 2.2).

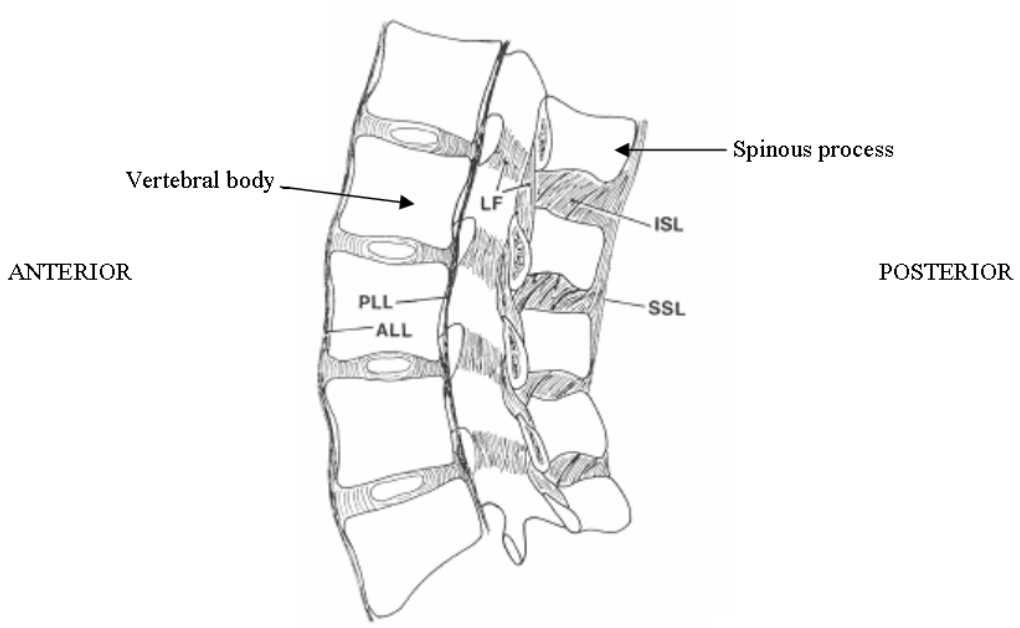

Figure 2.1: Sagittal view of the lumbar spine. Note the ligament attachment sites on the posterior boney elements. ISL – interspinous ligament, SSL – supraspinous ligament, LF – ligamentum flavum, PPL – posterior longitudinal ligament, ALL – anterior longitudinal ligament. Image from Adams et al., 2006, *The biomechanics of back pain*, pg 21.

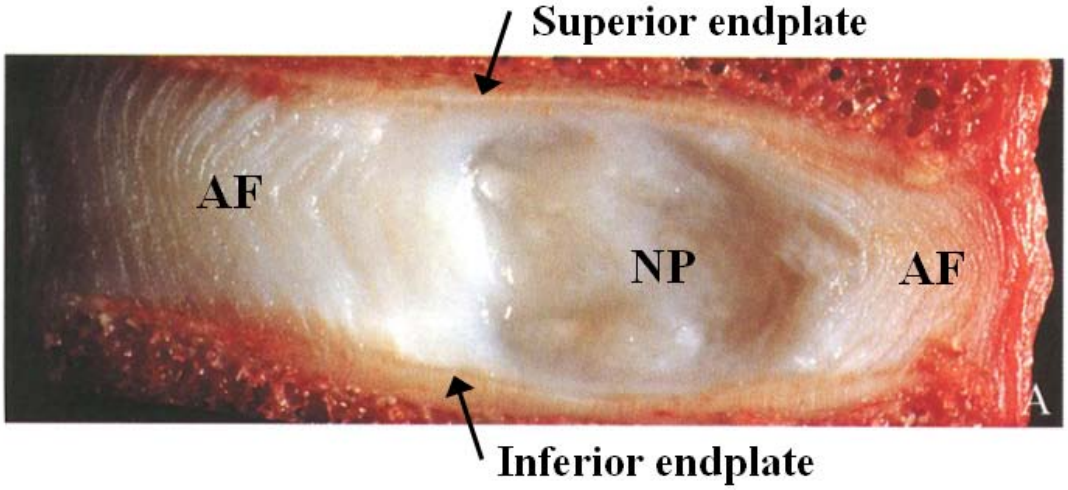

Figure 2.2: Sagittal view of the intervertebral disc including the nucleus pulpous (NP), annulus fibrosus (AF), and endplates. Image from Adams et al., 2006, *The biomechanics of back pain*.

2.1.2 Intervertebral Disc

The IVD is a fibrocartilaginous structure (Eyre & Muir, 1976; Hayes et al., 2001) found between each adjacent vertebra in the spine. It is attached at the endplates of the vertebral bodies, and the contribution of the IVDs across the entire spine represent between 20 and 33% of the height of the whole vertebral column (White & Panjabi, 1990). The IVD is comprised of the gelatinous nucleus pulposus found in the most inner part of the IVD, which is surrounded by the annulus fibrosus. The nucleus is comprised of approximately 85% water and the annulus is approximately 78% water (Lipson, 1981). The IVD partially functions to dissipate shock (Cassidy et al., 1989; Guerin & Elliott, 2006; Holzapfel et al., 2005; Inerot & Axelsson, 1991; Inoue, 1981; Johnson et al., 1982) and allows for extensive movement between the vertebrae (Cassidy et al., 1989; Guerin & Elliott, 2006; Klein & Hukins, 1982a).

2.1.2.1 Nucleus Pulposus

The nucleus contains primarily type II collagen fibres (Eyre & Muir, 1974; Eyre & Muir, 1976; Hayes et al., 2001), is rich with proteoglycans (Berthet-Colominas et al., 1982 (bovine)), and contains chondrocyte-like cells similar to those seen in articular cartilage (Bruehlmann et al., 2002; Errington et al., 1998; Hayes et al., 2001; McNeilly et al., 1996; Pritchard et al., 2002). These cells are spherical in shape (Bruehlmann et al., 2002; Errington et al., 1998; Pritchard et al., 2002) and the type II collagen synthesized by these cells is thought to resist compressive forces (Hayes et al., 2001). It is the proteoglycans that are responsible for the high fluid environment of the nucleus. The proteoglycans create a negatively charged environment due to their polarity such that it

allows for an influx of fluid into the nucleus. This increase in fluid is what creates the hydrostatic nature of the IVD.

2.1.2.2 Annulus Fibrosus

The fibrocartilaginous annulus is a highly complex and organized structure of alternating ply-like sheets called lamella, first described by Beadle in 1932. The morphology of the collagen and disc cells varies throughout the annulus such that two distinct regions can be dissociated, the inner annulus and the outer annulus. The annulus is also rich with proteoglycans (Inerot & Axelsson, 1991), although not to the same extent as the nucleus (Berthet-Colominas et al., 1982).

The inner annulus is most similar to the nucleus in that the majority of the collagen present in this area is type II collagen (Berthet-Colominas et al., 1982; Bruehlmann et al., 2002; Errington et al., 1998; Eyre & Muir, 1974; Eyre & Muir, 1976; Hayes et al., 2001) with minimal type I collagen present. In the inner annulus of humans, the chondrocyte-like spherical cells have one or two short processes radiating from the cell bodies in a seemingly unorganized fashion (Bruehlmann et al., 2002; Inoue, 1981; Postacchini et al., 1984) and are thought to act as mechanoreceptors by detecting compressive loads (Errington et al., 1998; McNeilly et al., 1996). The thickness of each lamella in the inner annulus is approximately 300 μm in the human intervertebral disc (Cassidy et al., 1989; Marchand & Ahmed, 1990).

The outer annulus is quite different from the inner annulus in regards to the collagen type present and the morphology and function of the cells. The outer annulus is comprised mostly, if not completely, of type I collagen fibres (Berthet-Colominas et al., 1982 (bovine); Bruehlmann et al., 2002 (bovine); Errington et al., 1998 (bovine) ; Eyre &

Muir, 1974 (porcine); Eyre & Muir, 1976 (porcine); Hayes et al., 2001 (rat)); however, the transition from type II to type I collagen is not bounded by a distinct separation point, but rather a gradual and uniform transformation from the interior to exterior of the annulus fibrosus (Berthet-Colominas et al., 1982; Cassidy et al., 1989 (human); Eyre & Muir, 1976). These type I collagen fibres are more akin to those found in tendon or ligaments (Bruehlmann et al., 2002; Errington et al., 1998; Hayes et al., 2001; Lo et al., 2002 (review – human and animal); McNeily et al., 1996 (rat); Pritchard et al., 2002 (porcine)) and are considered to resist tensile rather than compressive forces (Hayes et al., 2001). The fibrochondrocyte-like disc cells responsible for synthesizing the type I collagen are quite elongated and fusiform in shape (Bruehlmann et al., 2002; Errington et al., 1998; Postacchini et al., 1984 (rat); Pritchard et al., 2002). These cells are also equipped with long processes radiating from the cell bodies parallel to the collagen fibres (Bruehlmann et al., 2002; Errington et al., 1998; Postacchini et al., 1984; Pritchard et al., 2001) which are also thought to act as mechanoreceptors (Errington et al., 1998; McNeily et al., 1996). The density of the fibrochondrocyte-like elongated cells found in the matrix of the outer annulus is quite high with over four times the number of cells as compared to the density of chondrocyte-like spherical cells in the nucleus (Hastreiter et al., 2001 (human)). The thickness of the lamellae in the outer annulus tends to be less than that in the inner annulus (Tampier, 2006 (human and porcine)) with an average thickness of 130 μm (Cassidy et al., 1989 (human); Marchand & Ahmed, 1990 (human); Tsuji et al., 1993 (human)).

2.1.2.3 Lamellar Anatomy

The collagen fibres, both type I in the outer annulus, and type II in the inner annulus, are oriented in such a fashion to create distinctive fibre bundles visible to the naked eye. These fibre bundles run obliquely to the spine compressive axis with alternating angle directions in adjacent layers (Marchand & Ahmed, 1990) (Figure 2.3). The angle of inclination of these bundles has been documented extensively and ranges from 45-60° from the compressive axis (Cassidy et al., 1989 (human); Hickey & Hukins, 1980 (human); Holzapfel et al., 2005 (human); Klein & Hukins, 1982a (rabbit); Marchand & Ahmed, 1990 (human); Tampier, 2006 (human and porcine); Tsuji et al., 1993 (human)). However, debate still exists as to whether the angle of inclination differs between the outer and inner annulus layers and between anterior and posterior annulus layers (Cassidy et al., 1989 (human); Holzapfel et al., 2005 (human); Tampier, 2006 (human and porcine)).

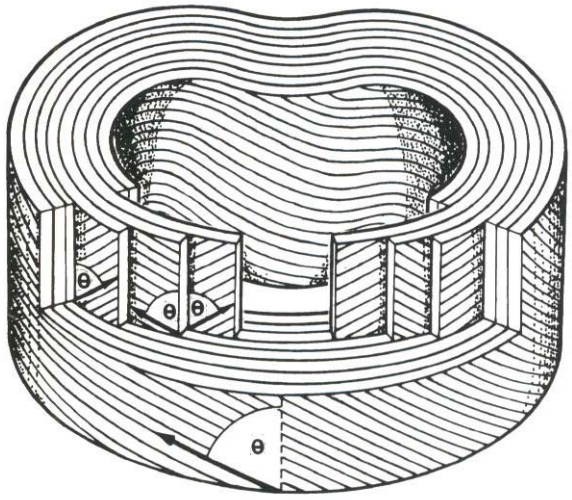

Figure 2.3: Annulus fibrosus fibre orientation in the intervertebral disc. Note the alternating fibre direction in adjacent lamellae. Image from Adams et al., 2006, *The biomechanics of back pain*, pg 15

The annulus is generally comprised of 15 to 25 layers (Cassidy et al., 1989 (human); Marchand & Ahmed, 1990 (human); Tampier, 2006 (human and porcine)). However, the fibre bundles often form incomplete layers such that two adjacent layers merge into each other (Marchand & Ahmed, 1990 (human); Tsuji et al., 1993 (human)). Specifically, Tsuji et al. (1993) found that the posterior annulus had fewer distinct lamellae, and subsequently a greater number of incomplete lamellae as compared to the anterior annulus.

During loaded states of the IVD, the orientation of the collagen fibres in the lamellae will change due to disc height changes. Specifically, when axially loaded in compression, the fibre orientation changes such that the fibres become closer to horizontal (Klein & Hukins, 1982a (rabbit)), and in circumferential tension, the fibres reorient themselves in the direction of loading and become more horizontal (Guerin & Elliott, 2006 (human)). Changes in fibre orientation also occur as a result of posture changes. When flexed, the anterior fibres orient themselves such that the fibre angle becomes smaller (closer to horizontal) and the posterior fibres become more vertically aligned. The opposite occurs during extension (Klein & Hukins, 1982b (rabbit)). Further, under torsional loading, the fibres in every second layer become slack and thus their angle of orientation decreases to become closer to vertical, while the fibres in the alternating layers become taut and become more horizontal (Klein & Hukins, 1982b).

2.1.2.4 Inter-lamellar Matrix

In between two adjoining lamellae lies an adhesive layer of cells and structures. These cells are much different in morphology from those found in either the nucleus or within the lamellae of the annulus. Inter-lamellar cells are disc shaped, flat cells with

many projecting processes that form a stellate pattern (Bruehlmann et al., 2002 (bovine)). These processes interconnect to create a lattice formation similar to that surrounding ligament tissue (Lo et al., 2002). Pezowicz and colleagues (2005) published an elegant imagery study of the connections and structural complexity between each of the lamellar layers harvested from ox tails and the effect of such connections under tension both along and perpendicular to the collagen fibres (Figure 2.4). Despite this complex architecture, Fujita et al. (1997) demonstrated delamination of the inter-lamellar matrix within the human annulus in response to transverse tension (tension applied perpendicular to the direction of the collagen fibre bundles).

Figure 2.4: Annulus fibrosus from ox tail following tensile strain. Note the formation of a cleft (W) in the superior lamella, which reveals the underlying lamella and intricate arrangement of collagen fibres. Image from Pezowicz et al., 2005.

2.2 Material Properties of the IVD

2.2.1 Lamellae Mechanics

2.2.1.1 Traditionally Examined Material Properties of the Annulus Fibrosus

Certain material properties have been more commonly examined when testing annular tissue. The most common property examined being Young's modulus, which can be determined from the slope of the linear portion of a stress/strain curve. Generally Young's modulus has been determined from unidirectional tensile tests of the annulus and can provide information about the normalized stiffness of the tissue of interest. Skaggs et al. (1994), Ebara et al. (1996), Fujita et al. (1997), and Holzapfel et al. (2005) (human annular samples were examined in each study) have all documented Young's modulus for both multiple and single lamella. However, each of these studies only examined tension applied in one direction at a time, either parallel to the fibre orientation or perpendicular to it.

Another commonly examined property is the ultimate strength, or tensile strength of a tissue. This is the maximum stress a material can withstand before failure. Skaggs et al. (1994), Ebara et al. (1996), and Fujita et al. (1997) each documented the tensile strength of multiple lamellae sections of the annulus during tensile strain.

Less commonly examined properties include the yield point, which is the point where a material is no longer elastically deforming but is now plastically deforming, end of toe region stress and strain, and material toughness, which relates to a material's ability to store energy prior to failing. Material toughness is determined by integrating the stress-stain curve. This means a tough material must be ductile, or must be able to deform greatly before failing, yet be strong as well. Fujita et al. (1997) reported the yield point

during multiple lamellae tensile testing and Chuang et al. (2007) documented the toughness of annulus tissue as a result of increased collagen crosslinks within the fibre in the inter-lamellar matrix in the bovine annulus formed through aglycone treatments. Collagen crosslinks are covalent bonds formed within the collagen fibre that provide tensile strength to the collagen (Bailey et al., 1974).

2.2.1.2 Tensile Loading

Each lamella in the IVD consists of bundles of parallel collagen fibres. These individual sheets are subjected to tensile forces similar to that in the whole IVD. These tensile forces occur parallel to the collagen fibres (Skaggs et al., 1994 (human)), perpendicular to the collagen fibres, and circumferentially around the disc (Ebara et al., 1996 (human)) (Figure 2.5). Various studies have tried to document these tensile forces in single (Holzapfel et al., 2005; Skaggs et al., 1994; both human studies) as well as multiple layers of the annulus (Ebara et al., 1996 (human); Pezowicz et al., 2005 (ox)). Further, tensile forces at various locations of the disc, both anterior versus posterior, as well as outer versus inner AF, have been examined (Ebara et al., 1996; Holzapfel et al., 2005; Skaggs et al., 1994).

Adams & Green (1993) and Green et al. (1993) initiated the investigation of the human annulus tensile behaviour by examining the vertical tensile strength of thick sections of the anterior and posterior annulus. They found that tensile strength was highest in the direction of the collagen fibres (Green et al., 1993) and that a portion of this strength was attributed to the intra-lamellar connections and not just the collagen fibres themselves (Adams & Green, 1993).

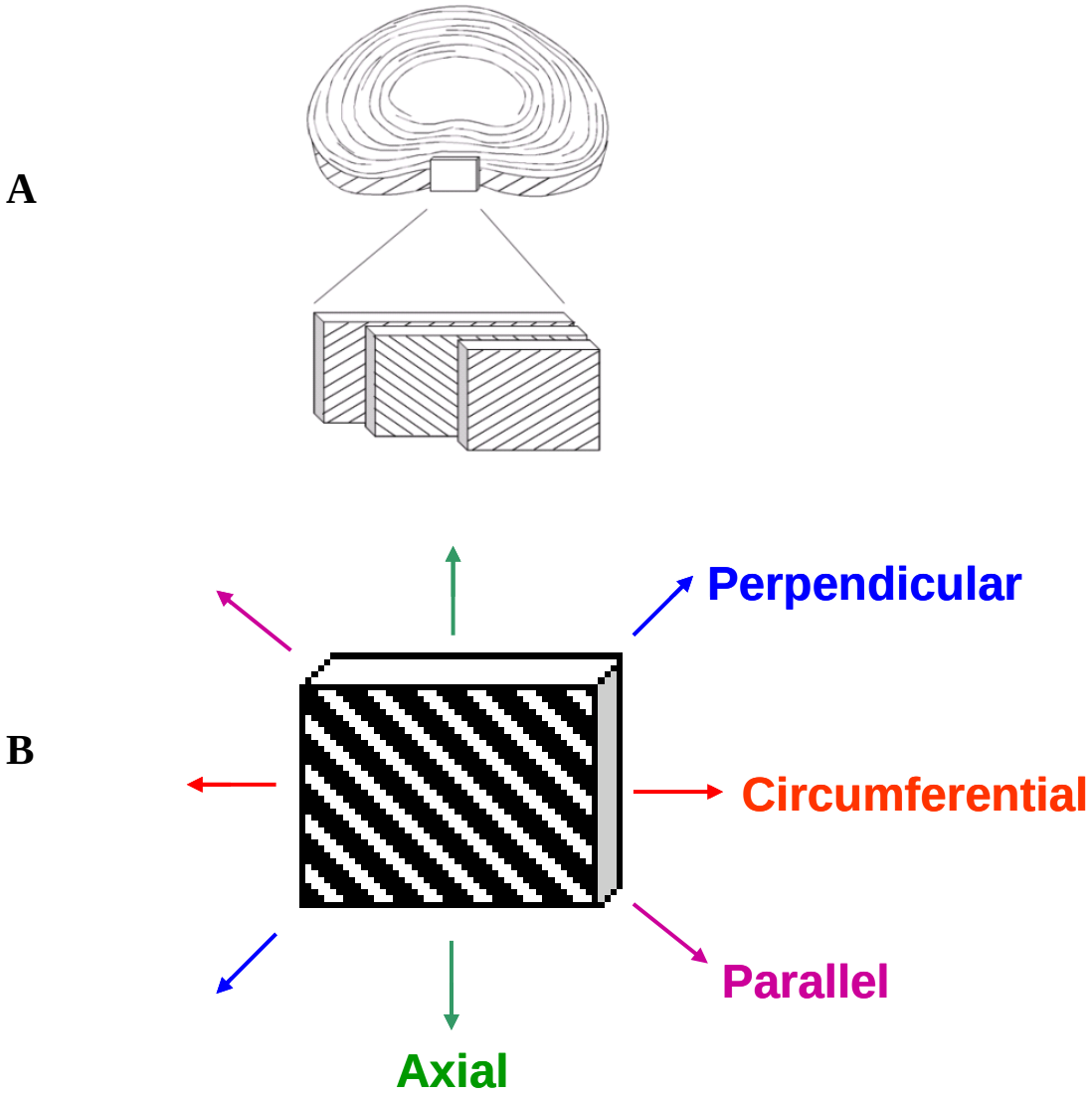

Figure 2.5: Schematic representation of each of the examined directions of tension in the literature. A) Shows location of extracted annulus tissue B) extracted annulus tissue and arrows indicating direction of previously researched tension.

Skaggs and colleagues (1994) examined single human lamellae and found that, when stretched parallel to the collagen fibres at a very slow strain rate, failure stresses for anterior annulus tissue were higher than for posterior-lateral annulus tissue and failure stresses for outer annulus samples were higher as compared to those from the inner annulus. These reported failure stresses (mean (S.D)) were 10.3 MPa (8.4) in the anterior outer region, 3.6 MPa (2.0) in the anterior inner region, 5.6 MPa (3.2) in the posterior outer region, and 5.8 MPa (2.9) in the posterior inner region. Ebara et al. (1996) documented similar regional findings in terms of the modulus of multiple layers stretched circumferentially (parallel to the endplates). Ebara et al. (1996) found that, in general, anterior samples were stiffer than posterior samples, and that samples from the outer region were more stiff than from the inner region. Ebara et al. (1996) documented mean modulus values ranging between approximately 8 MPa and 50 MPa.

Skaggs at al. (1994) also found that failure strain was higher for posterior-lateral annulus tissue as compared to anterior despite the fact that no visible morphological differences exist between the anterior and posterior annulus, and found higher failure strains for inner annulus versus outer annulus tissues. Skaggs et al. (1994) also found that adjacent single lamellae did not have differing tensile strength suggesting local uniformity in the annulus.

A more recent study conducted by Pezowicz and colleagues (2005) examined the tensile strength of a multi-lamellar section of the outer annulus (thickness of 1.1mm) from ox tails under isolated separate testing conditions of either strain applied parallel or perpendicular to the collagen fibres. They observed the classic uncrimping of the collagen fibres, a reversible change, and then with further strain, eventual rupture. Most

interesting, however, was their findings with the perpendicular testing. Pezowicz et al. (2005) found that minimal stress was required to pull the adjacent parallel fibres apart, and when these fibres did pull apart, distinct clefts formed and the inter-lamellar layer beneath was visible. They concluded from the formation of these clefts that the inter-fibre adhesion must be quite low and must not significantly contribute to the strength of the lamellae. Further, these clefts were the first visual documentation of the currently proposed mechanism of herniation progression (Moore et al., 1996; Tampier, 2006) in which the nucleus squeezes through the annulus pushing through weak inter-fibre bonds/clefts rather than rupturing the annular fibres.

Following the study conducted by Pezowicz and colleagues (2005), Holzapfel et al., (2005) published the first paper to examine the tensile strength of individual lamellae from human lumbar IVD. They examined both the tensile strength parallel to the collagen fibre orientation a well as perpendicular to the fibres, however again not simultaneously. Further, when they examined the parallel strength, the annulus section remained attached to the endplates of the adjacent vertebral bodies, as they believed this provided a more physiological value of the tensile strength of the annulus. Holzapfel et al. (2005) examined human annulus lamellae from the outer and inner regions of both the antero-lateral and posterior sections of the annulus. They found that the outer annulus was stiffer than the inner annulus, and that the antero-lateral annulus was stiffer than the posterior annulus when the force was applied in line with the direction of the collagen fibres. For the perpendicular testing, only the antero-lateral section of the annulus at an intermediate depth was examined. They found a mean elastic modulus for these tests of 0.22 MPa

while the moduli for the tensile tests conducted parallel to the fibre orientation were over 100 times this magnitude (28-78 MPa).

2.2.1.3 Biaxial Tensile Testing

The tensile properties of various tissues have been examined under biaxial loading scenarios. For example mitral valve tissue (Grashow et al., 2006; May-Newman & Yin, 1995), pericardium tissue (Lee et al., 1985; Sacks & Chuong, 1998), lung tissue (Debes & Fung, 1992), and arteries (Debes & Fung, 1995) have all be examined in terms of the mechanical properties under biaxial tensile load. Generally speaking, biaxial tensile load is more representative of the loading profile that these tissues would be exposed to *in vivo* and it is therefore important to be aware of potential differences in the mechanical response between uniaxial and biaxial testing scenarios. In addition to these studies, two papers have examined biaxial loading of the annulus (Bass et al., 2004 (human); Bruehlmann et al., 2004 (bovine)). However, the work by Bruehlmann et al. (2004) primarily focused on cellular deformation as a result of biaxial strain rather than the mechanical properties of the annulus as a whole. Bass et al (2004), on the other hand, examined the mechanical properties of the human annulus, and found significantly greater stress values for a given strain when under biaxial tension as compared to uniaxial tension. However, Bass et al., (2004) were not able to comment on regional difference as only anterior superficial sections were examined.

2.2.1.4 Inter-lamellar Shear Strength

Studies have attempted to predict the magnitude of inter-lamellar shear force using modelling approaches such as finite element models (Goel et al., 1995; Yin & Elliott, 2005). For example Goel et al. (1995) used a finite element model to predict the

shear stresses in the inter-lamellar septum. They estimated the shear stress to be as high as 270 kPa in the posterior-lateral region. They further suggested that these shear stresses may contribute to delamination of the annular layers in posterior-lateral layers.

More recently studies have actually measured these shear forces in annulus tissue. Iatridis et al. (1999) and Fujita et al. (2000) initiated investigations of the shear behaviour of human annulus tissue. Iatridis et al. (1999) focused on the effect of applied torsional shear strains on thin transverse slices of the anterior annulus. They examined various rates and magnitudes of applied shear strain and found that both affected the shear modulus such that higher strain rates resulted in higher shear moduli while larger strain magnitudes resulted in lower shear moduli. Fujita et al. (2000), on the other hand, focused on the effect of shear strain on cubes of human annulus tissue from various regions of the IVD. Specifically, Fujita et al. (2000) applied shear strains by placing the tissue samples between two parallel sandpaper wrapped plates that linearly translated in opposite directions. Fujita et al. (2000) applied these shear strains (incremented from 2.5 to 10% strain, each strain held for 20 min) in each plane of the cube such that the strains were applied both parallel to and perpendicular to the direction of the annulus lamellae, however the two strain directions were not applied simultaneously. Cube specimens were tested as it was thought that the shear behaviour observed would be a good approximation of the shear behaviour of the inter-lamellar matrix since the collagen fibres were not under any tension during these tests. Fujita et al. (2000) also applied similar strains to pre-strained 2mm thick sheets (multiple lamellae) of anterior annulus tissue in the vertical direction (anatomical axial direction) as well as in the horizontal direction (parallel to the endplates) such that shear strains were never applied in the pure direction of the collagen

fibre bundles. Tissue sheets that were shear strained in the axial direction had a pre-strain in the circumferential axis and vice versa. The results from the cube tissue samples indicted that the highest shear modulus for the cube sections occurred when the shear strain was applied in plane with the lamellae, possibly due to the added tensile stiffness from inter-lamellar collagen connections. Results from the sheet tissue samples revealed that both the axial shear modulus and circumferential modulus were higher for tissue sheets from the outer versus inner annulus, potentially due to the presence of different collagen types, and that the magnitude of pre-strain only increased the axial shear modulus and not the circumferential shear modulus. Fujita et al. (2000) also found that the shear moduli for the sheet tissue samples were twice as high in the axial axis as compared to the circumferential axis.

A recent study by Chuang et al. (2007) examined the effect of additional inter-lamellar collagen crosslinks on the tensile properties of bovine annulus tissue. By exposing the tissue to genipin, a natural fruit extract capable of increasing the number of fibril bonds, Chuang and colleagues (2007) were able to assess the effect of added crosslinks in the matrix of bovine annular samples. They found that the tissues exposed to genipin had higher ultimate tensile strength, increased toughness, and increased yield stress in the circumferential tensile direction; the direction in which normal annulus tissue is under the greatest stress.

2.3 Intervertebral Disc Herniation

2.3.1 Stages of Herniation

As described in detail in sections 2.1.2.1 and 2.1.2.2, the IVD is comprised of a gelatinous centre called the nucleus pulposus, which is surrounded by a more fibrosus structure comprised of layers of alternating collagen fibre orientation called the annulus fibrosus. While it is clear that there is no true distinct separating barrier between these two structures, they do possess distinct differences in composition and function. Like any other structure in the body, the intervertebral disc is vulnerable to injury, for example disc herniation. Disc herniation is characterised by the extrusion, generally in the posterior direction (Haughton, 1988; Mobbs & Steel, 2007), of the nucleus through the annulus. Disc herniation is generally classified as a protrusion or a prolapse (Yasuma et al., 1986). A protrusion is characterised by a nuclear, annular, or nuclear/annular bulge generally in the posterior direction that extends into the spinal canal. A prolapse is characterized by actual nuclear extrusion through the annulus and posterior longitudinal ligament into the spinal canal (Yasuma et al., 1986). Adams & Hutton (1985) detailed the theoretical events or stages of the IVD herniation process. They stated that the early stages are marked by lamella dissociation or delamination of the IVD. This is followed with the nucleus breaching through each lamella layer, and ending with complete extrusion of the nucleus through the outer most layer of the annulus.

Recent work by Tampier et al. (2007) noted that herniation is not characterized by fibre tearing, or a nucleus path that propagates through the annulus in a straight line. Rather Tampier et al. (2007) found that the nucleus migrates through the lamellae of the annulus looking for the weakest spots to protrude into the adjacent lamella (Figure 2.6).

Tampier et al. (2007) documented the nucleus protruding through clefts, which had developed in each lamella (Figure 2.7). As previously mentioned, similar clefts were formed when the annular tissue was stretched in the transverse (perpendicular to the collagen orientation) direction (Pezowicz et al., 2005). Further, Tampier et al. (2007) observed inter-lamellar delamination as a result of this migrating nucleus.

Herniations generally occur in the posterior or posterior-lateral direction (Haughton, 1988; Mobbs & Steel, 2007). While the reason for this is most likely due to posture (see section 3.1.2) it has been hypothesized that the greater number of incomplete layers (when a bundle of a layer is woven though a bundle in an adjacent layer) found in the posterior annulus may reduce its strength relative to the anterior annulus (Tsuji et al., 1993).

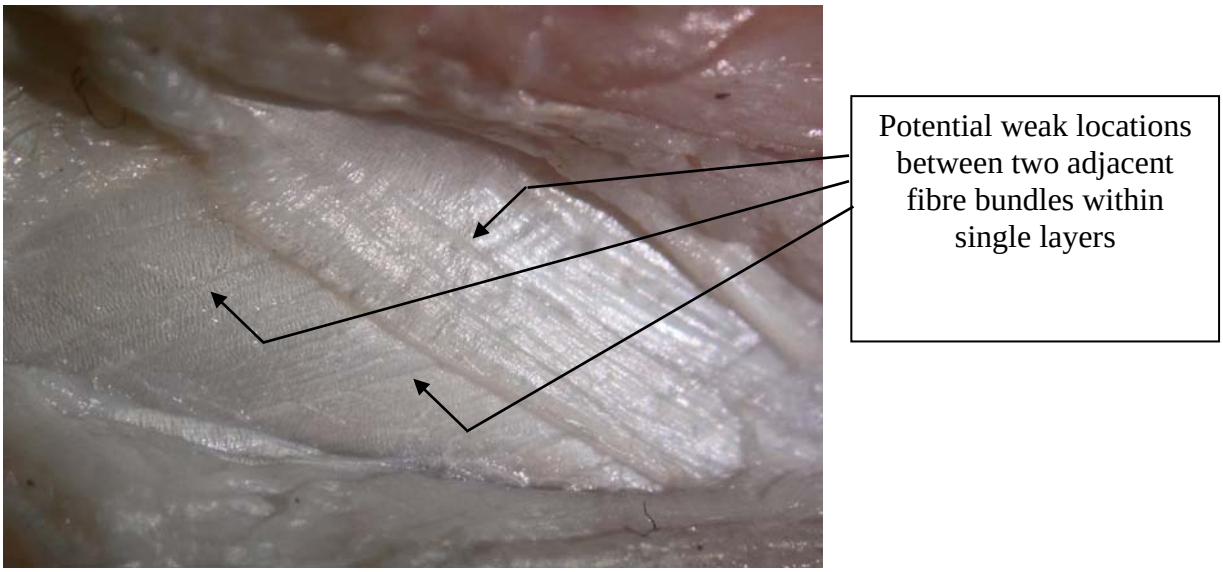

Figure 2.6: Magnified view of porcine outer anterior annulus fibrosus lamellae. Areas noted with arrows are potential weak locations in individual lamellae due to the visible collagen bundle segregations.

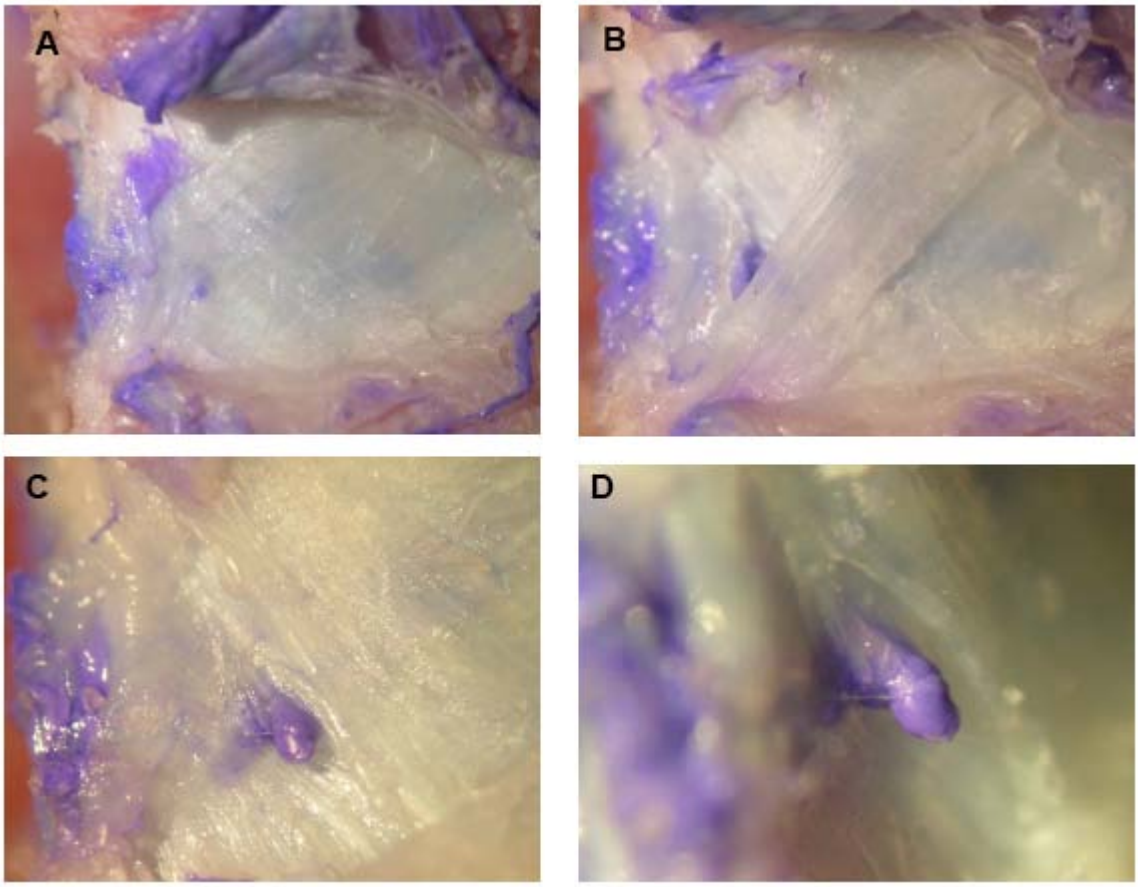

Figure 2.7: Dissection of the annulus fibrosus tissue following the initiation of disc herniation. The more outer lamellae do not show nuclear material (a and b), but the more inner lamellae (c and d) show that the nucleus pulposus has begun to penetrate the annulus fibrosus through formed clefts in the lamellae. Figure reproduced from Tampier et al., 2007, with permission.

2.3.2 Risks Factors

Disc herniation has been associated with various occupational activities and exposures. Specifically, in occupational environments heavy physical work and manual handling have been associated with an increased risk of disc herniation (Videman et al., 1990; Viikari-Juntura, 1997). Further, *in vitro* studies have found that static hyperflexion combined with compression (Adams & Hutton, 1982), repetitive compressive loading and combined flexion (Gordon et al., 1991) and repetitive flexion combined with mild compression (Adams & Hutton, 1983; Aultman et al., 2005; Callaghan & McGill, 2001) are all successful methods of developing both delamination as well as complete disc herniations. Repetitive spine flexion combined with static compression is a common pattern observed during repetitive lifting tasks and is most likely the reason disc herniations are generally posterior/posterior-lateral in direction. In addition to heavy physical work, manual lifting, and repetitive spinal flexion, exposure to whole body vibration (WBV) is another risk factor for the development of disc herniations (Viikari-Juntura, 1997; Virtanen et al., 2007).

2.3.2.1 Whole Body Vibration

Little is known about the relationship between WBV and the development of disc herniations other than the fact that a strong association exists between the two. It is well documented that the natural frequency of the human torso is between 4Hz and 6Hz (Dupuis, 1989; Panjabi et al., 1986; Pope et al., 1998; Wilder et al., 1982), which is also the approximate frequency to which individuals are exposed in situations such as automobile or truck driving (Mansfield, 2005). Further, it has been shown that these exposure frequencies do not diminish at the spine level, and in fact can augment the

amplitude of vibration measured at the lumbar spine (Panjabi et al., 1986; Pope et al., 1998), which may contribute to disc herniation initiation and/or propagation. A review on WBV and low back pain by Wilder and Pope (1996) also hypothesized that the stresses placed on the inner lamellae of the posterior annulus due to flexion are exacerbated with vibration. Further Wilder (1993) theorized that vibration may induce rocking motions of the pelvis, which may translate to the spine. If vibration exposure does result in increased motion at the spine, in particular increased cyclic flexion, it is possible that it could accelerate the initiation of delamination and disc herniation. The reason for this acceleration may lie in the fact that vibration, or cyclic loading, negatively affects the fatigue life of many engineering materials (Dowling, 1993; Hertzberg, 1996; Hertzberg & Manson, 1980; Riddell et al., 1966) and biological tissues such as vertebral bone (Parkinson & Callaghan, 2007) and ligaments (Weisman et al., 1980). Weisman et al. in 1980, showed that ligaments in a rat model become weaker as a response to low magnitude cyclic loading. Perhaps a similar occurrence happens in annular tissue given that both outer annulus lamellae and ligaments are primarily composed of type I collagen fibres (Bruehlmann et al., 2002; Errington et al., 1998; Hayes et al., 2001; Lo et al., 2002; McNeily et al., 1996; Pritchard et al., 2002).

It has also been shown that vibration negatively affects the integrity of the inter-lamellar matrix of the annulus. Ishihara et al. (1992) found that exposure to vibration resulted in a significant reduction in proteoglycan synthesis in the nucleus and the inner annulus. Reduced proteoglycan synthesis may eventually weaken the inter-lamellar matrix and the strength of the annulus tissue as proteoglycans are a major structural component of the inter-lamellar matrix and serve to support cells. Yamazaki et al. (2002)

further examined the expressions of various genes in a rabbit model and found that exposure to vibration reduced the expression of the aggrecan gene, confirming the possibility of reduced proteoglycan synthesis with vibration.

2.4 Summary

While information pertaining to the tensile strength of the annulus is available, this information is lacking for individual lamella. In particular, no study to date has examined the response of simultaneous tensile strain in the parallel and perpendicular direction of a single lamella (Figure 2.5), which may actually be closer to how the tensile strains are applied *in vivo*. In addition, little attention has been given to the inter-lamellar matrix of the annulus, in particular its mechanical properties. Further, the effect of vibration on the tensile strength of individual lamella, the inter-lamellar matrix, or on any annulus tissue sample has not been investigated. This information is of importance given the strong association between exposure to vibration and material fatigue as well as between exposure to WBV and the occurrence of disc herniation.

Chapter 3

A comparison of uniaxial and biaxial mechanical properties of the annulus fibrosus: A porcine model

Chapter Synopsis

The annulus fibrosus experiences multi-direction tensile load *in vivo*. Yet, very few studies have examined this unique multi-directional loading scenario, and instead have simplified the mechanics by solely examining the material properties and responses of the annulus under uniaxial tensile loading. Therefore, our understanding of how this complex, multi-layered tissue responds to daily loading may be deficient. The objective of this study was to determine the mechanical properties of annular samples under uniaxial and biaxial tensile loading. Two-layer annulus tissue samples were isolated from porcine IVDs from four locations; anterior-superficial, anterior-deep, posterior/lateral-superficial and posterior/lateral-deep. These tissues were then subjected to three 20% strain conditions: uniaxial; constrained uniaxial; and biaxial strain. Uniaxial strain was applied in the circumferential direction (parallel to the end-plates), while biaxial strain was applied simultaneously in the circumferential and axial (in-line with the compressive axis) directions. Constrained uniaxial strain consisted of 20% strain in the circumferential direction while holding the tissue stationary in the axial direction. The maximal stress and elastic moduli determined from the biaxial tests were significantly higher than those observed during both the uniaxial tests (maximal stress 97.1% higher during biaxial tests; elastic moduli 117.9% higher during biaxial tests) and constrained uniaxial tests (maximal stress 46.8% higher during biaxial tests; elastic moduli 82.9% higher during biaxial tests). These findings suggest the annulus may be able to carry higher stresses *in vivo* when under multi-directional tension. These findings should be considered when

modeling the disc to more accurately determine the responses of the annulus under tension.

3.1 Introduction

The intervertebral disc is a multi-structural fibrocartilage tissue (Eyre & Muir, 1976; Hayes et al., 2001) designed to allow movement (Cassidy et al., 1989; Guerin & Elliott, 2006; Klein & Hukins, 1982a) and withstand compression in the spine (Cassidy et al., 1989; Guerin & Elliott, 2006; Holzapfel et al., 2005; Inerot & Axelsson, 1991; Inoue, 1981; Johnson et al., 1982) The material properties of the annulus fibrosus have been extensively researched; thick sections comprising of many layers of the annulus have been studied as well as single lamellae. Adams & Green (1993) and Green et al. (2003) commenced this area of research when they examined the tensile material properties of multi layered sections of the human annulus. Such sections of the annulus were further researched by Ebara et al. (1996) and Pezowicz et al. (2005). Additionally, Skaggs and colleagues in 1994 followed by Holzapfel and colleagues in 2005, furthered our understanding of the tensile material properties of the annulus by examining single isolated lamellae. One aspect common to all of these studies is the examination of only uniaxial tension of the annulus. However, a healthy intervertebral disc is subjected to multidirectional tensile loads *in vivo* (Edwards et al., 2001; McNally & Adams, 1992; Shirazi-Adl et al., 1984; Stokes, 1987; van Deursen et al, 2001) and needs to be examined as such. Many studies have examined the response to biaxial tension in collagenous tissues other than the annulus, including, but not limited to, mitral value tissue (Grashow et al., 2006; May-Newman & Yin, 1995), pericardium tissue (Lee et al., 1985; Sacks & Chuong, 1998), lung tissue (Debes & Fung, 1992), and arteries (Debes & Fung, 1995). Only two papers, to the author's knowledge, have examined the biaxial tensile response of annular tissue (Bass et al., 2004 (human); Bruehlmann et al., 2004 (bovine)).

Bruehlmann and colleagues (2004) examined the outer layers of the annulus under biaxial strain to determine the intercellular mechanics of the annulus. Bass et al. (2004) on the other hand, examined the uniaxial and biaxial mechanical properties of multi layer samples of the annulus and found that biaxial tension resulted in much higher stress values as compared to the uniaxial tensile tests. However, both Bass et al. (2004) and Bruehlmann et al. (2004) only examined the outer layers and did not examine any differences between anterior and posterior tissue of the annulus. Therefore, our knowledge of biaxial tensile loading across the entire annulus still remains largely unknown.

The purpose of the current study was therefore to examine the uniaxial and biaxial tensile response of two-layered annulus tissue samples obtained from four unique locations of the porcine intervertebral disc: the anterior superficial region, the anterior deep region, the posterior superficial region, and the posterior deep region of the annulus.

3.2 Methods

3.2.1 Tissue Preparation

Thirty-four annulus tissue samples were obtained from the anterior and posterior/lateral regions of 17 porcine functional spine units (FSU) (6 from the spinal level c3/c4, 11 from the spinal level c5/c6). These specimens were obtained fresh-frozen from a common source to control for variables such as age, mass, activity level, and diet. Previous research has confirmed anatomical, geometric, and functional similarities between the porcine cervical and human lumbar spine (Oxland et al., 1991; Yingling et

al., 1999). Frozen specimens were thawed at room temperature for 12-15 hours prior to dissection.

Each tissue sample from the anterior and posterior region consisted of two adjacent lamellae layers, and were obtained from the superficial and deep regions of the annulus, resulting in eight unique tissue sample extraction locations: four from c3/c4 FSUs and four from c5/c6 FSUs from the following locations: anterior superficial, anterior deep, posterior/lateral superficial, and posterior/lateral deep. The superficial tissue samples were obtained from the outer most layers (layers 1-4) while the deep tissue samples were obtained from more inner layers (layers 5-10); however these tissue samples are still somewhat superficial relative to the entire annulus size (approximately 15-25 layers). Deeper tissue samples could not be obtained as the increasing concentration of type II collagen fibres in the inner layers make dissecting distinct layers unfeasible.

Four tissue samples were tested for each extraction location, with the exception of the anterior superficial and anterior deep locations of c5/c6 intervertebral discs in which five tissues were tested, yielding 34 tissue samples. Each tissue sample was dissected from the FSU using a stereoscopic zoom microscope (Nikon SMZ 1000, Nikon Instruments Inc, Melville, NY, USA) to ensure that only two layers were included in the tissue sample. Tissues were oriented such that tension could be applied in the circumferential direction and in the axial direction (Figure 3.1). Axial tension is in the direction of spinal compression, while circumferential tension is perpendicular to the compressive axis. Each sample was approximately 4 mm by 4 mm with a mean thickness

of 0.36 mm. Saline (0.91% w/v of NaCl) was used to keep each tissue sample hydrated during preparation and testing.

3.2.2 Tissue Testing Protocol

Each tissue sample was mounted in a strain controlled biaxial material testing apparatus specifically designed for soft biomaterials (BioTester 5000, CellScale, Waterloo, ON, Canada) (Figures 3.2 and 3.3a), which uses a unique rake design to secure the tissue in place (Figure 3.3b). Once each tissue sample was secured in the testing apparatus, tension was applied to ensure that each tissue was taut at the start of each testing protocol, but was not under any excessive tension (no tension greater than 5 mN). Once the tissue sample was at this initial tensile state, the testing protocol commenced. Each tissue sample underwent three repeats of 10% strain over 10 seconds for preconditioning. Initial pilot work found that three repeats at this strain magnitude resulted in a repeatable stress-strain response of the tissue. Following preconditioning, the tissue then underwent 20% true strain over 20 seconds under the following conditions: uniaxial strain, biaxial strain, and constrained uniaxial strain. Uniaxial strain tests only had one set of rakes inserted in the tissue in the circumferential direction. Biaxial strain tests had sets of rakes inserted in both the circumferential and axial directions, each strained simultaneously to 20% true strain. Constrained uniaxial tests also had both sets of rakes inserted into the tissue, but strain was only applied in the circumferential direction, while the axial rakes remained stationary, thereby constraining any deformation or tissue narrowing in the axial direction. This test type was included to represent the constraining effect of the attachment to endplates of the vertebral bodies *in vivo*. The

three test types were presented quasi-randomly, such that the biaxial and constrained uniaxial tests had to be conducted in sequence to reduce the number of rake punctures to the tissue. However, the order in which these two tests were presented with respect to one another was randomized and the order of these two tests with respect to the uniaxial test was also randomized.

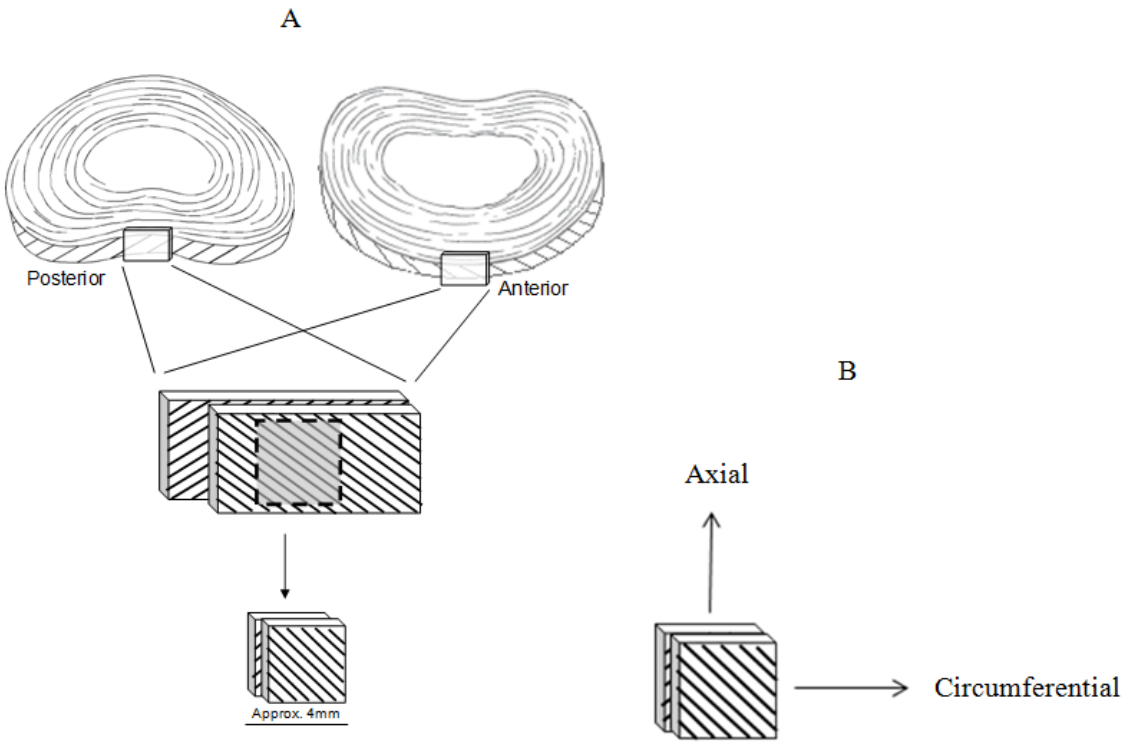

Figure 3.1: a) Depiction of dissection procedures to obtain annulus fibrosus tissue samples with only two adjacent lamellae. b) Direction of axial and circumferential tension. Axial tension is in the direction of spinal compression, while circumferential tension is perpendicular to the compressive axis.

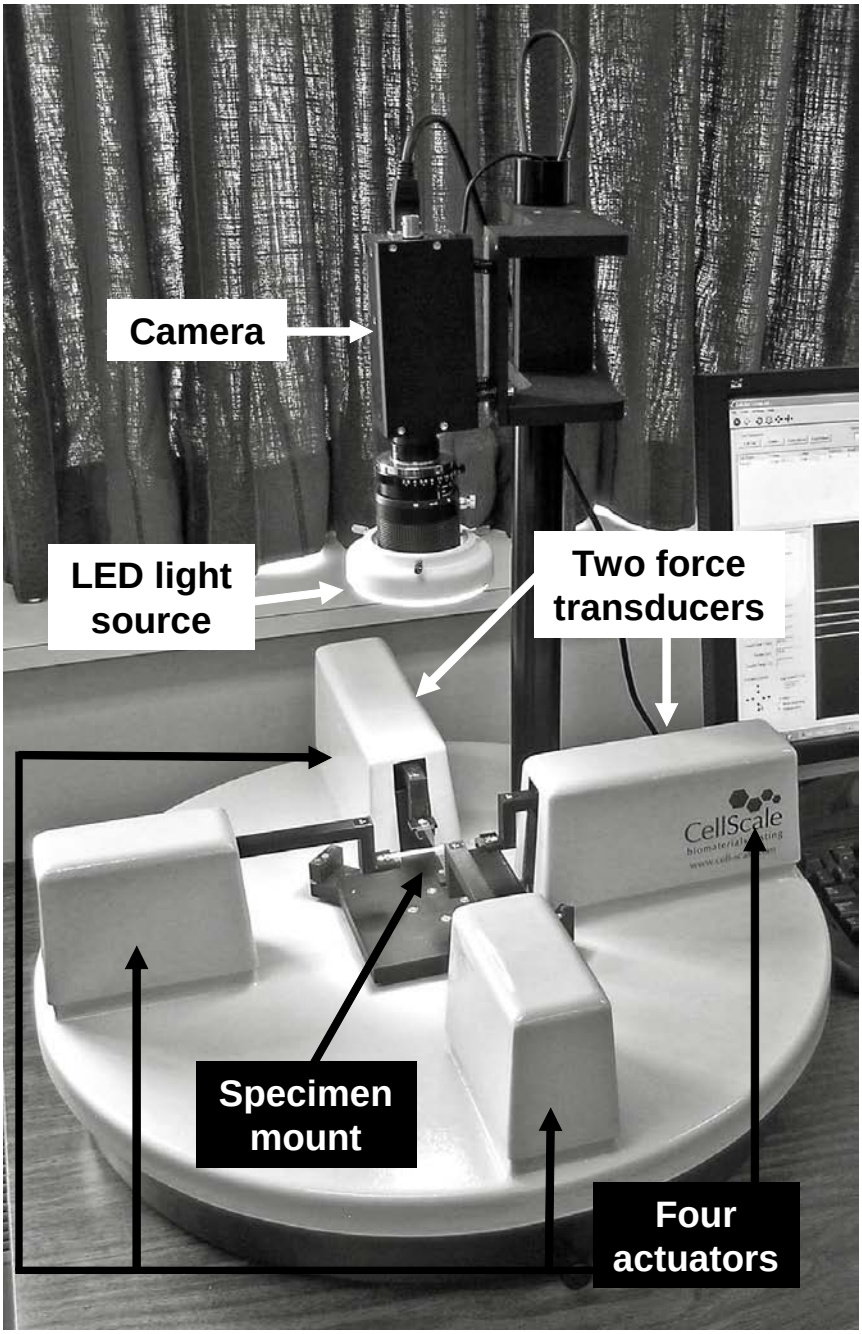

Figure 3.2: BioTester 5000 biaxial material testing apparatus.

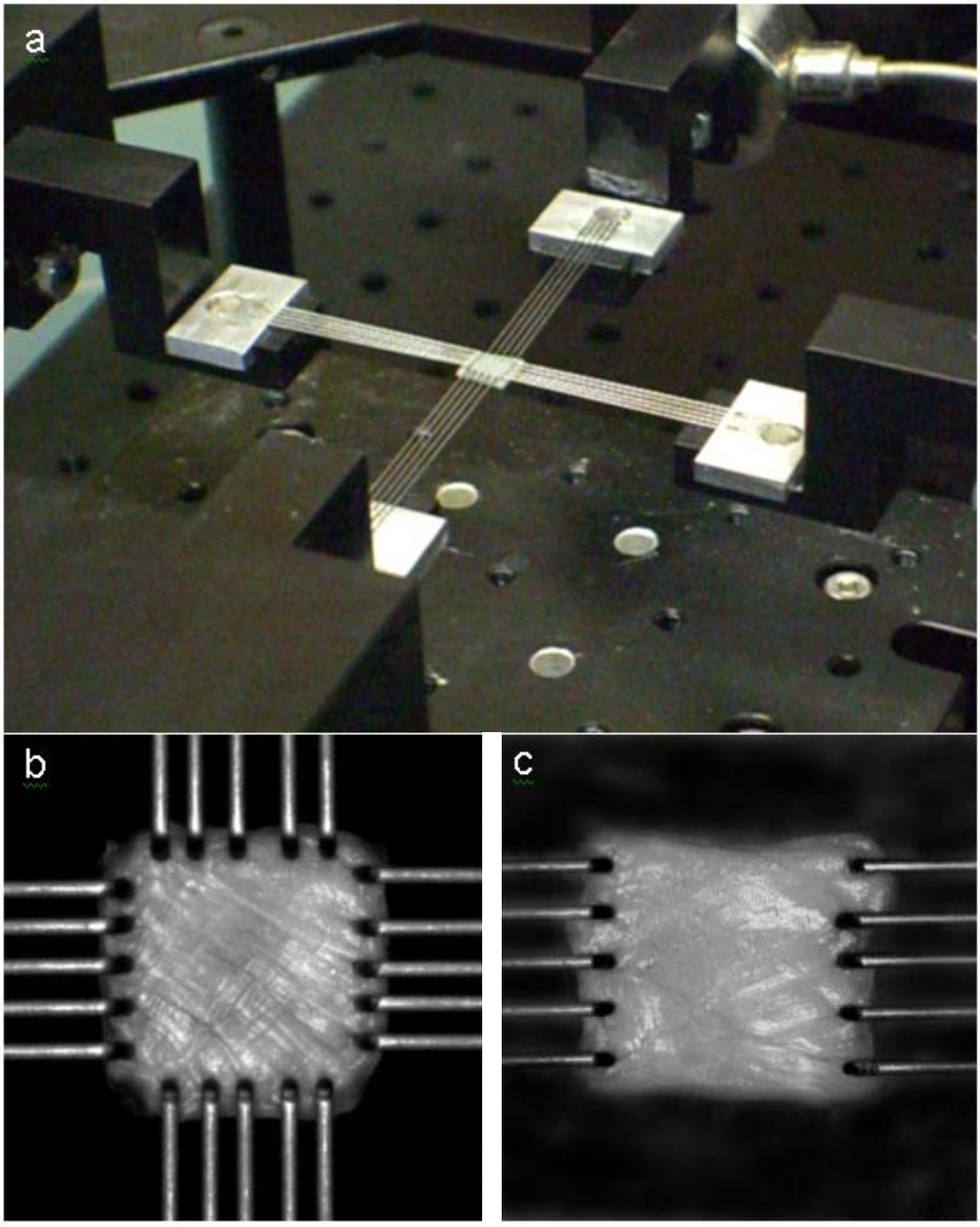

Figure 3.3: a) Biaxial tensile testing apparatus. Four rakes secure the tissue during biaxial tension, and two rakes are used for uniaxial tension. b) Biaxial configuration with four rakes inserted into the tissue, and c) Uniaxial configuration with two rakes inserted into the tissue.

3.2.3 Data Analysis

During each strain test, force and rake displacement information were recorded using the BioTester 5000 custom software, LabJoy 5.80 (Figure 3.4). Force was normalized using the cross sectional area of each tissue sample in order to determine stress magnitudes. Cross-sectional area was determined for each tissue sample using a digital caliper to determine tissue thickness, and tissue width was determined via calibrated image digitization (ImageJ version 1.42, public domain image software distributed by the National Institutes of Health) (Figure 3.5). Displacement was normalized in order to determine strain. Stress-strain profiles in the circumferential direction were then generated to determine the elastic modulus of the tissue for each of the three test types. Variables of interest were elastic modulus, maximal stress, and maximal strain.

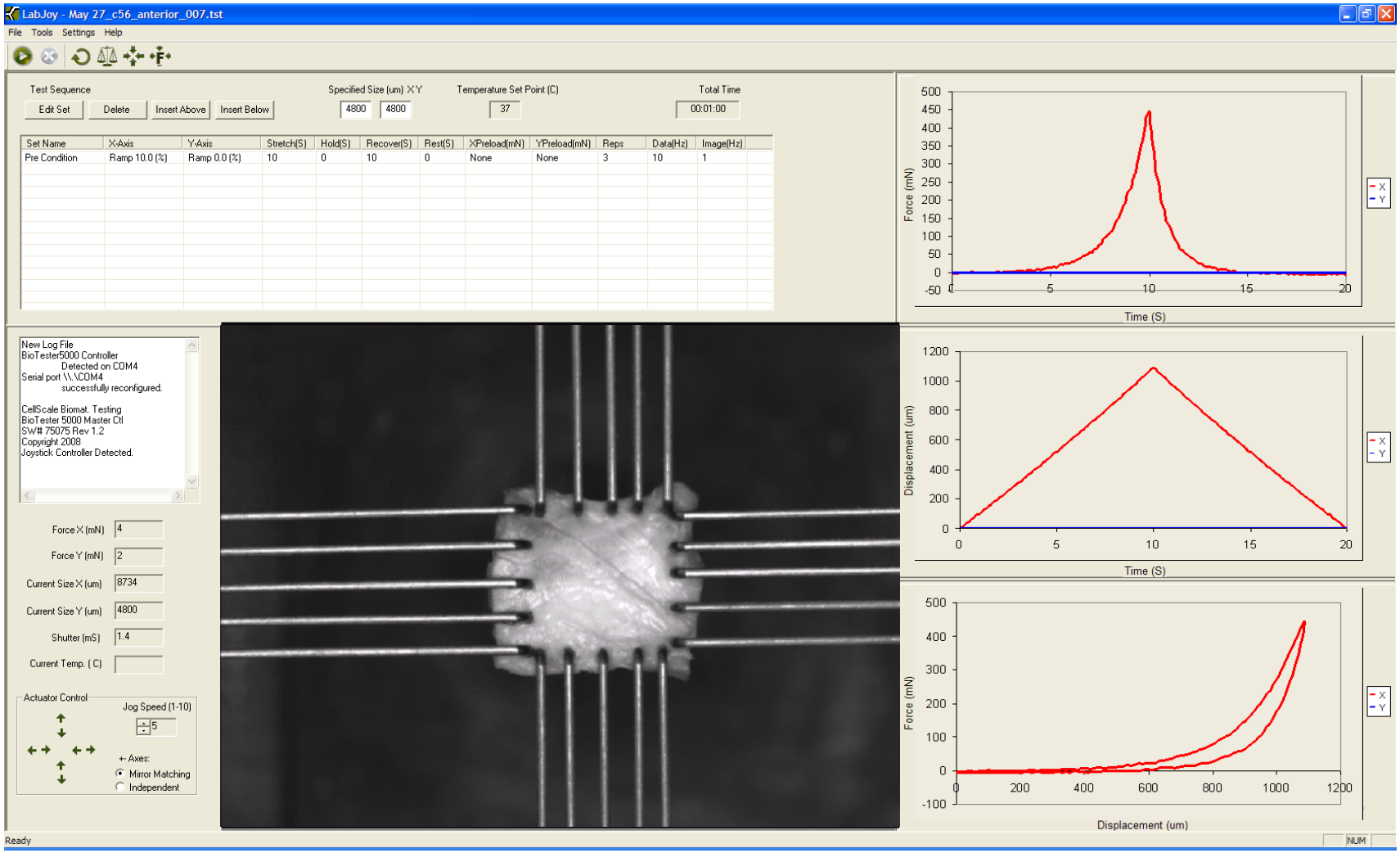

Figure 3.4: Graphical user interface for LabJoy 5.80. Graphs on right hand side display real-time force-time, displacement-time and force-displacement graphs.

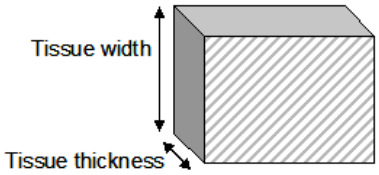

Figure 3.5: Cross-sectional area of each tissue sample was calculated in order to determine the stress in the circumferential direction. This was calculated by multiplying the tissue thickness (as measured with displacement measurement sensor) by the tissue width (as measured via calibrated image digitization).

3.2.4 Statistical Analysis

Cross-sectional area was determined for all tissue samples and a three-way mixed model general linear model (GLM) was conducted to determine the effect of tissue extraction location. The three factors, each describing the site of tissue extraction, were 1) FSU type (c3/c4 or c5/c6), 2) location in the intervertebral disc (anterior or posterior/lateral) and 3) depth of the tissue sample (superficial or deep). A second GLM was conducted on the tissue tests. Specifically, the elastic modulus and maximal stress during each tensile test (dependent variables) were assessed using a four-way GLM in order to determine the effect of the independent variable test type (repeated measure: uniaxial, constrained uniaxial, or biaxial) along with the effect of the three levels of tissue extraction site (independent variables) stated above in the three-way GLM. An alpha level of 0.05 was used to determine significance for all statistical tests. Tukey post-hoc tests were further conducted on the test type (uniaxial, biaxial, constrained uniaxial) factor.

3.3 Results

3.3.1 Tissue Characteristics

The average cross-sectional area of the 34 tissue samples was 1.59 mm^2 (S.D. 0.82 mm^2). No significant difference in cross-sectional area was observed between tissue samples obtained from c3/c4 intervertebral discs as compared to c5/c6 intervertebral discs ($p = 0.596$, statistical power = 18.2%), nor between superficial and deep tissue samples ($p = 0.334$, statistical power = 23.8%). A significant difference between the cross-sectional area of tissue samples obtained from the anterior annulus as compared to the posterior annulus was observed ($p = 0.041$, Cohen's d effect size = 0.84) with anterior tissues having greater cross-sectional areas than posterior tissue samples (1.89 mm^2 (S.D. 0.96 mm^2), 1.26 mm^2 (S.D. 0.46 mm^2), respectively).

3.3.2 Tensile Tests

All tissue samples demonstrated a non-linear stress-strain profile when strained from 0 to 20% true strain, resulting in an average engineering strain of 22.78% (S.D. 0.21%) (Figure 3.6). However, once the tissue was strained beyond its toe region, all tissue samples demonstrated a linear elastic region, and when fit to a linear curve, had a mean R^2 value of 0.99 (S.D. 0.01). The linear portion of the curve began at a mean engineering strain of 18.72% (S.D. 1.96%) and was not found to be significantly different across test type ($p = 0.270$, statistical power = 37.2%), FSU type ($p = 0.117$, statistical power = 31.2%), or location on the intervertebral disc (anterior or posterior, $p = 0.191$, statistical power = 33.6%), but was significantly different between tissue sample depth ($p = 0.023$, Cohen's d effect size = 0.60). The linear portion began at an average strain of

18.14% (S.D. 1.33%) for the superficial tissue samples, and an average strain of 19.28% (S.D. 2.33%) for the deep tissue samples.

The slope of the linear portion of the stress-strain curve, or the elastic modulus, was found to be significantly affected by the tensile test type ($p = 0.0004$, Cohen's d effect size = 0.79). Post-hoc tests revealed significant differences between the moduli calculated during the biaxial tests and the uniaxial tests, and between the biaxial and constrained uniaxial tests. The mean elastic modulus during the biaxial tests was 117.9% higher than that during the uniaxial tests and 82.9% higher that during the constrained uniaxial tests. However, no significant differences were observed between the moduli of the tissues during uniaxial tension and constrained uniaxial tension. A similar finding was observed for maximal stress at 20% true strain between the three tensile test types ($p = 0.002$, Cohen's d effect size = 0.70). Post-hoc tests revealed significant differences between the maximal stress magnitude reached during the biaxial tests and the uniaxial tests, and between the biaxial and constrained uniaxial tests. The mean maximal stress reached during the biaxial tests was 97.1% higher than that during the uniaxial tests and 46.8% higher that during the constrained uniaxial tests. However, no significant differences were observed between the maximal stress reached by the tissues during uniaxial tension and constrained uniaxial tension. Further, no statistically significant differences were observed in the maximal stress reached or the elastic moduli between the four tissue sample locations. Tables 3.1 and 3.2 summarize the calculated elastic moduli, and the maximal stress for each tissue location as well as for each tensile test. No significant interactions between the four factors were observed.

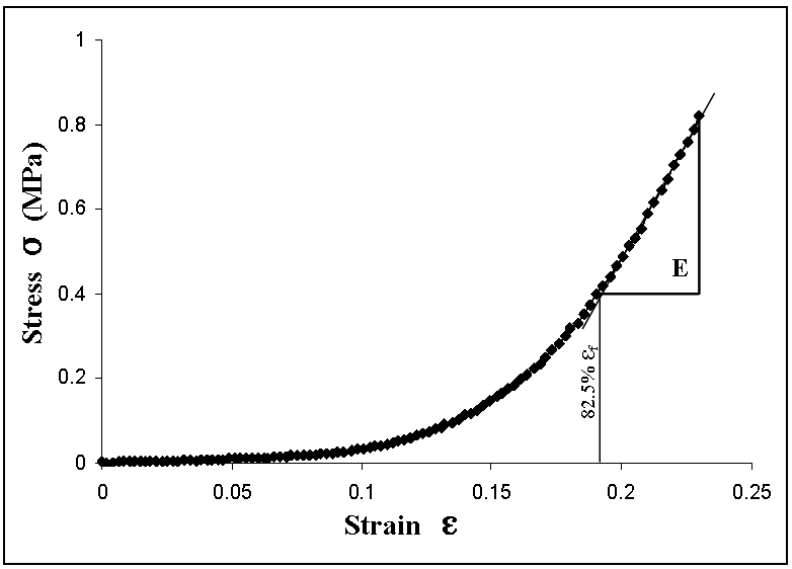

Figure 3.6: Representative stress-strain curve in the circumferential direction. Tissues were strained to 20% true strain, or 23% engineering strain. The elastic modulus (E) was determined by taking the slope of the linear portion of the stress-strain curve. This linear portion, on average, started at 82.5% of the final strain magnitude (γf).

Table 3.1: Mean and standard deviation values for the elastic modulus and maximum stress reached at 20% true strain for all tissues, as well as for each tissue location.

	Elastic Modulus (MPa)	Maximal Stress (MPa)
All Tissues (n = 34)	4.66 (S.D. 4.68)	0.50 (S.D. 0.59)
Anterior Superficial (n = 9)	5.17 (S.D. 5.00)	0.58 (S.D. 0.63)
Anterior Deep (n = 9)	4.84 (S.D. 5.05)	0.62 (S.D. 0.81)
Posterior Superficial (n = 8)	3.97 (S.D. 5.21)	0.37 (S.D. 0.42)
Posterior Deep (n = 8)	4.53 (S.D. 3.39)	0.40 (S.D. 0.29)

Table 3.2: Mean and standard deviation values for the elastic modulus and maximum stress reached at 20% uniaxial strain, 20% constrained uniaxial strain, and 20% biaxial strain. Values with asterisk are significantly different from values without asterisk.

	Elastic Modulus (MPa)		Maximal Stress (MPa)	
Uniaxial	3.19 (S.D. 2.51)		0.35 (S.D. 0.35)	
Constrained Uniaxial	3.80 (S.D. 3.72)		0.47 (S.D. 0.73)	
Biaxial	6.95 (S.D. 6.20)	*	0.69 (S.D. 0.59)	*

3.4 Discussion

The current study examined the annular mechanical properties and tissue responses to uniaxial and biaxial tensile strain. Two major observations were made: first, it was observed that during the biaxial tensile tests, the maximal stress reached and the mean elastic modulus were higher than that observed during the uniaxial tensile tests (both unconstrained and constrained). Second, four unique locations of the annulus were examined, and it was observed that the maximal stress reached during the tensile strain and the elastic moduli during these tests were not significantly different between the four locations.

The annulus is a uniquely designed composite structure comprised of layers of obliquely aligned collagen fibres. The outer annulus, in particular, is comprised mostly of type I collagen fibres (Berthet-Colominas et al., 1982; Bruehlmann et al., 2002; Errington et al., 1998; Eyre & Muir, 1974; Eyre & Muir, 1976; Hayes et al., 2001). These type I fibres are more akin to those found in tendon or ligaments (Bruehlmann et al., 2002; Errington et al., 1998; Hayes et al., 2001; Lo et al., 2002; McNeily et al., 1996; Pritchard et al., 2002) and are considered to resist tensile forces (Hayes et al., 2001). Further, in a healthy intervertebral disc, the tension experienced by the annulus is multidirectional in nature (Edwards et al., 2001; McNally & Adams, 1992; Shirazi-Adl et al., 1984; Stokes, 1987; van Deursen et al., 2001). Despite this complex physiological loading, only two studies, to the author's knowledge, have examined the multidirectional tensile loading in human annulus tissue (Bass et al., 2004) as well as bovine annulus tissue (Bruehlmann et al., 2004). The current study has further examined the altered mechanical properties, including stress response and tissue elastic modulus, at four unique locations within the

annulus and as a result of uniaxial, biaxial, and constrained uniaxial tension, which replicated the constraint of the endplates. This endplate constraint was the opposite of that simulated by Bass and colleagues (2004) who examined constrained uniaxial tension by holding the circumferential direction stationary, while simultaneously straining in the axial direction.

The current study documented significant increases in the circumferential stress reached at 20% true strain (equivalent to approximately 23% engineering strain) during biaxial tension, as compared to uniaxial and constrained uniaxial tension. This is consistent with the findings of Bass et al. (2004), who found that when annulus samples (which were comprised of a number of lamellae) were strained to 7% axial strain required 0.16MPa axial stress to reach this strain under uniaxial tension, but 0.56MPa when under biaxial tension. The current study observed peak stress values of 0.35 MPa under uniaxial tension and 0.69 MPa under biaxial tension. Further, significantly higher elastic modulus values were quantified in the circumferential direction during biaxial tension as compared to both the uniaxial and constrained uniaxial tension. Interesting, however, was that the stress at 20% true strain and the elastic modulus during uniaxial and constrained uniaxial tension were not significantly different from one another. This was a surprising observation, as the force measured in the axial direction during the constrained uniaxial tension was thought to be large enough to significantly increase the force required to strain the circumferential axis to the 20% strain. However, the increase in stiffness that one would expect as a result of the constraining effect of the axial rakes may have been nullified by the inability for the fibres to realign to the same extent as what was observed during the unconstrained uniaxial tests. Such substantial realignment increases the

stiffness of the tissue, as it has been shown that annulus tissue is far stiffer inline with the collagen fibres as compared to perpendicular to them (Holzapfel et al., 2005).

The annulus is loaded *in vivo* under multidirectional tension, and this study confirms the need to examine the tissue response to such loading as it differs greatly from uniaxial tension, confirming the findings of Bass and colleagues (2004). In addition, this study further demonstrates that uniaxial tension may closely mimic the state of the annulus during certain situations where the tension applied in one axis is minimal, similar to that created in the constrained uniaxial tensile state.

The current study also documented cross-sectional area, elastic moduli, and stress values from four locations of the annulus during uniaxial and biaxial tension and found no differences in the properties at these locations. Tissue samples isolated from the posterior/lateral annulus, regardless of tissue extraction depth (superficial versus deep), were found to be significantly thinner than those from the anterior region, similar to that observed by Holzapfel et al. (2005), in human annular tissue. Holzapel et al. (2005) as well as Skaggs et al. (1994) did, however, find differences in the elastic moduli of tissues extracted from different locations, specifically lower moduli in tissues obtained from the deep layers of the annulus. These inconsistent findings may be a result of the size of tissue tested. Both Holzapfel et al. (2005) and Skaggs et al. (1994) examined single layers of the annulus, while the current study examined bi-layered samples, which likely possess different mechanical properties. It is plausible that when the annulus is examined as a multilayer structure, any differences between location are no longer evident. The tissue as a composite structure rather than a single isolated layer, may not actually differ with respect to its mechanical properties at different depths or at different regions of the disc

and thus be non-homogeneous. It is important to note that the current study only examined tissue samples obtained from the outer half of the annulus, while Holzapfel et al. (2005) and Skaggs et al. (1994) may have been able to isolate even deeper layers than the current study, which could possess different mechanical properties than the outer most layers.

The current study also observed larger toe regions in the stress-strain curves of tissues extracted from the deep layers of the annulus as compared to the superficial layers. This may be related to the concentration of type II collagen fibres found in the deeper layers of the annulus as compared to the superficial layers (Berthet-Colominas et al., 1982; Cassidy et al., 1989; Eyre & Muir, 1976), and the length of the toe region of the stress-strain curve may be affected by uncrimping of both type I and type II collagen fibres.

The tissues examined in the current study were obtained from porcine cervical intervertebral discs and may be considered a limitation. However, the porcine cervical spine has been shown to be anatomically and functionally similar to the human lumbar spine, with the advantage of controlling for factors that are difficult, if not impossible, to control for in humans. The current study examined tissues from differing depths; however all tissue samples were still only obtained from predominantly the outer half of the annulus, and therefore this study cannot comment on the mechanical properties or tissue responses to uniaxial or biaxial strain in the deepest most layers of the annulus. Another limitation of the current study was the inability to quantify the failure stress or the elastic modulus just prior to failure, due to the repeated measures design of the study. Therefore, mechanical properties of the annulus tissue were only determined at true strain

magnitudes of 20%. Last, the order of the three tensile tests was not completely randomized in an attempt to minimize the number of times the tissue was pierced by the rakes; however, every attempt to randomize other components of the collection was made to reduce any effect of test order.

3.5 Conclusion

The annulus is naturally loaded under multidirectional strain *in vivo*, yet limited research has investigated the response of this tissue to such loading. The current study showed that with biaxial tension applied to bi-layer tissue samples, the annulus displays a stiffer response and is subjected to higher stresses at a given strain as compared to uniaxial and constrained uniaxial tension. However, the mechanical properties do not differ between uniaxial and constrained uniaxial tension, suggesting that for certain *in vivo* situations where tension in one axis may be minimal, the response of the annulus may mimic that observed during purely unconstrained uniaxial tension. Further, when modeling the mechanical responses of the disc, it is important to take into consideration the substantial differences found in this study between uniaxial and biaxial tensile loading of the annulus, as dramatically different loading scenarios could result depending on how the strain patterns are modelled and whether uniaxial or biaxial mechanical properties are utilized. This study also examined the material properties and annulus response to uniaxial and biaxial tensile strain between four unique locations of the annulus and found no significant differences between the locations. This suggests that when the annulus is examined as a bi-layered structure, its mechanical properties may not differ substantially at different locations of the annulus.

Chapter 4

An examination of the effect of strain rate on the tensile mechanical properties of the annulus fibrosus

Chapter Synopsis

Disc herniation is considered a cumulative injury, in that repetitive stress on the posterior annulus can result in the nucleus pulposus penetrating the annulus fibrosus and eventually extruding posteriorly into the spinal canal. However, the annulus is viscoelastic in nature, and therefore could express different mechanical responses to applied strain at varying rates. Other viscoelastic tissues, including tendons and ligaments, have shown altered mechanical responses to different rates of applied strain, but the response of the annulus to varying rates of strain is largely unknown. The current study examined the mechanical properties of 20 two-layer samples of annulus tissue at three distinct rates of applied 20% biaxial strain (20% strain over 20 seconds (slow), over 10 seconds (medium), and over 5 seconds (fast)) as these three rates are considered physiologically relevant in the annulus fibrosus to terms of leading to disc herniation. No differences in the stiffness or maximal stress in each of the two directions of applied strain were observed between the three strain rates. Specifically, the average (S.D.) moduli calculated at the fast, medium, and slow rates, respectively in the axial direction were 7.42 MPa (6.06), 7.77 MPa (6.61), and 7.63 MPa (6.67) and in the circumferential direction 8.22 MPa (8.4), 8.63 MPa (9.00), and 8.49 MPa (8.69). The maximal stresses reached during the slow, medium, and fast rates, respectively in the axial direction were 0.39 MPa (0.35), 0.40 MPa (0.36), and 0.40 MPa (0.26) and in the circumferential direction 0.43 MPa (0.46), 0.44 MPa (0.46), and 0.45 MPa (0.47). These results indicate that at submaximal strain magnitudes over a range of physiological rates, the annulus is strain rate independent.

4.1 Introduction

The annulus fibrosus is a collagenous tissue that undergoes multi-directional tensile strain during many scenarios in vivo (Edwards et al., 2001; McNally & Adams, 1992; Shirazi-Adl et al., 1984; Stokes, 1987; van Deursen et al, 2001), and is commonly injured during the disc herniation process. Disc herniation has been shown to occur in a porcine model as a result of repetitive bending of the intervertebral joints combined with moderate compression (Callaghan & McGill, 2001), and is therefore considered a cumulative or repetitive injury to the annulus, and it is hypothesized that herniation progresses through clefts formed in the annulus (Pezowicz et al., 2005; Tampier et al., 2007) as a result of repeated tensile strains on the lamellae. The annulus does not commonly become injured as a result of high loading rates; in these cases it is the vertebral bodies that are most at risk (Brinckmann et al., 1989; Gunning et al., 2001; Lundin et al., 1998; Yingling et al., 1997).

Whether disc herniation is initiated or how quickly it progresses is related to the tensile strength of each layer of the annulus, with weaker layers being penetrated by the nucleus pulposus more quickly and easily. Understanding the properties of the annulus, including its tensile strength, is necessary to determine how herniation will commence and propagate as a result of a given exposure. The notion of strain rate dependence in soft tissues is not new. The viscoelasticity of soft tissues such as tendons and ligaments has been extensively documented for decades through strain rate tests as well as through creep, stress-relaxation, and hysteresis tests (for example Solomonow, 2004; Woo et al., 2000). While there is no debate as to the viscoelastic nature of these tissues, the effect of physiological strain rates is not clear. While many studies have documented the responses

of tendon, ligaments, and other soft tissues, at a wide range of strain rates, no clear conclusion exists pertaining to the dependence of mechanical response of these tissue to changing strain rates. In general, it is widely accepted that bone is strain rate dependent (Carter & Caler, 1985; Keaveny & Hayes, 1993), but more controversy exists with soft tissues.

The mechanical properties of soft tissues such as tendons (Haut, 1983 (rat); Wren et al., 2001 (human); Lynch et al., 2003 (ovine)) and ligaments (Crowninshield and Pope, 1976 (rat); Noyes et al., 1974 (monkey); Woo et al., 1990 (rabbit); Yamamoto & Hayashi, 1998 (rabbit)) have been found to be affected by the rate at which they are strained, such that higher peak stresses result for a given strain at faster applied strain rates. In terms of tissue stiffness, the modulus values of tendons documented by Lynch et al. (2003), Wren et al. (2001), Haut (1983), and Yamamoto and Hayashi (1998) were all unaffected by strain rate. However, others, who have examined ligaments, have observed increases in tissue modulus values with higher strain rates (Danto & Woo, 1993 (rabbit); Haut & Little, 1969 (canine); Ticker et al., 1996 (human)). Contrary to these findings were observed by Crisco et al. (2002) (rabbit) and Blevins et al. (1994) (human) who both found strain-rate independence in ligaments in terms of peak stress and modulus values. However, it is unknown as to whether the annulus responds in a similar fashion. If the annulus is found to be affected by the rate of strain, and in particular, reaches higher stresses at higher rates of strain, this could affect the initiation and propagation of disc herniation and be a critical factor in modeling the pathway of this injury.

While soft tissues such as ligaments and tendons have been extensively researched in terms of strain rate dependence, the annulus has not been as thoroughly

examined. Karsa et al. (2004) examined the effect of various strain rates (ranging from 0.07%/sec to 333%/sec) on ovine annular tissue that was still attached to the vertebral bodies, and found that, when tensile strained to failure, the modulus of the annulus-vertebral body unit was higher during the fast strain rate as compared to the low strain rate, but no differences in peak stress were observed. In another study, the inter-lamellar matrix (connective tissue between each layer of the annulus) mechanical properties were examined at various rates of strain ranging from 0.005%/sec to 50%/sec, yet no differences were observed in modulus or maximal stress reached (Fujita et al., 2007 (human)). Understanding how the mechanical properties of the annulus of the intervertebral disc change as a result of varying strain rate has important implications in terms of injury potential. If the responses of the annulus tissues are strain-rate dependent, both the initiation and progression of injury such as herniation would also be dependent of the rate of strain applied to the annulus.

The purpose of this study was to determine if the tensile mechanical properties of the annulus are strain rate dependent, within a range of rates that are physiologically relevant for producing chronic herniation-type damage, at sub-acute failure strains.

4.2 Methods

4.2.1 Tissue Dissection and Preparation

Twenty annular tissue samples were dissected and prepared from five intervertebral discs. These intervertebral discs were obtained from five porcine spines, at the cervical level of c5/c6, which had been previously frozen and thawed for 12-15 hours prior to dissection. Porcine cervical spines have been shown to be both functionally and

anatomically similar to human lumbar spines (Oxland et al., 1991; Yingling et al., 1999). Using an animal model rather than human cadaveric spines permits control over factors such as age, diet, activity level, and mass. These 20 tissue samples were obtained from four regions of the annulus (five samples from each region) including the superficial layers of the anterior region, the deep layers of the anterior region, the superficial layers of the posterior/lateral region, and the deep layers of the posterior/lateral region. The superficial region was that of the outer most layers (layers 1-4) while the deep region was that of the more inner layers (layers 5-10); however these deep tissue samples are still somewhat superficial relative to the entire annulus size (approximately 15-25 layers). Deeper tissue samples could not be obtained as the increasing concentration of type II collagen fibres in the inner layers make dissecting distinct layers unfeasible.

Each tissue sample was dissected from the annulus using a light microscope. Tissue samples from each region of the annulus were comprised of two adjacent lamellae. Each tissue sample was approximately 4mm by 4mm with an average thickness of 0.28mm (S.D. 0.09mm). Tissue samples were trimmed to be approximately square in shape similar to that in Chapter 3 (Figure 3.1a) with two sides parallel to the endplates (circumferential direction) and two sides parallel to the compressive axis of the intervertebral disc (axial direction) from which the tissue sample was dissected (Figure 3.1b).

4.2.2 Tissue Mounting and Testing

Each tissue was mounted in the BioTester 5000 (Cellscale, Waterloo, ON, Canada); a biaxial tensile material testing apparatus specially designed to test soft

biomaterials (Figure 3.2 in Chapter 3). This apparatus secures the tissues by means of a unique system that utilizes rakes, which pierce the tissue. Each tissue sample was secured using four rakes (Figure 4.1a) in order to be able to apply biaxial tension. Biaxial tension was examined rather than uniaxial tension as the annulus tissue experiences multi-directional tension *in vivo*. Tension was applied in the direction of the axial compressive axis (termed axial) as well as the circumferential axis (perpendicular to the compressive axis) (Figure 4.1b). Once secured, the tissue was strained such that the tissue was taut, but without applying more than 5 mN of tension. This starting tension was considered the point of zero strain. A preconditioning test consisting of three repeats of 10% strain at a rate of 1%/sec was conducted prior to data collection.

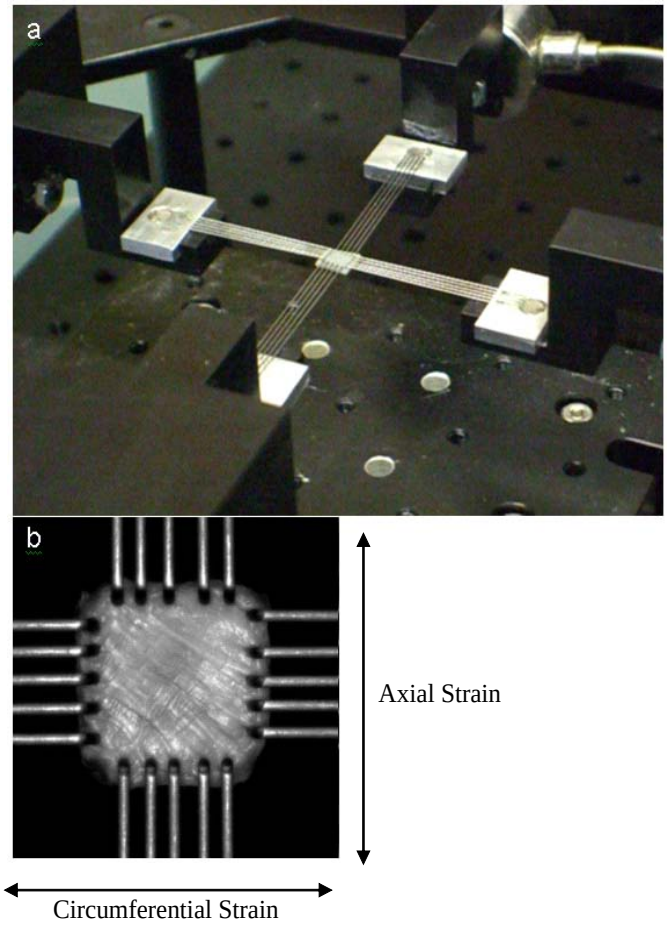

Figure 4.1: a) Biaxial testing apparatus set-up. Four rakes that are in series with actuators secure the tissue in place, which apply the strain. b) Image of a two-layered sample of the annulus fibrosus mounted in the testing apparatus. Strain was applied in the axial and circumferential directions.

Each tissue then underwent a series of twelve 20% biaxial strain tests. Twenty percent strain was chosen as a physiological magnitude as it would be less than the average maximum strain the posterior annulus would experience during 15° joint flexion (White & Panjabi, 1990); the maximum each individual intervertebral joint generally is capable of rotating. Three different strain rates were tested: 20% strain/20 seconds (slow: 1%/sec), 20% strain/10 second (medium: 2%/sec), and 20% strain/5 seconds (fast: 4%/sec); each rate was tested four times per tissue. The first four tests were presented with zero rest in between, followed by a 5 second static rest period at zero strain, followed by another four consecutive tests, then another 5 second static rest period, and a final set of four consecutive tests (Figure 4.2). The force reached during each test that immediately followed a period of rest was generally higher than the other three tests within a group of four, and were therefore removed from analysis, yielding nine tests for analysis. The strain rate for each of these nine tests were quasi-randomized in order to have three repeats for each of the three strain rates; slow, medium, and fast (1%/sec, 2%/sec, 4%/sec, respectively).

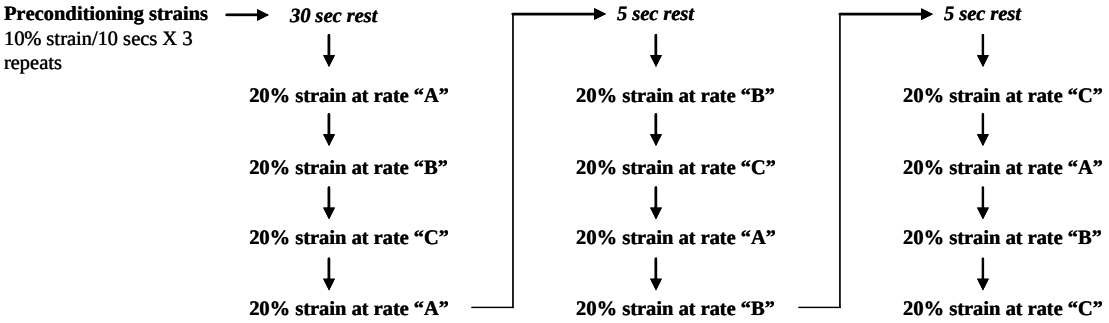

Figure 4.2: Data collection time line. Strain rates "A", "B", and "C" represent the three strain rates examined. The particular strain rate which was represented by each of the letters "A", "B", and "C" was randomized across the 20 tissues tested. The first 20% strain test within each block was excluded from analysis to yield three repeats at each of the three strain rates examined.

4.2.3 Data Analysis

Force and rake displacement in the axial and circumferential directions were sampled at 10 Hz during each of the strain tests using the BioTester 5000 custom software, LabJoy 5.80 (Cellscale, Waterloo, ON, Canada). Stress was calculated from the force outputs by dividing by the cross-sectional area of the tissue samples, and strain was calculated by normalizing the displacement of the rakes in each of the axial and circumferential directions. These calculations yielded stress-strain profiles in the axial direction, as well as in the circumferential direction. The elastic modulus was determined from the linear portion to the right of the toe region of each stress-strain profile for each test at each strain rate. Variables of interest were maximal stress in both the axial and circumferential directions and the elastic modulus in both directions for each of the three strain rates.

4.2.4 Statistical Analysis

A four-way repeated measures mixed model general linear model (GLM) was conducted in order to determine the effect of strain rate (repeated measure three levels; slow, medium, fast), tissue location (two levels; anterior, posterior), tissue depth (two levels; superficial, deep), and direction of applied strain (two levels; axial, circumferential) on maximal stress and elastic modulus in both the axial and circumferential direction. An alpha level of 0.05 was set for all statistical tests, and Tukey post hoc tests were further conducted on the independent variable, strain rate.

4.3 Results

Three strain rates were examined; fast (4%/sec), medium (2%/sec), and slow (1%/sec) and it was found that these strain rates did not significantly affect the maximal stress (at 20% strain), nor did they affect the elastic modulus. This was observed in both the axial and circumferential direction. The mean (standard deviation) maximal stress reached during the fast, medium, and slow strain rates in the circumferential direction were 0.45 MPa (0.47), 0.44 MPa (0.46), and 0.43 MPa (0.46), respectively ($p = 0.16$, statistical power = 6.6%). In the axial direction, mean (standard deviation) maximal stress reached during the fast, medium, and slow strain rates were 0.40 MPa (0.36), 0.40 MPa (0.36), and 0.39 MPa (0.35), respectively ($p = 0.26$, statistical power = 6.0%) (Figure 4.3). The mean (standard deviation) elastic moduli calculated during the fast, medium, and slow strain rates in the circumferential direction were 8.22 MPa (8.4), 8.63 MPa (9.00), and 8.49 MPa (8.69), respectively ($p = 0.17$, statistical power = 6.7%). In the axial direction, mean (standard deviation) elastic moduli during the fast, medium, and slow strain rates were 7.42 MPa (6.06), 7.77 MPa (6.61), and 7.63 MPa (6.67), respectively ($p = 0.21$, statistical power = 7.1%) (Figure 4.4). These peak stress and moduli values are fairly comparable to those documented in Chapter 3 (for biaxial tests: mean peak stress of 6.95 (S.D. 6.20) MPa and mean modulus of 0.45 (S.D. 0.59) MPa).

In terms of the comparison between the maximal stress and elastic moduli in the circumferential versus axial direction, no significant differences were observed. The mean (standard deviation) maximal stress collapsed across all strain rates in the circumferential direction was 0.44 MPa (0.46) and 0.39 MPa (0.36) in the axial direction ($p = 0.73$, statistical power = 10.3%). In terms of the calculated elastic modulus, the mean

(standard deviation) elastic modulus collapsed across all strain rates in the circumferential direction was 8.45 MPa (8.65) and 7.61 MPa (6.42) in the axial direction ($p = 0.73$, statistical power = 9.7%). A significant three-way interaction was observed for the elastic modulus variable ($p = 0.003$), between the factors strain rate, tissue location (anterior versus posterior) and direction of applied strain (axial versus circumferential). Moduli values tended to be lower in tissues harvested from the posterior annulus as compared to the anterior, and this difference was more predominant in the circumferential direction than the axial direction. In terms of strain rate, the difference in the circumferential moduli values between anterior and posterior tissues was fairly consistent across the three rates of strain, but in the axial direction, this difference was much larger in the fast strain rate tests.

It is important to note that the large standard deviations presented in Figures 4.3 and 4.5 are collapsed across all tissue samples, and could be misinterpreted as high variability impeding the ability to detect any significant difference between the three strain rates. However, the within specimen variability, and thus the actual differences observed between the three strain rates within a specimen, was much smaller. The average standard deviation between the three strain rates within a specimen was 0.08 MPa for the maximal stress in the circumferential direction (as compared to 0.46 MPa across all specimens); 0.06 MPa for the maximal stress in the axial direction (as compared to 0.36 MPa across all specimens); 1.02 MPa for the elastic modulus in the circumferential direction (as compared to 8.65MPa across all specimens); and 1.11 MPa for the elastic modulus in the axial direction (as compared to 6.42 MPa across all

specimens). Figure 4.5 illustrates the substantial similarities observed in the stress-strain profiles between the three strain rates.

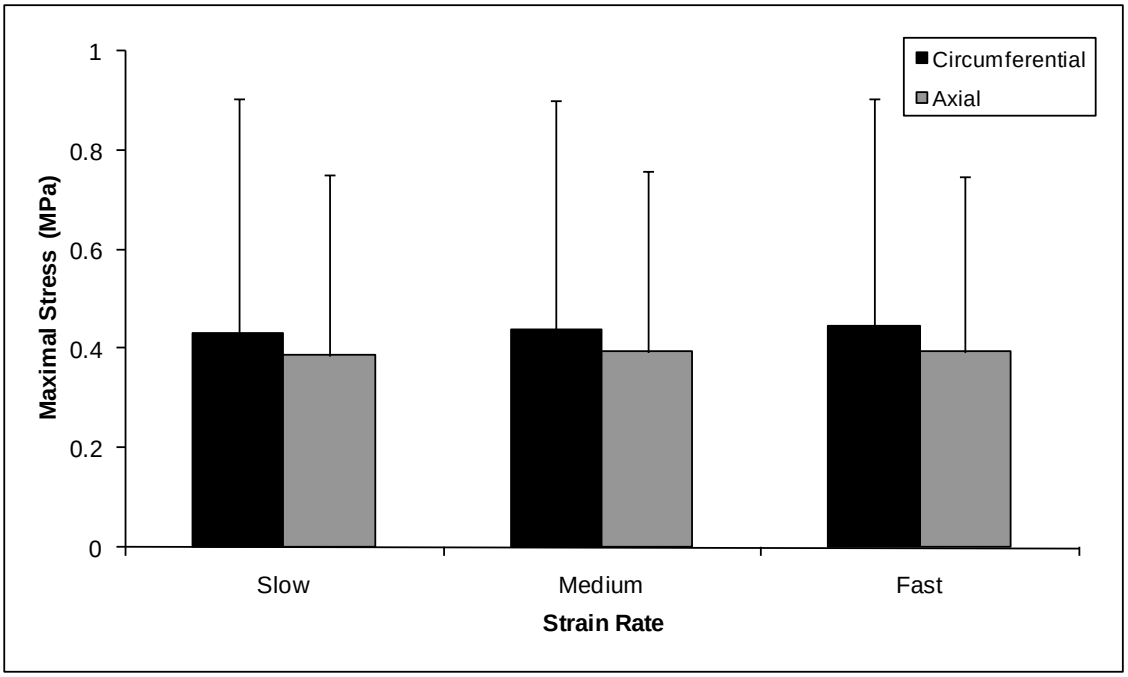

Figure 4.3: Mean maximal stress collapsed across all tissue samples for slow (20% strain/20 sec), medium (20% strain/10 sec) and fast (20% strain/5 sec) strain rates in the axial and circumferential directions. Error bars denote 1 standard deviation.

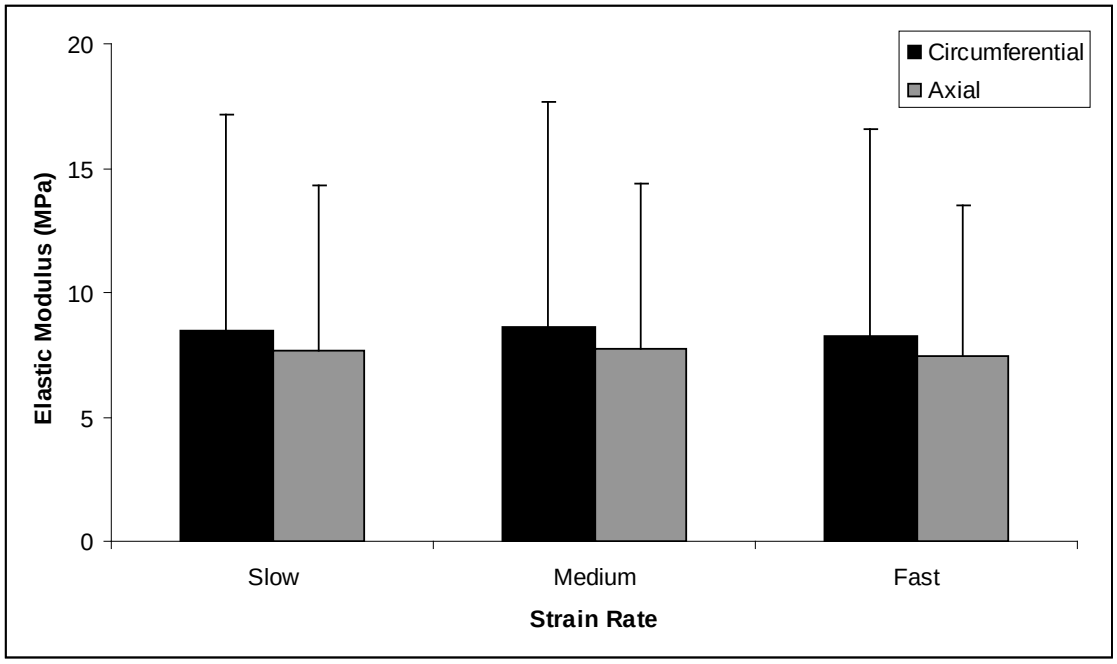

Figure 4.4: Mean elastic moduli collapsed across all tissue samples for slow (20% strain/20 sec), medium (20% strain/10 sec) and fast (20% strain/5 sec) strain rates in the axial and circumferential directions. Error bars denote 1 standard deviation.

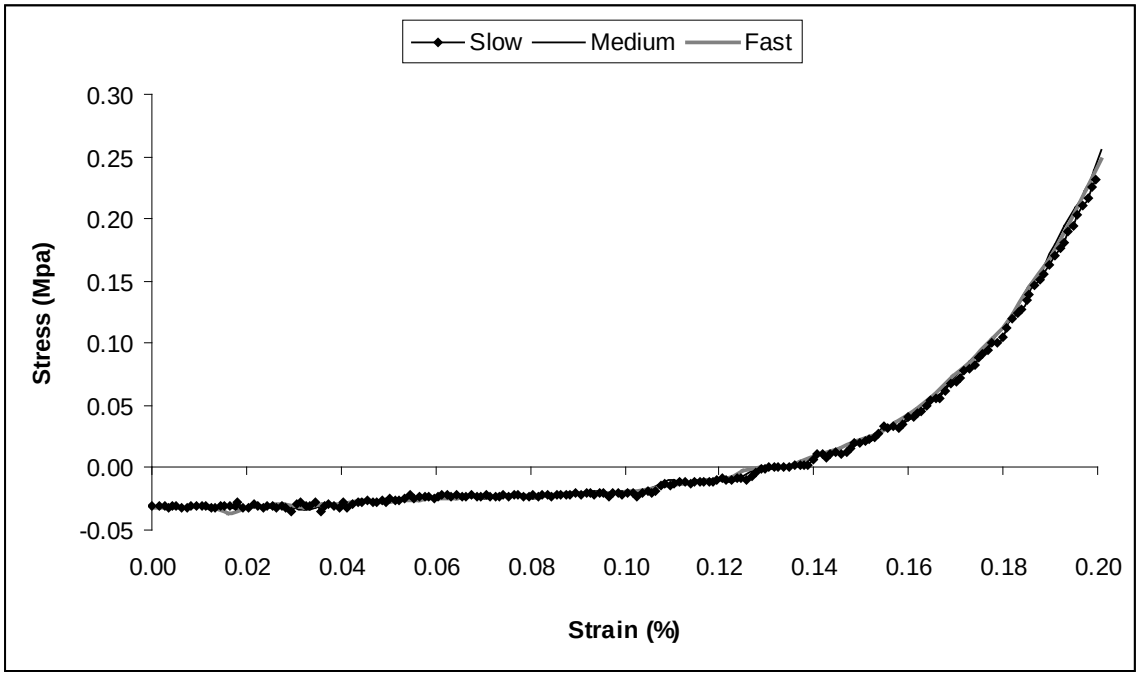

Figure 4.5: Stress-strain profiles of a two-layered annular tissue sample obtained from the superficial layers of the posterior annulus during each of the three rates of strain: slow (20% strain/20 sec), medium (20% strain/10 sec) and fast (20% strain/5 sec).

4.4 Discussion

The current study examined the biaxial strain-rate dependence of two-layered annulus samples. Three biaxial strain rates were examined, 20% strain over 20 seconds (1%/sec), 20% strain over 10 seconds (2%/sec), and 20% strain over 5 seconds (4%/sec), and it was found that no differences existed in terms of the stiffness of the tissue (elastic modulus) or the maximal stress reached over 20% strain. These findings suggest that between zero and 20% strain, the annulus is strain rate-independent at rates that are physiologically relevant for producing repetitive or cumulative injury to this type of tissue. This independence exists in tissue samples obtained from both the anterior and posterior region of the annulus fibrosus as well as from both superficial and deep layers. Last, the current study examined the effect of strain rate on both the circumferential and axial mechanical properties of the annulus, and found that the properties in both directions were strain rate-independent and were not significantly different from one another.

Debate exists as to whether biologic tissues are strain rate dependent or independent. For example, bone material properties have been found to be dependent on strain rate such that with increasing rates of strain, bone is stiffer and fails at higher stress magnitudes (Carter & Caler, 1985; Keaveny & Hayes, 1993). Biologic soft tissues, on the other hand, have not been found to be consistently strain rate dependent or independent. Tendons, for example, have been researched quite extensively with regards to the effect of strain rate on their mechanical properties. Yamamoto and Hayashi (1998) examined the properties of the patellar tendon harvested from rabbits at three different rates of strain (ranging from 0.556%/sec up to 1250%/sec) to failure and found no differences in

the elastic moduli, indicating no effect of strain rate on tissue stiffness, but did however observe a significant increase in the maximal stress reached with increasing strain rate. Investigations have also included the Achilles tendon (Wren et al., 2001), rat-tail tendon (Haut, 1983), and sheep flexor tendon in the hind limb (Lynch et al., 2003), all of which observed higher failure stresses with higher strain rates but did not all observe differences in the tissue stiffness. Of these three studies, Lynch et al. (2003) and Wren et al. (2001) examined non-acute, physiologically realistic strain rates (0.01%/sec - 1%/sec and 1%/sec – 10%/sec, respectively), while Haut (1983) strained the rat-tail tendon at a rate of up to 720%/sec, a rate achievable only during very abrupt loading. Ligaments have also exhibited increases in failure stress with increased strain rates (Crowninshield & Pope, 1976; Noyes et al., 1974; Woo et al., 1990) while others observed strain rate independence (Blevins et al., 1994; Crisco et al., 2002). Each of the aforementioned studies, with the exception of Crowninshield and Pope (1976) also reported tissue moduli values yet no significant effect of strain rate was observed in terms of this property. Further, each of these studies examined strain rates which are not achievable through voluntary movement (ranging from 3660%/sec to 19,000%/sec), but only through acute injurious situations, with the exception of Noyes et al. (1974), who examined slower strain rates (ranging from less than 1%/sec up to over 60%/sec) that are likely more representative of voluntary movements. Others have also documented increased stiffness in ligaments as a result of increased strain rate (Danto & Woo, 1993; Haut & Little, 1969; Ticker et al., 1996). Contrary to the majority of the studies mentioned above, these latter three studies each examined much slower strain rates (ranging from 0.03%/sec to 10%/sec), more likely to be achievable during voluntary movement.

The strain rates examined in the current study were limited to those across a range that represents rates that would be achievable voluntarily and not as a result of acute injury, and therefore it is unknown how these mechanical properties would change at higher strain rates. Under compressive loading the fibres of the annulus become more horizontally aligned (Klein & Hukins, 1982a) and are subjected to circumferential tension; however, if this compressive load is applied at a high rate, the result is not injury to the AF, but instead damage the vertebral bodies (Brinckmann et al., 1989; Gunning et al., 2001; Lundin et al., 1998; Yingling et al., 1997). Therefore, the authors feel that the strain rates examined in the current study more closely represented rates that would result in injury to the annulus. In particular, herniation is one of the most common types of injury of the annulus, which tends to be both initiated and propagated through repeated voluntary flexion/extension of the intervertebral joint at, most likely, slower rates of strain. Further, herniation progresses through clefts formed in each layer of the annulus as a result of such tensile strain.

The current study was unique with respect to its repeated measures design, which allowed the examination of all three strain rates within each tissue sample. However, due to this design, tissues were not strained until failure, making this study dissimilar to most other tendon or ligament strain rate studies. Yamamoto and Hayashi (1998) strained patellar tendons to failure and while they found greater stiffness at higher strain rates, this did not appear to be the case at sub-failure strain. A similar finding was observed by Grashow et al. (2006) in sub-failure strain tests of the mitral valve in the heart. The stress-strain profiles, and thus stiffness, of these tissues at sub-failure strains were similar at different strain rates. These studies suggest that strain rate often does not appear to

have an effect on the mechanical properties of soft tissues at strains below failure. This observation is similar to what was observed in the current study. It would appear that certain tissues are strain rate dependent in terms of stiffness and many are in terms of failure stress, but this may only hold true at very high strains. The current study aimed to examine more physiologic strain magnitudes that individuals may be subjected to on a daily basis, and that are hypothesized to cause damage to the annulus resulting in herniation. To enable us to comment on any differences in sub-failure versus failure strain magnitudes, and the effect of strain rate on such strain magnitudes, two additional tissue samples were strained to failure at different strain rates. These two additional tissue samples were obtained from a single harvested sample (which was cut in half to yield the two samples in order to reduce tissue variability) from the superficial anterior layers of a c5/c6 porcine motion segment. Both tissue samples underwent the same protocol as each of the other 20 samples tested in this study (i.e. four repeats at each strain rate), and it was again confirmed that when strained to 20%, no differences were observed the maximal stress nor the modulus between the three strain rates. These two tissues then underwent a failure protocol; one at the fast strain rate (20%/5 sec) and the other at the slow rate (20%/20 sec). The tissue strained at the fast rate failed at 21.4% strain in the circumferential direction and 21.3% in the axial direction. The tissue strained at the slow rate failed at 24.0% and 23.8% in the circumferential and axial directions, respectively. However, the tissue strained at the fast rate failed at a peak stress of 0.83MPa and 0.57MPa in the circumferential and axial directions, respectively, while the tissue strained at the slow rate failed at much lower stresses; 0.55MPa and 0.28MPa in the circumferential and axial directions, respectively. A similar observation was made in

terms of the modulus in the axial direction with a modulus of 5.31MPa for the fast strained tissue and 4.08MPa for the slow strained tissue. However, in the circumferential direction, the modulus was higher for the slow strained tissue as compared to the fast (8.40MPa at the slow strain rate as compared to 7.66MPa at the high strain rate). Further work is required to confirm these differences between sub-failure and failure strains. The annulus may exhibit strain rate dependent responses, but only in high strain failure conditions.

The current study was the first to measure the mechanical properties of the annulus at varying strain rates without attachment to the adjacent vertebral bodies. Previous work has examined the effect of different displacement rates on the functional spine unit (intervertebral disc and surrounding vertebral bodies) as a whole. A range of displacement rates have been studied, but all with the same conclusion; increases in stiffness and failure load are evident with increasing displacement rates (Brown et al., 2008; Elias et al., 2006; Nuckley et al., 2005; Race et al., 2000). However, the relationship found by Elias et al. (2006) was deemed weak and an additional study (Yingling et al., 1997) failed to find any association between failure loads and the rate of compression. These conflicting findings demonstrate the debate which still remains regarding the mechanical properties of spinal segments and strain rate, not dissimilar to the uncertainty regarding the effect of rate on other soft tissues such as ligaments and tendons. Last, only one study has attempted to determine the strain-rate dependence of mechanical properties of the annulus (Kasra et al., 2004 (ovine); however, segments of the adjacent vertebral bodies were still affixed to the annulus, thus still not enabling the separation of the effect of strain rate on the annulus alone and its influence on the

bone/soft tissue interface properties. In particular, Kasra and colleagues (2004) examined the mechanical properties during both sub-failure and failure tests. They found that during the sub-failure tests, the modulus was lowest during the medium strain rate (as compared to slow and high) but was highest during the fast strain rate during the failure tests. Their sub-failure finding does not suggest a strong link between strain rate and stiffness, as one would expect to observe a consistent trend of increasing stiffness with increasing strain rate. Thus, Kasra et al. (2004) provides additional support to the findings of the current study, that during sub-failure strains, the material properties of the annulus are strain rate independent.

It is important to address limitations in the current study. First, the use of a porcine model may not be directly comparable to the human intervertebral disc, but has been shown to be anatomically and functionally similar to human (Oxland et al., 1991; Yingling et al., 1999). Further, testing layers of the annulus absent from the adjacent bone does not mimic the response of this tissue *in vivo*, but does allow investigation of the annulus isolated from any other tissue that might alter its response to various rates of applied strain. Last, the rates of strain examined in this study were quite slow, representing voluntary movement, and do not represent the entire range of rates that the intervertebral joints are capable of achieving. The range of these strain rates was limited and therefore it was not possible to comment on the viscoelastic nature of the annulus at extremely high strain rates.

4.5 Conclusion

It is concluded that within the range of zero to 20% strain, the mechanical properties of two-layered samples of the annulus, in particular the elastic modulus and maximal stress, are strain rate independent at lower strain rates achievable through voluntary movement. Further, this independence was observed in both the anterior and posterior region of the annulus as well as in deep and superficial sections. This study examined the mechanical properties in both the axial and circumferential directions, and concluded that the elastic modulus and maximal stress do not differ in these two directions. This information is especially relevant as the annulus rarely fails as a result of extremely high strain rates, at which the damage would occur in the boney elements of the spine, and concludes that at strain rates achievable through voluntary motion that could result in herniation, the tensile response of the annulus tissue is not affected by strain rate.

Chapter 5

Mechanical properties of the annulus fibrosus and the consequence of vibration: An examination of the intra-lamellar matrix.

Chapter Synopsis

Whole body vibration has been associated with the increased reporting of low back pain and an increased risk of disc herniation; however the mechanism responsible for this association is unclear. It is theorized that disc herniation propagates through the annular layers via clefts that form in the ground substance between the collagen fibre bundles within each lamella. Given that cyclic loading has been associated with fatigue failure in other biologic tissues such as ligaments, it was hypothesized that exposure to vibration may have a similar effect on the annulus fibrosus by weakening the intra-lamellar matrix, thus leading to an increased risk of cleft formation. The current study examined the effect of exposure to 5 Hz axial vibration on the mechanical properties of single layers of the annulus when tested under uniaxial strain to failure perpendicular to the orientation of the collagen fibres. This orientation effectively isolated the intra-lamellar matrix of annular lamella. Vibration had minimal effect on the mechanical properties with the exception of the strain magnitude at the end of the toe region of the stress-strain curve. Vibrated tissues did, however, show significantly larger toe regions (49.7% as compared to 31.4% observed in the control tissues, $p = 0.027$), which may be due to damage of elastin fibres located between adjacent collagen fibres within a single lamella. Elastin functions to minimize tissue extensibility as well as tensile strain recovery and therefore, over time, a reduction in tensile strain recovery due to damaged elastin may lead in an increased risk of cleft formation between adjacent collagen fibres, which could in turn lead to disc herniation.

5.1 Introduction

Previous research has shown that the propagation of disc herniation does not involve aggressive tearing through the fibres of each lamella of the annulus, but rather the nucleus pulposus squeezes through adjacent bundles of collagen fibres within each lamella (Moore et al., 1996; Tampier et al., 2007). The nucleus of the disc forcefully pushes up against each layer, straining the layer, until clefts form in the lamellae (between adjacent collagen fibre bundles) at the weakest location, allowing the nucleus to propagate to the next layer. Few studies have quantified the forces required to separate the collagen bundles in single annular layers; forces which are related to the mechanical properties of the intra-lamellar matrix. Further, no study has attempted to determine how the annulus responds to transverse tensile strain (strain applied perpendicular to the orientation of the collagen fibres) following exposure to factors that have been linked with disc herniation, such as whole body vibration. Vibration, or low-magnitude cyclic loading, has been shown to negatively alter the strength of various engineering materials (Dowling, 1993; Hertzberg, 1980; Hertzberg and Manson, 1980; Riddell et al., 1966) as well as biological materials such as ligaments (Weisman et al., 1980 (rat)) which contain similar components to the annulus tissue, predominately type I collagen. Therefore, it is likely that a similar negative effect would be observed with annulus tissue that has been subjected to vibration. Further, exposure to whole body vibration has been shown to be heavily associated with the prevalence and incidence of low back pain (Bovenzi & Hulshof, 1999; Lis et al., 2007; Robb & Mansfield, 2007) as well as disc herniation (Viikari-Juntura, 1997; Virtanen et al., 2007).

In addition to the obliquely oriented collagen fibres of the annulus, the matrix found between the collagen bundles, called the intra-lamellar matrix, contains various components that may assist in providing strength and support against tensile strain. For example, it has been hypothesized that the proteoglycans in the annulus actually entangle themselves around the collagen fibres creating a strong fibre-matrix bond capable of withstanding tensile strain (Adams & Green, 1993). Additionally, Pezowicz et al. (2005) documented a complex network of fibrous links within the annulus that help bind adjacent collagen fibres within each layer of the annulus, which also adds structural support and helps to resist strain applied perpendicular to the orientation of the collagen fibres (Pezowicz et al., 2005). Similar fibrous links, called the translamellar bridging network, have been identified in between the layers of the annulus and are comprised of type VI collagen (Melrose et al., 2008; Schollum et al., 2008; an ovine model was used in both studies). This similar bridging network is hypothesized to be the major tensile load-bearing structure in the intra-lamellar matrix. If these structures fail in response to tensile strain applied perpendicular to the orientation of the collagen fibres, the result is the formation of a cleft in the intra-lamellar matrix. The final major structure located in the intra-lamellar matrix is elastin (Yu et al., 2002; Yu et al., 2005), which is primarily responsible for assisting connective tissue recovery following tensile strain (Smith & Fazzalari, 2009).

Previous work has examined the formation of clefts in the intra-lamellar matrix as a result of transverse tensile strain (Pezowicz et al., 2005). The formation of clefts is thought to be a possible mechanism for herniation propagation, in that if there was a reduction in the strength of bonds formed between collagen bundles within a layer, it may

affect the ability of the annulus to withstand transverse tensile strain. If the properties of the collagen bonds were to be altered such that they become weaker, possibly as a result of exposure to a cyclic loading or vibration, it is likely that these clefts would form with reduced tension and allow the nucleus to penetrate each layer with greater ease.

The only documented potential effects of vibration on the intra-lamellar matrix are those of Ishihara et al. (1992) and Yamazaki et al. (2002) who have shown that exposure to vibration results in a significant reduction in proteoglycan synthesis in the nucleus and the inner annulus. However, it is possible that vibration may also have a structural effect on the existing proteoglycans, type VI collagen bonds, and elastin, in addition to these cellular changes. Therefore, this study aimed to identify the effect of exposure to axial vibration on the mechanical properties of single layers of the annulus when strained perpendicular to the collagen fibre orientation. This works differs from that of Pezowicz et al. (2005) by linking the formation of clefts and the mechanical properties to a known injurious exposure, vibration.

5.2 Methods

5.2.1 Pre-loading and Compressive-loading Protocol

Fourteen porcine functional spine units (FSU) at the cervical level of c5/c6 were examined in this study. Previous research has confirmed anatomical, geometric, and functional similarities between the porcine cervical and human lumbar spine (Oxland et al., 1991; Yingling et al., 1999).

Muscle tissue was dissected away prior to testing to leave the osteo-ligamentous FSU. Once free of the surrounding musculature, the specimens were secured into two

custom aluminium cups with 16 gauge wire around the anterior and posterior spinal elements, and further secured with dental plaster (Denstone, Miles, South Bend, IN, USA). Each mounted FSU was subjected to a preconditioning 300 N compressive load for 15 minutes (Callaghan & McGill, 1995; Gunning et al., 2001; Yingling et al., 1997; Yingling et al., 1999) using a servohydraulic materials testing machine (8872, Instron Canada, Toronto, ON, Canada). A rotational brushless servomotor (Kollmorgen, Model AKM23D-BNCNC-00, Danaher Motion, Il, USA) was used to rotate the specimen about the flexion-extension axis and a torque transducer (SensorData Technologies Inc., Model T120-106-1 K, Sterling Heights, MI, USA) measured the moment applied to the specimen.

Following the 300 N preconditioning trial, seven FSUs were loaded under 1400 N static compression for two hours in a neutral posture. Neutral was defined as the location of lowest torque resistance about the flexion-extension axis, which was determined during the 15 minute preconditioning trial. These FSUs served as control specimens. The remaining seven FSUs underwent a vibration protocol following the 15 minute preconditioning. Vibration was applied through cyclic compression using the servohydraulic materials testing machine. Compression oscillated in a sinusoidal waveform between 1260 N and 1540 N (± 10% of 1400 N; therefore the total cumulative compression experienced by both groups was equal) at 5 Hz, the approximate natural frequency of the human torso (Pope et al., 1998; Dupuis, 1989; Panjabi et al., 1986; Wilder et al., 1982), and the approximate frequency to which individuals are exposed in situations such as automobile or truck driving (Mansfield, 2005). Following this loading

protocol, each FSU, both control and vibrated, were removed from the aluminium cups and the posterior elements were removed to expose the complete intervertebral disc.

5.2.2 Single Layer Specimen Dissection and Preparation

Sixteen single layer tissue samples were obtained (Figure 5.1) from the seven control FSUs and 16 were obtained from the seven vibrated FSUs yielding 32 tissue samples. These tissue samples were obtained from four locations in the AF: anterior superficial, anterior deep, posterior/lateral superficial, and posterior/lateral deep. The superficial region was that of the outer most layers (layers 1-4) while the deep region was that of the more inner layers (layers 5-10); however these deep tissue samples are still somewhat superficial relative to the entire annulus size (approximately 15-25 layers). While fourteen FSUs were tested, yielding a maximum of 56 samples (16 x 4 extraction sites), only 32 tissue samples were usable for tensile testing as some dissected tissues were not large enough to mount in the system used (described in more detail below). Each tissue sample was dissected from the intervertebral disc using a light microscope (Nikon SMZ 1000, Nikon Instruments Inc, Melville, NY, USA) in order to ensure that only one layer of the annulus had been isolated and that no damage had occurred during the dissection. The average thickness of the control tissues was 0.20 mm (±0.06) and 0.18 mm (±0.07) for the vibrated tissue samples ($p = 0.33$, statistical power = 21.9%) and was measured using a displacement measurement sensor (ZX-LD40L Smart Sensor, Omron Canada Inc, Toronto, ON) (Figure 5.2). The average cross sectional area of these tissues were 0.72 mm^2 (±0.26) and 0.60 mm^2 (±0.30) for the control and vibrated tissue sample, respectively ($p = 0.26$, statistical power = 33.2%).

Tissues were dissected such that strain could be applied perpendicular to the orientation of the collagen fibres (Figure 5.1b). Each tissue sample was subjected to tensile strains using a custom biaxial tensile testing system (BioTester 5000, CellScale, Waterloo Instruments Inc, Waterloo, ON) in the transverse direction (perpendicular to the orientation of the collagen fibres – Figure 5.3). Tissues were secured in the tensile testing system via tungsten rakes (Figure 5.1). Once mounted in the testing system, each tissue was initially strained such that the tissue was taut, but without applying more than 5 mN of tension. This starting tension was considered the point of zero strain. Each tissue sample was preconditioned with three repeats of 10% strain at a rate of 1% strain/sec and then subsequently strained to failure at a rate of 2% strain/sec.

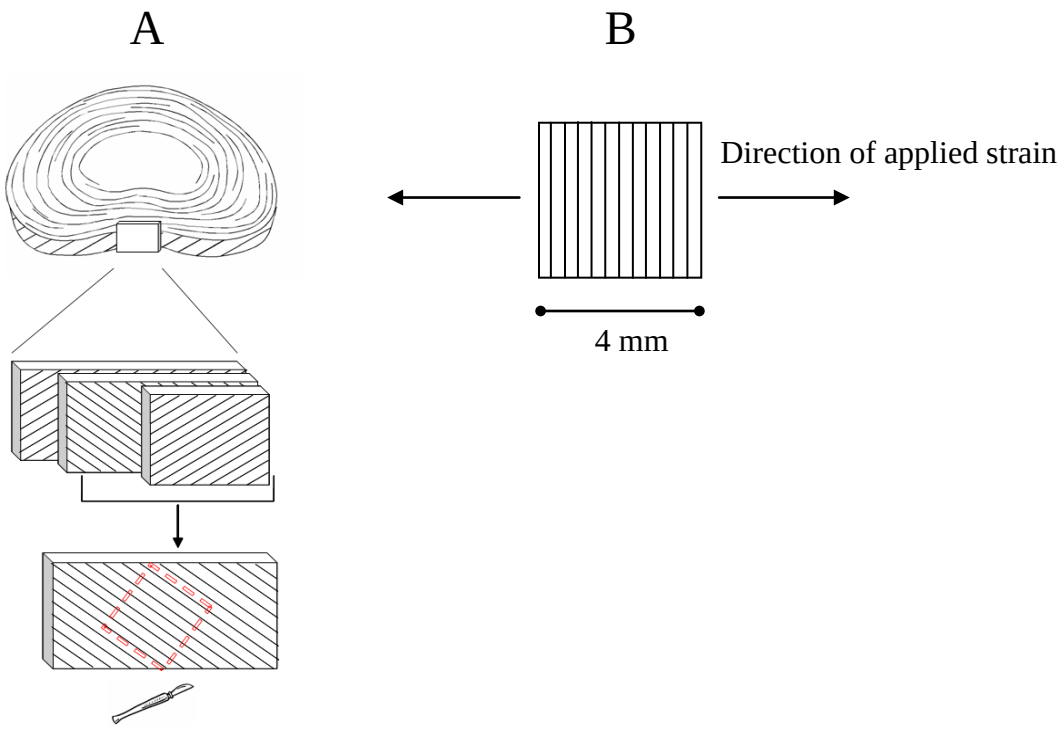

Figure 5.1: A) Schematic representation of tissue harvest. Single layers of the annulus from the anterior and posterior-lateral region, and from both superficial and deep sections were obtained. B) Tissues (approximately 4x4 mm) were cut such that the orientation of the collagen fibres ran vertically and tension was applied perpendicular to the orientation (shown by arrows).

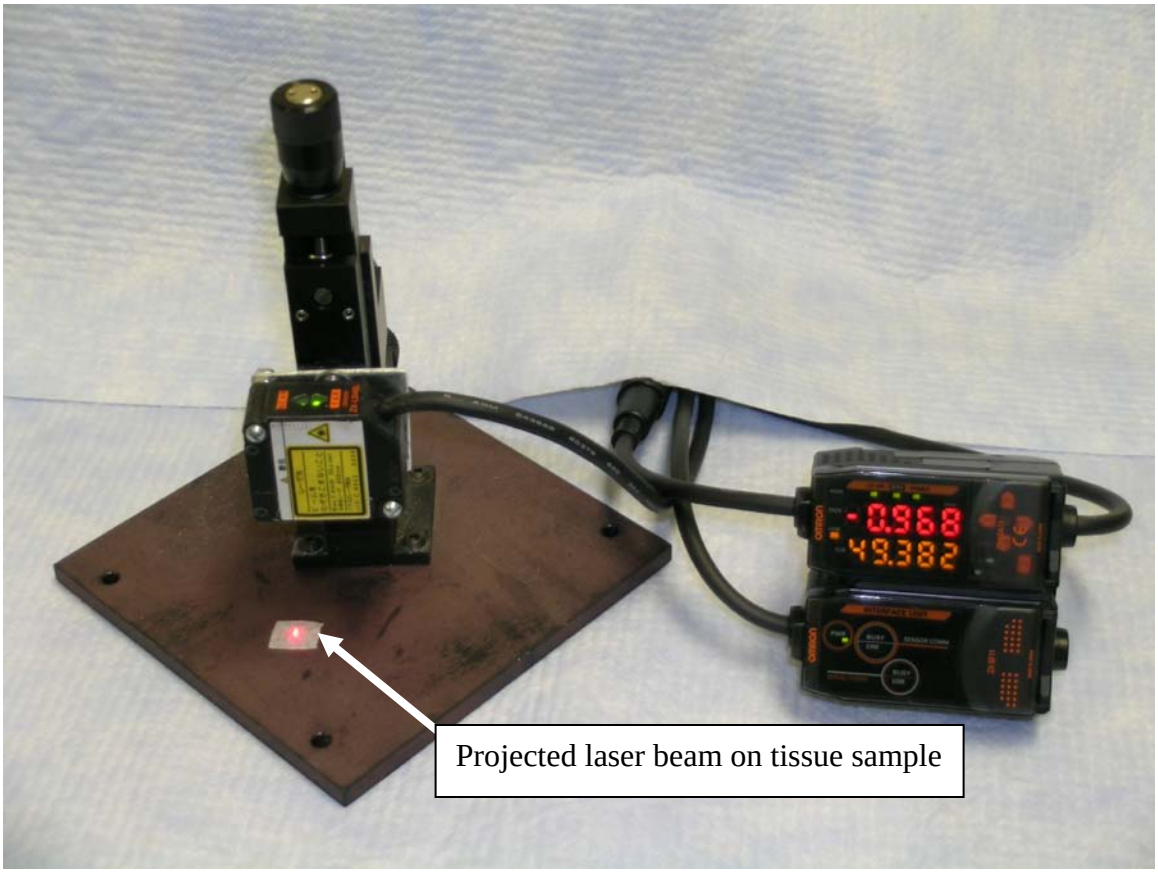

Figure 5.2: Displacement measurement sensor. A calibrated laser beam (indicated by arrow) is projected onto the surface of the tissue in order to determine the tissue thickness.

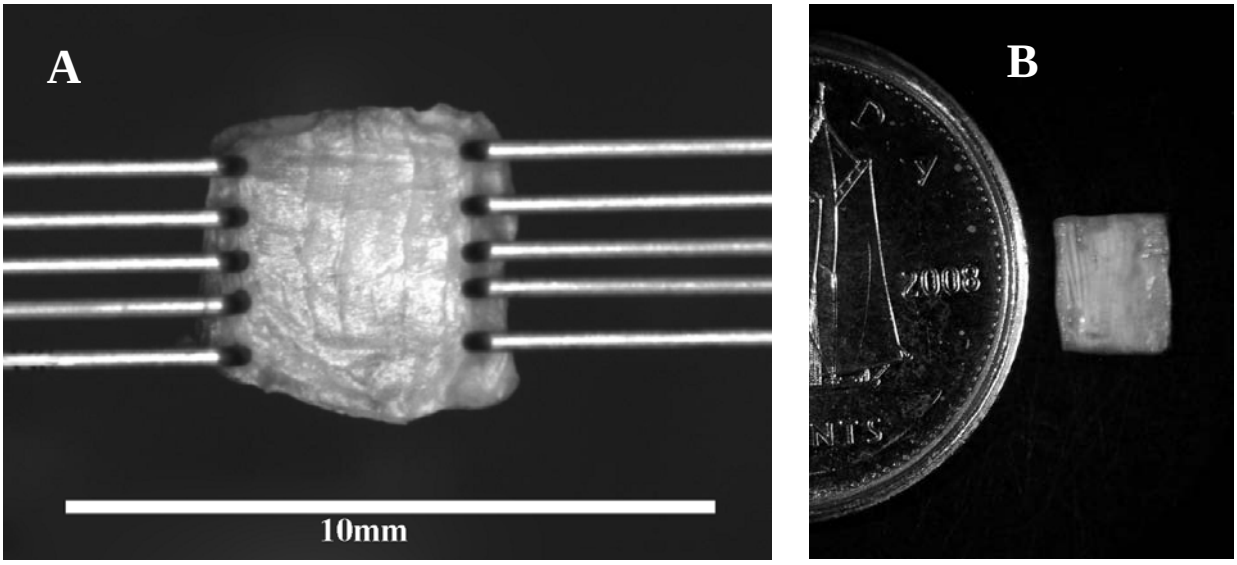

Figure 5.3: A) Single layer annular tissue mounted via rakes in the strain-controlled testing apparatus. Note the vertically aligned collagen fibres. White horizontal bar represents 10 mm. B) Sample tissue and a dime shown for relative size comparison.

5.2.3 Data Analysis

Force and rake displacement data were obtained during each failure test using the BioTester 5000 custom software, LabJoy 5.80, and were sampled at 10Hz. Cross-sectional areas were calculated for each tissue sample and were used to determine stress values during the failure tests and strain data were calculated by normalizing the displacement of the rakes. Multiple variables were obtained from these stress-strain profiles and are shown in Figure 5.4.

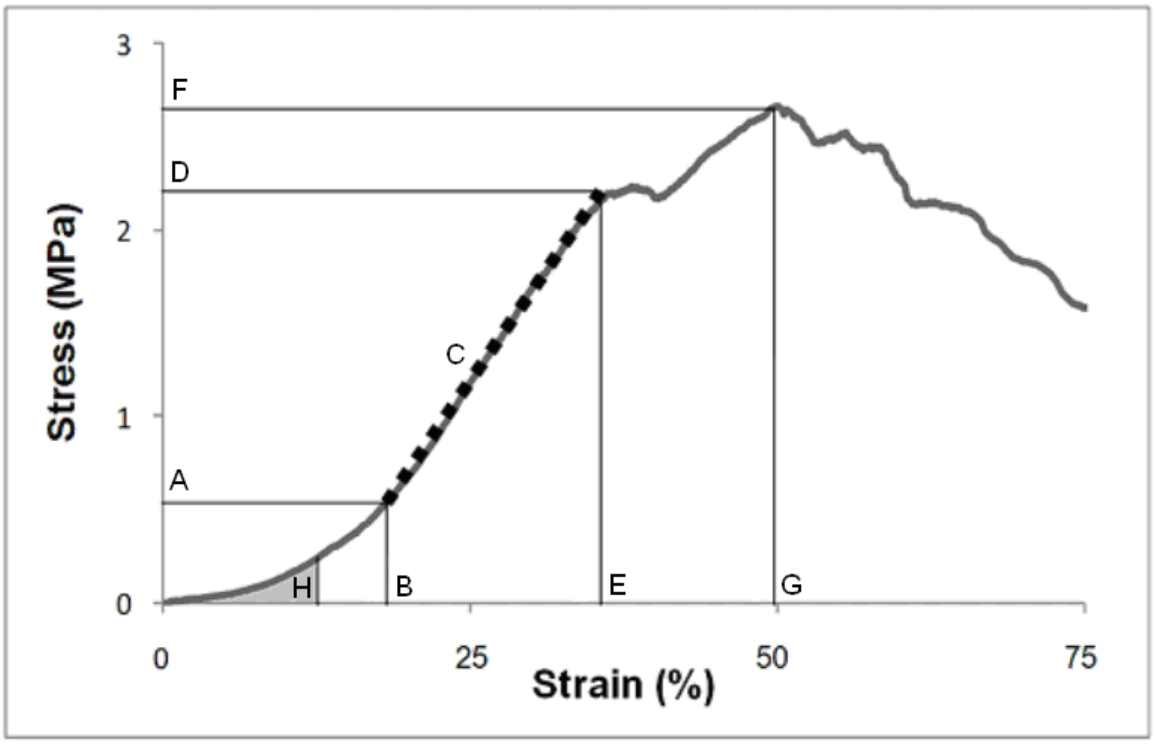

Figure 5.4: Representative stress-strain curve identifying variables of interest. A) Stress at the end of toe region (MPa) ; B) strain at the end of the toe region (% strain); C) Elastic modulus (MPa); D) stress at initial failure (MPa); E) strain at initial failure (% strain); F) tensile strength (MPa); G) Failure strain (% strain); H) usable material toughness.

5.2.3.1 Toe Region

The toe region, or the initial non-linear portion of the stress-strain curve, was examined for each specimen. Specifically, the strain magnitude at the end of the toe region, defined as the region prior to the beginning of the linear region, was recorded as well as the stress at this point in the stress-strain curve.

5.2.3.2 Linear Region

The linear region of each stress-strain curve was also examined for each specimen. The elastic modulus or slope of the linear region was calculated. Additionally, image detection analysis (LabJoy 5.80) was used in order to determine the deformation of each tissue in the axis orthogonal (vertical) to the axis of applied strain. This information was used to determine Poisson's ratio in the linear region of the stress-strain curve and was calculated using the following equation:

Eq. 5.1 $$\nu = -(\varepsilon_{\text{perpendicular to collagen orientation}} / \varepsilon_{\text{parallel to collagen orientation}})$$

where $\varepsilon_{\text{perpendicular to collagen orientation}}$ is the strain applied by the rakes and $\varepsilon_{\text{parallel to collagen orientation}}$ is the compressive strain (narrowing of the tissue) in the vertical direction (parallel to collagen orientation).

5.2.3.3 Initial Failure

The stress and corresponding strain at the first detection of failure was determined for each tissue. Initial failure was the point at which there was either 1) a sudden drop in stress without an initial decrease in the slope of the linear region, 2) a decrease in the slope of the linear region indicative of entering into a plastic, non-recoverable region.

5.2.3.4 Tensile Strength and Failure Strain

Tensile strength is the maximum stress value for each specimen. The strain at this stress was also recorded and termed failure strain.

5.2.3.5 Material Toughness

Material toughness was determined by calculating the area under the stress-strain curve between zero strain and 12.5% strain. The toughness from zero to 12.5% strain was considered “usable toughness”, as 12.5% strain was the average value of the documented failure strains by Skaggs et al. (1994). These failure strains were for tissues strained in the direction of the collagen fibres; the opposite orientation of those in the current study. It was assumed for the current study that, *in vivo*, if a layer of the annulus is strained to 12.5% perpendicular to the orientation of the fibres (the orientation examined in the current study) then adjacent layers which are in an opposite orientation would be close to their maximal (failure) strain. This assumes that layers of the annulus are tightly bound together and when one layer strains, the adjacent layers concurrently strain. Therefore, any energy absorbed beyond 12.5% strain perpendicular to the orientation of the collagen fibres (as in this investigation) may not be exploitable *in vivo* during non-failure strains.

5.2.4 Statistical Analysis

A three-way ANOVA was conducted to determine the effect of condition (vibration versus control), tissue location (two levels; anterior, posterior-lateral), and tissue depth (two levels; superficial, deep) on the aforementioned variables. An alpha level of 0.05 was set for all statistical tests.

5.3 Results

5.3.1 Effect of Vibration

Sixteen single layer annular tissue samples were obtained from vibrated FSUs and 16 from control FSUs. No significant differences were observed between any of the variables investigated with the exception of the strain at the end of the toe region. For this variable, the tissues which had been subjected to two hours of vibration had significantly greater strain at the end of the toe region than those exposed to two hours of static compression ($p = 0.027$, Cohen's d effect size = 0.74). Specifically, vibrated tissues had a mean (standard deviation) of 49.7% strain (33%) while control tissues were found to have a mean (standard deviation) toe region of 31.4% strain (15%), $p = 0.027$. Tables 5.1 and 5.2 summarize these findings.

5.3.2 Effect of Tissue Site Extraction

Of the 32 tissues harvested, eight were obtained from the anterior superficial section of the AF, eight from the anterior deep section, eight from the posterior/lateral superficial section, and eight from posterior/lateral deep section. Tissue harvest location had an effect on the strain at the end of the toe region ($p = 0.027$) and the Poisson's ratio ($p = 0.026$). In both these variables, a significant interaction between tissue location (anterior/ posterior-lateral) and tissue depth (superficial/deep) was observed. Figure 5.5 depicts these interactions.

Table 5.1: Average (standard deviation) values for each of the variables examined collapsed across tissue harvest location for control tissues (n = 16) and vibrated tissues (n = 16). All variables, with the exception of the strain at the end of the toe region (identified with asterisk, p = 0.027) were not significantly different between the control and vibrated tissues (p>0.05).

	End of Toe Region Strain (%)	End of Toe Region Stress (MPa)	Elastic Modulus (MPa)	Poisson's Ratio
Control (n=16)	31.4 (15.4)	0.33 (0.24)	3.41 (2.61)	0.49 (0.35)
Vibration (n=16)	49.7 (32.6) *	0.59 (0.63)	2.91 (2.06)	0.61 (0.29)
statistical power (%)	n/a	45.9	14.8	27.8

	First Initial FailureStrain (%)	First Initial Failure Stress (MPa)	Failure Strain (%)	Tensile Strength (MPa)	Toughness (kPa)
Control (n=16)	56.9 (23.0)	1.09 (1.06)	116.8 (50.2)	1.44 (1.26)	4.36 (3.79)
Vibration (n=16)	81.3 (46.1)	1.36 (1.45)	115.2 (42.9)	1.62 (1.63)	4.29 (3.79)
statistical power (%)	59.9	14.8	6.1	9.8	5.6

Table 5.2: Average (standard deviation) values for each of the variables examined collapsed across exposure (control versus vibrated) for each tissue harvest location (n=8 for each location). No significant main effect was observed for any variable (p>0.05).

	End of Toe Region Strain (%)	End of Toe Region Stress (MPa)	Elastic Modulus (MPa)	Poisson's Ratio
Anterior Superficial (n=8)	42.5 (26.7)	0.27 (0.23)	2.88 (2.43)	0.46 (0.29)
Anterior Deep (n=8)	27.8 (9.9)	0.34 (0.13)	3.02 (1.67)	0.64 (0.19)
Posterior Superficial (n=8)	34.9 (14.8)	0.63 (0.58)	4.10 (2.83)	0.75 (0.46)
Posterior Deep (n=8)	57.0 (40.1)	0.61 (0.73)	2.65 (2.43)	0.39 (0.24)

	First Initial FailureStrain (%)	First Initial Failure Stress (MPa)	Failure Strain (%)	Tensile Strength (MPa)	Toughness (kPa)
Anterior Superficial (n=8)	72.9 (50.3)	0.69 (0.58)	119.8 (66.1)	1.25 (1.32)	4.90 (5.09)
Anterior Deep (n=8)	51.1 (15.5)	0.99 (0.58)	94.5 (32.3)	1.17 (0.62)	5.09 (4.22)
Posterior Superficial (n=8)	64.7 (19.1)	1.81 (1.58)	113.5 (35.8)	2.16 (1.83)	4.18 (2.32)
Posterior Deep (n=8)	87.6 (49.4)	1.41 (1.74)	136.2 (40.5)	1.53 (1.72)	3.13 (3.11)

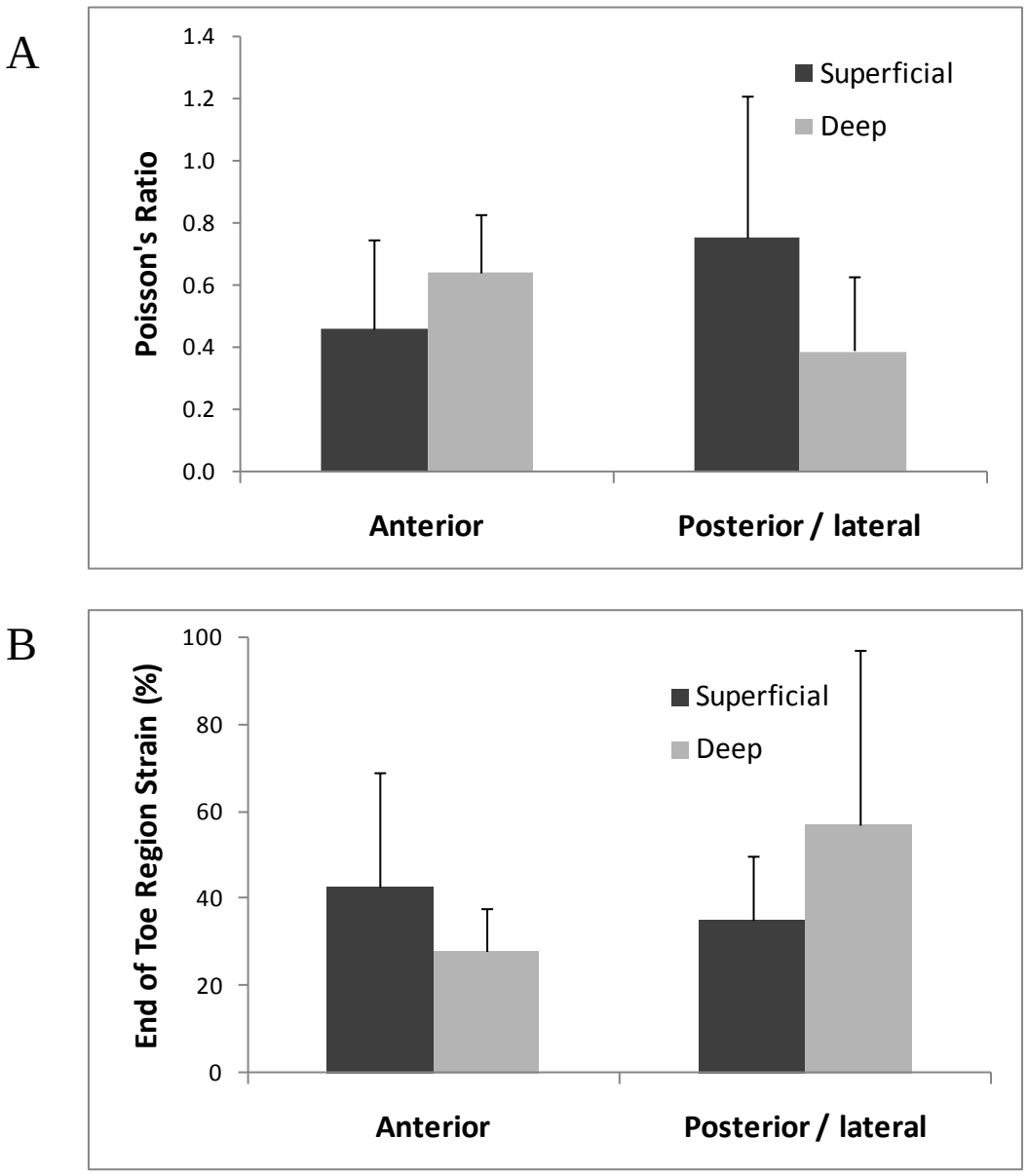

Figure 5.5: Interaction between tissue harvest location (anterior versus posterior/lateral) and depth (superficial versus deep) for A) strain at the end of toe region (% strain) ($p=0.027$) and B) Poisson's ratio ($p=0.026$).

5.4 Discussion

Vibration has been linked with an increased risk of disc herniation (Viikari-Juntura, 1997; Virtanen et al., 2007), but this link has been minimally explored and no hypothesized mechanism between vibration and herniation has been proposed. The current study aimed to compare the mechanical properties of the intra-lamellar matrix in discs subjected to vibration and control discs in order to determine if the mechanism of injury lies in changes to the mechanical properties of this matrix. The only property that was significantly affected by vibration was the strain magnitude of the toe region of the stress-strain curve, which was larger in tissues that had been subjected to vibration. Many additional mechanical properties, including failure stress and strain, elastic modulus, and material toughness, were not significantly affected by vibration. These findings suggest that vibration has a minimal effect on the material properties of the intra-lamellar matrix, but may alter the mechanics within the toe region.

The toe region is a non-linear portion of the stress-strain profile that occurs prior to the linear elastic region. This region is generally associated with uncrimping of fibres, namely the collagen fibres in the case of tendons and ligaments. However, in the current study, tension was applied perpendicular to the orientation of the collagen fibres and therefore the uncrimping associated with the toe region was not likely to be that of collagen fibres (primarily type I in the annulus) but more associated with the mechanical properties of other components of the intra-lamellar matrix. These other components, in particular type VI collagen fibres, proteoglycans, and elastin, are involved in providing structural support by assisting in bearing tensile load, maintaining hydration and thus cell adhesion, and assisting in recovery following tensile strain (Adams & Green, 1993; Pezowicz et al., 2005; Smith & Fazzalari, 2009), respectively. Since failure strength was not significantly affected by vibration, it is less likely that any collagen

fibres, in particular the type VI, were damaged. Rather, the affected structures were more likely elastin, and to a lesser extent, proteoglycans.

Elastin is found in the intra-lamellar matrix and functions to assist in connective tissue recovery following sub-failure tensile strain. In the case of the single layer annular tissues examined in this study, elastin would serve to keep adjacent type I collagen fibres in the lamellae tightly bound to one another. Additionally, due to the high elastic modulus of elastin (Smith & Fazzalari, 2009), it also helps minimize a tissue's extensibility. Previous work has shown that, in the absence of elastin, the annulus is less stiff in the toe region as well as the linear region, and shows significantly greater extensibility (Smith et al., 2008). Further, the importance of elastin is thought to be even greater in the toe region as it assists in collagen re-crimp, which is vital in terms of energy absorption (Adams et al., 2006). This study found significantly larger toe regions, and thus extensibility, in the annular layers exposed to vibration as compared to the control tissues; and with no observed difference in the stress magnitude at the end of the toe region, these vibrated tissues were also less stiff in the toe region. These findings indicate that elastin was likely the most affected structure in the intra-lamellar matrix.

In addition to elastin, proteoglycans may have also been affected by the vibration. A reduction in proteoglycan synthesis has been observed in the annulus following vibration (Ishihara et al., 1992; Yamazaki et al., 2002); however, it is possible vibration had an effect on the mechanical properties of the existing proteoglycans as well. Proteoglycans entangle themselves around the collagen fibres to create strong fibre-matrix bonds (Adams & Green, 1993), which, if damaged, could also allow increased deformation in the intra-lamellar matrix. If, however, elastin was the structure that was the primary target of damage, it is likely, with prolonged vibration exposure, that the ability for the intra-lamellar matrix to recover following

tensile strain would further diminish. This could result in an increased risk of forming clefts in between the obliquely orientated collagen fibres within any given layer, which in turn would increase the risk of disc herniation when compounded with the addition of focal stresses applied by the nucleus.

It is interesting to note that the toe regions for both the vibrated and control tissues were extended outside of the assumed usable region of 12.5% strain (based on documented failure strains of single annular layers strained parallel to the orientation of the collagen fibres (Skaggs et al., 1994; see section 5.2.3.5). This suggests that *in vivo*, single layers of the annulus may rarely be strained to the end of the toe region in the perpendicular orientation, making the mechanical properties within the toe region even more important to consider. It is likely that only after some initial damage has occurred will individual layers strain beyond the toe region in the perpendicular direction. For example, disc herniations are characterized by nucleus progression through the annulus. Once the nucleus has penetrated a layer, the result is often delamination, or disruption of the inter-lamellar matrix. In this scenario, the layers become more loosely bound, allowing them to experience greater local strains (beyond 12.5%) as a result of posterior migration of the nucleus. During this migration, the nucleus applies localized tensile strains to one annular layer, possibly well beyond the toe region towards failure strains, as the layers are no longer bound as tightly due to delamination. These strains eventually cause the components of the intra-lamellar matrix to fail, thus creating a cleft between adjacent collagen fibres within that single layer.

In terms of tissue harvest location, significant effects were found for toe region strain and Poisson's ratio. For both variables a significant interaction between anterior and posterior-lateral, and superficial and deep was observed. It is not evident why tissue harvest location had these

effects, and further research is required to better understand these regional differences. However, it can be concluded that exposure to vibration does not appear to have a significant affect on these regional differences as no statistical interactions between vibration exposure and tissue harvest location were evident. It is interesting to note, however, that the Poisson's ratios observed in this study often exceeded 0.5, which is the maximum ratio an isotropic material can have, providing evidence of anisotropy of the annulus.

Previous literature has examined tensile moduli of single layers of the annulus. Moduli values ranging from 28-78 MPa (Holzapfel et al., 2005) and 59-136 MPa (Skaggs et al., 1994) were observed when the annulus was strained parallel to the direction of the collagen fibres. These values are much higher than the moduli values observed in the current study, however, this was to be expected based on the direction of applied strain. Holzapfel et al., (2005) also examined the tensile moduli perpendicular to the collagen orientation (similar to the current study) and observed average moduli values 0.22 MPa. This mean value is less than what was observed in the current study (3.41 MPa for control tissues); however, this is likely because Holzapfel et al. (2005) reported toe-region moduli, rather than moduli in the linear region, which was measured in the current study. Holzapfel et al. (2005) also examined human annular samples, which may also contribute to the different moduli values that were observed in the current study. Pezowicz et al., (2005) also examined the mechanical properties of single layer annular samples both parallel and perpendicular to the collagen fibre direction. They did not report moduli values, but did report a mean peak stress value of 0.15MPa when strained perpendicular to the collagen fibre direction and 16.4 MPa along the fibre direction. The mean of 1.09 MPa observed in the control tissues in the current study is closer in magnitude to the 0.15

MPa observed by Pezowicz and colleagues' (2005) in the perpendicular orientation as compared to their finding of 16.4 MPa in the direction of the collagen fibres.

The current work examined single layers of the annulus after a novel vibration exposure, but is not absent of limitations. First, a porcine animal model was used and may not be directly comparable to humans. However, the use of an animal model allows for substantial control of things such as diet, age, and activity level, which are nearly impossible to control in a human population. Further, studies have shown that the cervical porcine spine is a good anatomical and functional match to human lumbar spines (Oxland et al., 1991; Yingling et al., 1999). Another limitation is the inability to test extremely deep layers. These layers have a higher concentration of proteoglycans and therefore are more hydrated and much harder to dissect a distinct layer, a problem not unique in this area of testing (Holzapfel et al., 2005). The variability of the mechanical properties may also be considered a limitation in this type of testing. Despite using an animal model, and normalizing forces and displacements to stresses and strains, the variability in tissue testing of this nature can be quite high and may impede chances of finding statistical differences. Last, the effect of vibration was only examined on neutrally loaded discs. Disc herniation is often the result of exposure during flexed postures or chronic repetitive flexion of the spinal joint and therefore it is important to examine the effect of exposure to vibration on the intervertebral disc as a whole during a protocol that results in disc herniation such as repetitive flexion.

5.5 Conclusion

The current study examined the tensile material properties of single layers of the annulus, under strains applied perpendicular to the orientation of the collagen fibres, and the effect of

vibration on these properties. No differences were observed between vibrated and control tissues for many of the variables examined suggesting that vibration may not have a substantial acute effect on the intra-lamellar matrix. It was, however, found that tissues exposed to vibration showed significantly larger toe region strains as compared to control tissues. These increased toe regions may be a mechanism for a greater risk of disc herniation as a result of vibration, and could be attributed to damage to components of the matrix, and in particular damage to the elastin. Compromised elastin could decrease the ability for single layers of the annulus to recover following tensile strain, which may increase the risk for cleft formation between adjacent collagen fibres, the mechanism of disc herniation propagation.

Chapter 6

Examining the mechanical properties of the inter-lamellar matrix and the effect of vibration exposure

Chapter Synopsis

Delamination, or the separation of the lamellae within the annulus fibrosus, is one of the stages of intervertebral disc herniation. Delamination occurs when the bonds adhering two adjacent layers, called the inter-lamellar matrix, fail. Therefore, in order to assist in preventing herniation, strong healthy bonds must exist. It is also vital to have a solid understanding of this bond in terms of when and how it fails. For example, vibration has been shown to be positively correlated with herniation, and it has been hypothesized that this positive link may be related to the effect of vibration on the inter-lamellar matrix. The purpose of this study was to identify the effect of exposure to axial vibration (5Hz) on the mechanical properties of the inter-lamellar matrix. A unique dissection protocol was applied to twenty-four tissue specimens in order to isolate the inter-lamellar matrix, and these samples were subsequently mechanically tested until failure at 2% strain/sec. Mechanical variables of interest included the stress and displacement at the end of the toe region, matrix moduli, and failure stress and displacement. The only variable significantly affected by exposure to vibration was failure displacement. Specifically, vibrated tissues failed at higher displacements than control tissues (a mean of 2.52mm as compared to 1.99mm). This increased extensibility is thought to be due to damaged elastin within the matrix as elastin functions to minimize displacement. Damaged elastin may lead to altered and sustained tensile loading on other structures such as collagen, which could subsequently fail and cause delamination.

6.1. Introduction

The intervertebral disc functions to dissipate shock (Cassidy et al., 1989; Guerin & Elliott, 2006; Holzapfel et al., 2005; Inerot & Axelsson, 1991; Inoue, 1981; Johnson et al., 1982) while also permitting substantial spinal range of motion (Cassidy et al., 1989; Guerin & Elliott, 2006; Klein & Hukins, 1982a). It is comprised of a gelatinous centre, the nucleus pulposus, which is surrounded by a composite laminate structure, the annulus fibrosus. Intervertebral disc herniation and associated initial stages (delamination for example) are the most common injuries to the disc. Herniation, in particular, is characterized by posterior migration of the nucleus through the layers of the annulus (Yasuma et al., 1986). Delamination, or separation of the annular layers, is thought to be one of the initial and potentially mandatory stages of herniation (Adams & Hutton, 1985), making the integrity of the bond between annular layers, called the inter-lamellar matrix, very important in terms of evaluating the risk of herniation. Further, modeling of the disc has suggested that shear stresses between the lamellae are what ultimately lead to delamination (Goel et al., 1995), reinforcing the need for strong inter-lamellar bonds and a sound understanding of its properties.

The inter-lamellar matrix (connective tissue found between layers of the annulus) is comprised of various structures including type VI collagen (Melrose et al., 2008; Schollum et al., 2008), proteoglycans (Adams & Green, 1993), and elastin (Yu et al., 2002; Yu et al., 2005). Each component plays a key role in maintaining the integrity of the annulus, including bearing tensile load, hydration, and tensile strain recovery, respectively. If any of these components were compromised, the annulus would be at an increased risk of delamination and consequently herniation. Relatively few studies have addressed the mechanics of the inter-lamellar matrix, the majority of which employed finite element models to examine the shear properties of the annulus

(Goel et al., 1995, Yin & Elliott, 2005). However, one study examined the shear properties of large human tissue samples from the annulus, which indirectly evaluated the stiffness of the inter-lamellar bonds (Fujita et al., 2000). These researchers shear-strained cubed samples containing multiple lamellae and therefore did not isolate the properties of the inter-lamellar matrix.

Given that the mechanical properties of the inter-lamellar matrix are likely related to herniation, it is reasonable to hypothesize that exposure to risk factors that have been linked to herniation may negatively alter these mechanical properties. For example, exposure to whole-body vibration has been shown to be positively linked to the risk of disc herniation (Viikari-Juntura, 1997; Virtanen et al., 2007), yet the mechanism is largely unknown. Cyclic loading has the potential to negatively affect many materials, ultimately leading to fatigue failure (Hertzberg, 1996; Hertzberg & Manson, 1980; Riddell et al., 1966), and a similar mechanism may be evident in the inter-lamellar matrix with exposure to vibration. The purpose of this study was two-fold. The first objective was to quantify the mechanical properties of the inter-lamellar matrix in healthy control discs and the second objective was to determine the effect of exposure to vibration on the mechanical properties of the inter-lamellar matrix in order to determine if the positive link between vibration and herniation lies in the properties of this matrix. Tissue samples were dissected such that the inter-lamellar matrix between two adjacent layers was isolated, in contrast to the previous work of Fujita et al., (2000).

6.2. Methods

6.2.1 Specimen Preparation

Thirteen functional porcine spine units (two adjacent vertebrae with intervening disc) were obtained from a common source. These spinal units were obtained from the cervical level, specifically at levels c3/c4 and c5/c6. The use of a porcine animal model, in particular at the cervical level, has been found to be an adequate representation of the human lumbar vertebra in terms of anatomical and functional structure (Oxland et al., 1991; Yingling et al., 1999).

Muscle surrounding the spinal joint was dissected away to leave only the osteo-ligamentous structure. Spinal units were then secured into custom-made aluminum cups using both dental plaster (Denstone, Miles, South Bend, IN, USA) and 16 gauge wire wrapped around the lamina, prior to mechanical testing.

6.2.2 Mechanical Testing

Mechanical testing was carried out using a materials testing machine (8872, Instron Canada, Toronto, ON, Canada). A rotational brushless servomotor (Kollmorgen, Model AKM23D-BNCNC-00, Danaher Motion, Il, USA) was used to rotate the specimen about the flexion-extension axis and a torque transducer (SensorData Technologies Inc., Model T120-106-1 K, Sterling Heights, MI, USA) measured the moment applied to the specimen. Initially, each spinal unit was preloaded for 15 minutes with a load magnitude of 300N. During this preloading test, the angle of lowest torque was identified about the flexion-extension axis, which was defined as neutral position. Following preloading, each spinal unit was loaded to 1400N axial compression for two hours. Seven of the 13 spinal units were statically compressed (constant load of 1400N) while the remaining six were cyclically compressed (ranging from 1260N to 1540N, or ±10% of 1400N, thus maintaining equal cumulative compressive load to the statically

loaded spinal units). The statically compressed spines served as control specimens, while the cyclically loaded served as the vibrated test group. A sinusoidal waveform with a frequency of 5Hz was used for the vibrated specimens, as 5 Hz is the natural frequency of the lumbar spine (Dupuis, 1989; Panjabi et al., 1986; Pope et al., 1998; Wilder et al., 1982).

Following mechanical testing, each spinal unit was removed from the aluminum cups and further dissected by cutting away the posterior elements. This additional dissection exposed the posterior region of the disc in preparation for subsequent mechanical testing of the annulus.

6.2.3 Annular Dissection and Preparation

A total of 24 annular tissue samples were obtained from the mechanically compressed functional spinal units; 12 control tissues and 12 vibrated tissues. These tissue samples were obtained from the superficial layers (outermost four layers) of the anterior (6 control; 6 vibrated) and posterior (6 control; 6 vibrated) annulus. Two tissue samples from each disc were not always feasible, which is why a sample size of 24 was obtained, rather than 26 (13 discs x 2 samples from each disc).

Tissue samples were dissected such that the sample contained two intact adjacent annular layers, but with single layer free ends (Figure 6.1$A_{(1)}$). This dissection essentially isolated the inter-lamellar matrix. Each tissue sample was kept moist via saline misting (0.91% w/v of NaCl) prior to and during mechanical testing.

6.2.4 Mechanical Testing of Tissue Samples

Each tissue sample was mounted in a custom tensile testing system (BioTester 5000, CellScale, Waterloo Instruments Inc, Waterloo, ON) designed for small and thin biological tissues. Tissues were secured via tungsten five-prong rakes (Figure 6.1: A_2-D) in each of the single layer free ends. Tissues were preconditioned with three repeats of 10% strain at a rate of

1%/sec. Following preconditioning, tissue samples were strained until failure at a rate of 2%/sec. Force and displacement were sampled at 10 Hz using custom software (LabJoy 5.80, CellScale, Waterloo Instruments Inc, Waterloo, ON) during each failure test.

6.2.5 Data Analysis

The modulus of the inter-lamellar matrix was determined by calculating the slope of the linear region of the stress-displacement curve. This modulus is similar to the shear modulus, *G*; however, it was assumed that the thickness of the inter-lamellar matrix was negligible relative to the thickness of the lamellae, and thus displacement rather than shear strain was examined (Figure 6.2). This modulus was termed the sliding modulus, *g*. In addition to inter-lamellar matrix modulus, shear stress and displacement at the end of the toe region were determined (τ_T and s_T, respectively), as well as failure shear stress and displacement magnitudes (τ_F and s_F, respectively) (Figure 6.1E).

6.2.6 Statistical Analysis

A two-way Analysis of Variance was conducted in order to determine the effect of condition: control versus vibration, and on tissue extraction location: anterior versus posterior. An alpha level of 0.05 was set for all statistical tests.

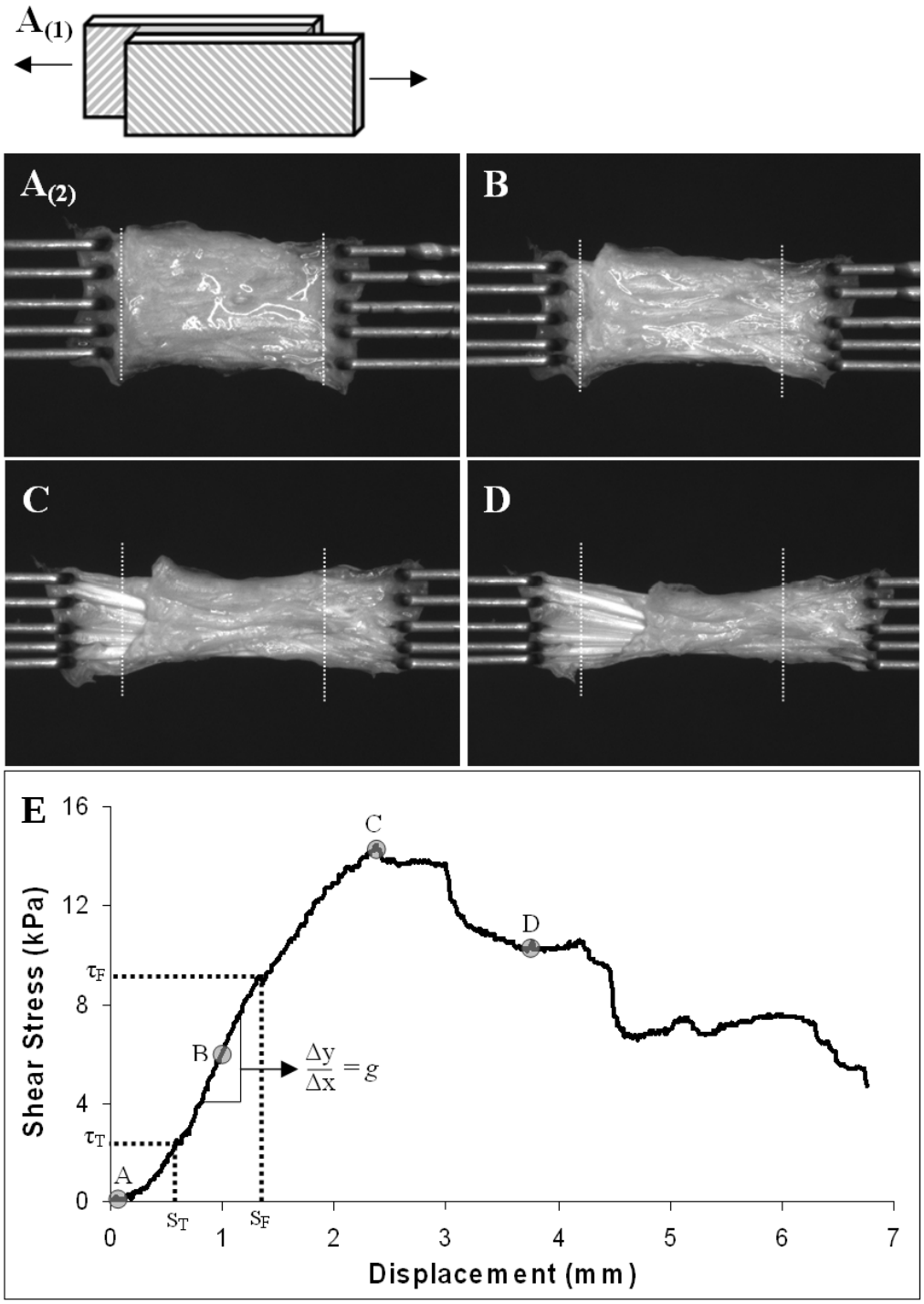

Figure 6.1: $A_{(1)}$: pictorial representation of the tissue sample dissection. $A_{(2)}$: Actual image of tissue at zero displacement. Dotted lines represent junction between single and bi-layered sections of the sample. Thus, each rake pierced only a single layer. B-D: Increasing displacement of tissue sample. Dotted lines represented original displacement. E: Shear stress-displacement curve identifying each mechanical property of interest as well as the location on the curve for each image ($A_{(2)}$-D).

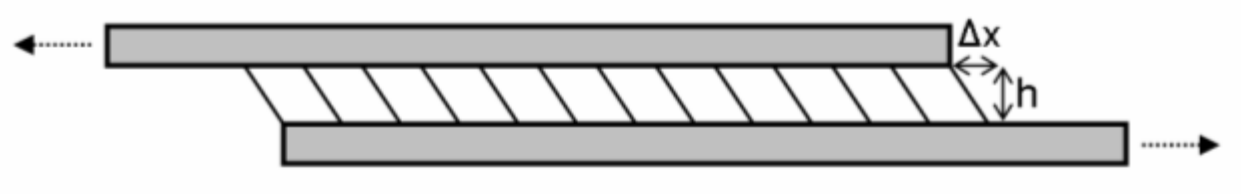

Figure 6.2: Schematic representation of shear strain. Grey portion represents each lamellae and the diagonal lines connect each lamellae represent the inter-lamellar matrix. Thickness of the inter-lamellar matrix (h) was assumed to be approaching zero, thus displacement (Δx) was of interest rather than shear strain. Arrows indict direction of displacement.

6.3. Results

6.3.1 The Effect of Vibration

Few differences were found between the control and vibrated tissues. For instance, no differences were observed in the inter-lamellar matrix sliding modulus, displacement and shear stress at the end of the toe region, or the failure shear stress. However, there was one variable that was affected by vibration, the displacement at failure. Failure displacement was significantly larger for the vibrated tissues as compared to the control tissues ($p = 0.047$, Cohen's d effect size = 0.90). Specifically, control tissues underwent a mean displacement of 1.99mm (S.D. 0.55) while the vibrated displaced to a mean of 2.52mm (S.D. 0.63) before failing. Table 6.1 summarizes the findings for the control and vibrated tissues.

6.3.2 The Effect of Tissue Location Extraction

No significant differences were found between tissues obtained from the anterior annulus as compared to the posterior annulus for any of the mechanical properties determined. Table 6.2 summarizes the findings for the anterior and posterior tissues.

Table 6.1: Mean (standard deviation) for each mechanical property as an effect of vibration. Each condition (control/vibration) had a sample size of 12. Italicized p value indicates significance. Units are as follows: τ_T and τ_F: kPa, s_T and s_F: mm, g: N/m^3

Mechanical Property		Control	Vibrated	*p value*	Statistical Power (%)
τ_T	Stress at Toe Region End	13.3 (10.9)	22.6 (19.4)	0.166	42.2
s_T	Displacement at Toe Region End	0.92 (0.50)	1.12 (0.55)	0.368	23.8
	Material Toughness	54.6 (43.1)	106.7 (74.6)	0.058	67.4
g	Sliding Modulus	4.80 x 10^7 (3.53 x 10^7)	7.07 x 10^7 (5.86 x 10^7)	0.270	31.0
τ_F	Failure Stress	72.4 (47.4)	111.5 (82.4)	0.185	41.3
s_F	Failure Displacement	1.99 (0.55)	2.52 (0.63)	**0.047**	n/a

Table 6.2: Mean (standard deviation) for each mechanical property as an effect of location. Each location (anterior/posterior) had a sample size of 12. Units are as follows: τ_T and τ_F: kPa, s_T and s_F: mm, g: N/m^3.

Mechanical Property		Anterior	Posterior	*p value*	Statistical Power (%)
τ_T	Stress at Toe Region End	13.7 (9.7)	22.1 (20.2)	0.207	36.5
s_T	Displacement at Toe Region End	1.10 (0.56)	0.94 (0.49)	0.461	18.4
	Material Toughness	76.0 (67.7)	85.4 (65.4)	0.721	9.7
g	Sliding Modulus	4.78 x 10^7 (3.13 x 10^7)	7.09 x 10^7 (6.08 x 10^7)	0.259	31.8
τ_F	Failure Stress	83.4 (61.0)	100.5 (77.3)	0.554	14.8
s_F	Failure Displacement	2.30 (0.74)	2.21 (0.55)	0.714	9.6

6.4. Discussion

Vibration, a known contributor to the risk of intervertebral disc herniation (Viikari-Juntura, 1997, Virtanen et al., 2007), was examined in terms of its effect on the mechanical properties of the inter-lamellar matrix of the annulus fibrosus. The properties of the inter-lamellar matrix were uniquely examined via a sliding tensile test. Specifically, two intact adjacent layers of the annulus were slid laterally (or parallel to the endplates) until failure. Few differences between healthy control and vibrated tissues were observed with the exception of the displacement at failure. Vibrated tissues slid to a greater displacement before failure than control tissues.

The inter-lamellar matrix is an important structure in the annulus. Similar to other composite materials, the annulus is stronger as a result of the adhesion of adjacent lamellae, as compared to the strength of individual lamellae in isolation (Adams & Green, 1993; Elliot & Setton, 2001; Schollum et al., 2008). The inter-lamellar matrix provides structural support, while still permitting some sliding between the layers. Finite element modeling has predicted that shear stresses between annular layers are responsible for annular delamination (Goel et al., 1995); therefore it is important to understand the properties of the inter-lamellar matrix in order to determine the potential for delamination in various loading scenarios such as vibration. Thus, to maintain the integrity of the disc, adhesion between adjacent layers must exist. To the author's knowledge, this study was the first to isolate and quantify the mechanical properties of the inter-lamellar matrix in both control discs and discs that had been exposed to vibration. However, previous work has examined the shear properties of multi-layered annular samples. Fujita et al. (2000) examined the shear behaviour of annular cubes (approximately 30 mm^3) by applying shear strain in-plane with the annular layers which indirectly examined gross response of the

total number of inter-lamellar matrices present in the sample. This resulted in multiple annular layers and multiple inter-lamellar matrices being tested, rather than solely the inter-lamellar matrix between two adjacent lamellae.

In terms of the effect of vibration, given that no effect on failure stress was observed, it is very plausible that vibration did not damage the collagen fibres of the inter-lamellar matrix (primarily type VI), as collagen is the major tensile load-bearing component of the inter-lamellar matrix (Adams et al., 2006). In addition to collagen, the inter-lamellar matrix is comprised primarily of proteoglycans and elastin (Yu et al., 2002; Yu et al., 2005). However, previous research has shown that the extensibility of a tissue, or how it will strain prior to failure, is primarily dependent on elastin (Smith et al., 2008; Smith & Fazzalari, 2009). Specifically, connective tissues will become more extensible when elastin is absent or if elastin is damaged. Therefore, based on the observed increase in displacement prior to failure in the vibrated tissues, vibration may have damaged the elastin in the inter-lamellar matrix.

Elastin is abundant in many connective tissues, including the inter-lamellar matrix of the annulus (Yu et al., 2002; Yu et al., 2005) and its primary purpose is to assist in recovery following strain (Smith & Fazzalari, 2009). Under normal loading, the annulus, including the inter-lamellar matrix, is subject to multi-directional loading (Edwards et al., 2001; McNally & Adams, 1992; Shirazi-Adl et al., 1984; Stokes, 1987; van Deursen et al., 2001). Elastin helps the tissue return to its original state of elongation following a reduction in tensile load. Without elastin, the ability to recover is substantially lessened which could result in residual strain on other matrix components including the type VI collagen fibres. These collagen fibres form a complex bridging network between adjacent lamellae and function as load bearers (Melrose et al., 2008; Schollum et al., 2009). Further, the collagen fibres are primarily responsible for

resisting delamination and could ultimately fail due to fatigue or prolonged loading. Once a tissue has delaminated, its potential to herniate is significantly higher. In fact, it has been proposed that some level of delamination within the annulus is necessary for herniation to progress, and that delamination is a stage that precedes posterior nuclear migration and protrusion (Adams & Hutton, 1985). In a previous study in this thesis, vibration was found to also increase the extensibility of the intra-lamellar matrix (connective tissue between collagen bundles within each lamella) within its toe region (Chapter 5). Both matrices are involved in resisting herniation progression and it appears that vibration has a similar negative effect on both components.

In terms of tissue harvest location, no differences were observed between tissues obtained from the anterior and posterior region of the annulus; however, only superficial sections were tested in this study. It is possible, due to previous findings of regional differences within the annulus, that similar differences would be observed here if both superficial and deep sections were observed. In general, outer annular tissue samples are more stiff (Holzapel et al., 2005) and fail at higher stresses (Skaggs et al., 1994). In another study, it was observed that the shear modulus between layers of the annulus was higher in the outer region as compared to the deep region (Fujita et al., 2000) and therefore it is likely that regional differences exist between superficial and deep tissues.

The current study examined the inter-lamellar matrix using a novel approach, however, limitations should be addressed. First, a porcine model was studied rather than human cadaveric tissue. However, published anatomical and functional similarities (Oxland et al., 1991; Yingling et al., 1999), as well as the ability to control many variables including age, weight, diet, and activity level, justified the use of a porcine model. Additionally, the inter-lamellar matrix may

not have been completed isolated, and the contribution of the individual layers of the annular lamellae may have been included in the magnitude of the properties measured. However, care was taken to ensure this contribution was minimized by inserting the rakes close to the junction between the single and bi-layered sections of the tissue (represented by the dotted lines in Figure 6.1$A_{(2)}$). Additional analysis revealed that the displacement contribution of the individual layers was less than 10% of the total displacement, which provided confidence that the inter-lamellar matrix was sufficiently isolated and the reported material properties are representative of the matrix.

6.5. Conclusion

The adhesion between adjacent lamellae in the annulus is vital to the integrity and strength of the annulus as a whole. Delamination, or the separation of these lamellae, is one of the stages of intervertebral disc herniation, which suggests that herniation progression is strongly related to the strength of the inter-lamellar matrix. This study examined the mechanical properties of the inter-lamellar matrix between two adjacent layers of the annulus following either two hours of static compression or two hours of vibratory compression. Vibrated tissues failed at greater displacements, but at similar shear stresses as the control tissues. This increased extensibility of the vibrated tissues is due to damage to components in the matrix, and in particular could be attributed to damage to the elastin fibres. Damaged elastin may lead to altered and sustained tensile loading on other structures such as collagen, which could subsequently fail and cause delamination.

Chapter 7

Does vibration influence the initiation of intervertebral disc herniation? An in-vitro analysis to determine a causal relationship

Chapter Synopsis

Exposure to vibration has been linked to an higher reporting of low back pain and in particular disc herniation via epidemiological studies. However, these studies are unable to determine causal relationships. *In vitro* tissue experimentation assists in determining if certain exposures, for example vibration, actually lead to herniation. The objectives of this study were two-fold. The first goal of this study was to determine the effect of exposure to axial vibration on the initiation and progression of disc herniation. Second, this study aimed to determine the effect of exposure to vibration and the presence of disc damage on the mechanical properties of individual lamella. Twenty functional spine units (FSU) were subjected to repetitive flexion-extension (6000 cycles), which has been shown to produce intervertebral disc herniation. While being exposed to the repeated motion profile, ten of these FSUs were statically compressed under 1400N (control group) and the 10 were cyclically compressed (1260N-1540N) at a frequency of 5 Hz (vibration group). Post collection, the intervertebral discs were further dissected and individual lamella of the annulus were tested under uniaxial tension to failure (tension applied perpendicular to the orientation of the collagen fibres) to assess the mechanical properties. Of the ten control FSUs, four had evidence of herniation initiation while eight of the ten vibrated FSUs showed herniation initiation ($p = 0.01$). No significant differences in disc height loss or FSU stiffness were observed between the control and vibrated groups. Further, no significant differences were observed between the two groups for any of the single lamella mechanical properties. However, this study has confirmed that vibration is a causal mechanical risk factor that significantly increases the occurrence of herniation.

7.1 Introduction

The intervertebral disc functions primarily to enable bending motion between adjacent vertebral bodies of the spine (Cassidy et al., 1989; Guerin & Elliott, 2006; Klein & Hukins, 1982a). Similar to any biological tissue, the disc is at risk of injury depending on the type, frequency and magnitudes of load they experience; interestingly, it is the ability to accommodate bending motions that put the disc at increased risk of herniation (Callaghan & McGill, 2001). Herniation is characterised by the posterior migration of the nucleus pulposus through the layers of the annulus fibrosus (Haughton, 1988), and can eventually result in complete prolapse into the spinal canal.

Herniation can result in debilitating pain (Adams et al., 2006) and affect quality of life if the extruded nuclear material compresses the spinal cord and/or nerve roots. It is therefore important to understand factors that increase the risk of herniation in order to mitigate this risk. Epidemiological studies have assisted in identifying relationships between mechanical exposures and disc herniation, but have been unable to definitively conclude that an exposure can directly lead to herniation. Researchers therefore have turned to *in vitro* or tissue experimentation to assess the effect of various exposures on injury initiation and progression. For example, epidemiological investigations have shown that repetitive lifting is positively correlated with low back pain (Macfarlane et al., 1997; Magora, 1974; Norman et al., 1998), and disc herniation (Videman et al., 1990); subsequent *in vitro* tissue experimentation has confirmed repetitive flexion-extension motion as a definitive mechanical cause of herniation by examining the degree of injury after such an exposure (Aultman et al., 2005; Callaghan & McGill, 2001). Similarly, exposure to vibration has been related to herniation via epidemiological studies (Viikari-Juntura, 1997; Virtanen et al., 2007), yet this relationship has not been examined at the tissue level, and

therefore it is not currently possible to conclude that vibratory loading does increase the risk of disc herniation.

A current hypothesis of the mechanical link between vibration and herniation is that vibration repetitively strains the layers of the annulus, potentially leading to fatigue failure of annular components including the intra and inter-lamellar matrices. Previous studies in this thesis have shown mechanical changes to both these matrices as a result of vibration exposure and based on these findings it is hypothesized that the mechanism lies in elastin damage and the resulting reduced ability of the tissue to recover from tensile strains (Chapters 5 and 6). If this is the case, then an accelerated initiation of herniation is expected in discs exposed to vibration. The purpose of this study was two-fold. The first objective was to assess the effect of a single dose exposure of vibration on the initiation of herniation in discs subjected to repetitive flexion and extension with moderate compression. The second objective was to examine the effect of this repetitive flexion/extension exposure on the mechanical properties of single lamellae.

7.2 Methods

7.2.1 Specimen Preparation

Twenty porcine cervical (c3/c4) functional spine units (two adjacent vertebrae and intervening disc) were obtained from a common source. Previous research has documented similarities between the porcine cervical spine and the human lumbar spine in terms of anatomy and function (Oxland et al., 1991; Yingling et al., 1999). Each spinal unit was dissected to remove surrounding muscle leaving only the osteo-ligamentous joint. Once dissected, each spinal unit was secured into custom-made aluminium cups via screws into the superior endplate of c3 and the inferior endplate of c4. Sixteen-gauge wire was also used to fix the specimen to the

cups by wrapping the wire around the lamina and securing the ends through the cups. Last, dental plaster (Denstone, Miles, South Bend, IN, USA) was used to fill around the specimen and wires to add additional fixation. The intervertebral disc of each spinal unit was then injected with a dye consisting of 0.7 cm^3 barium sulfate (radiopaque), blue dye (Coomassie Brilliant Blue G-mix: 0.25% dye; 2.5% MeOH; 97.25% distilled water), and water in a ratio of 2:1:2 (radiopaque: dye: water). This dye allowed for visual identification of the nucleus within the disc in X-ray films. Each spinal unit was wrapped in saline (0.91% w/v of NaCl) soaked gauze to maintain specimen moisture throughout collection.

7.2.2 Experiment 1 - Spinal Unit Mechanical Testing: Data Collection

Each spinal unit was initially preloaded with 300N of compression for 15 minutes using a servo-hydraulic dynamic materials testing apparatus (8872, Instron Canada, Toronto, ON, Canada). A rotational brushless servomotor (Kollmorgen, Model AKM23D-BNCNC-00, Danaher Motion, Il, USA) was used to rotate the specimen about its flexion-extension axis and a moment transducer (SensorData Technologies Inc., Model T120-106-1 K, Sterling Heights, MI, USA) measured the applied moment to the specimen. During this preloading trial, the angle of lowest moment was determined and defined as zero spinal flexion (neutral position). Following preloading, each spinal unit was rotated five times through a range of flexion and extension (termed passive test) at a rate of 0.5°/sec while under 300N of compression. The last three passive test repeats were used to determine the elastic region, or neutral zone, of the specimen. The end points of the neutral zone were set as the degree of flexion when the slope of the torque-angle curve rapidly increased during the rise (to determine flexion end point) and return (to determine extension end point) to the neutral position (Figure 7.1). These end-points served as the target flexion and extension angle during the experimental testing protocol.

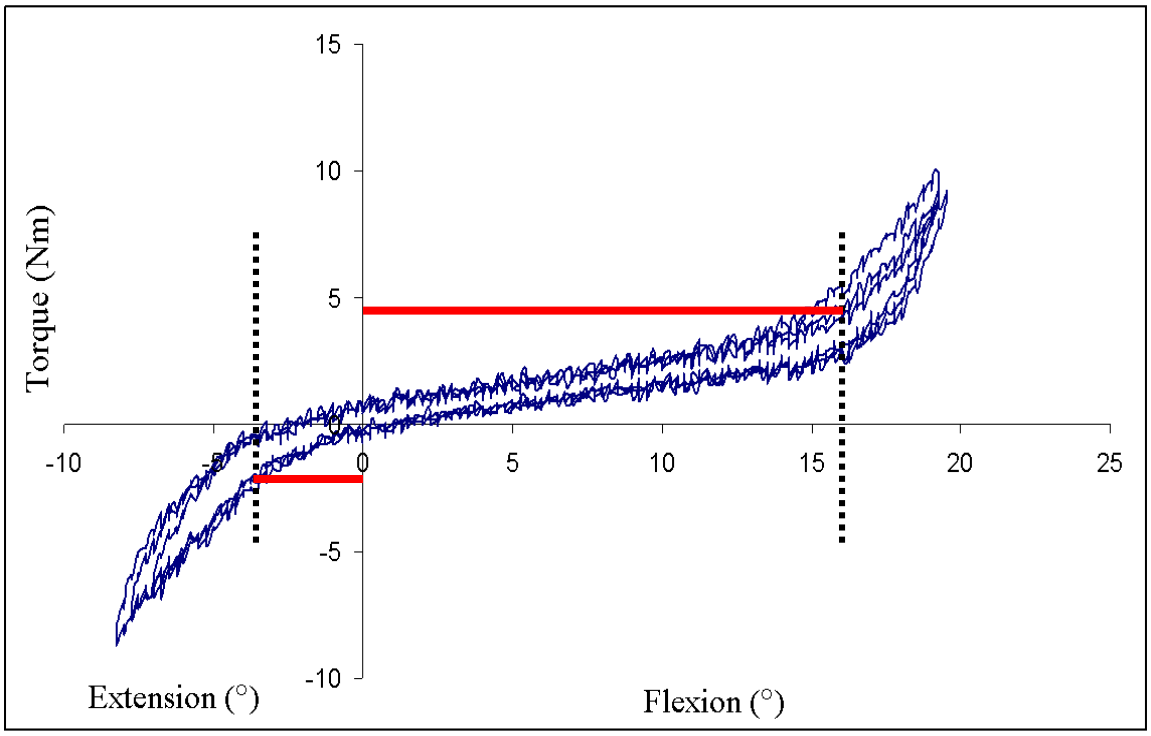

Figure 7.1: Example of a passive range of motion test (3 full flexion/extension cycles) for a functional spine unit. Dotted lines represent the end of the neutral zone in flexion and extension. These angles were set as the target flexion and extension angles in the herniation protocol. Solid lines indicate torque values at either end of the neutral zone. These values were used to calculate FSU stiffness.

Following the preload and range of motion tests, specimens were X-rayed in the sagittal plane and were subsequently developed with a digital X-ray system (Kodak DirectView CR500, Carestream, Toronto, Canada). Once X-rayed, specimens were mounted in the materials testing apparatus for the experimental testing protocol. Each spinal unit was subjected to a protocol shown to initiate intervertebral disc herniation (Callaghan & McGill, 2001). This protocol incorporates repeated spinal flexion and extension at a rate of 1 Hz in combination with moderate axial compressive load (1400N). Each spinal unit was randomly assigned to one to two groups: control (n = 10) or vibration (n = 10). The control group was subjected to a statically applied compressive load of 1400 N while simultaneously being flexed and extended at a rate of 1 Hz. The vibration group was subjected to a cyclically applied compressive load ranging from 1260N to 1540N (±10% of 1400N) at a frequency of 5 Hz (sinusoidal waveform) while simultaneously being flexed and extended at a rate of 1 Hz. Five Hz vibration was chosen as it is the natural frequency of the lumbar spine (Dupuis, 1989; Panjabi et al., 1986; Pope et al., 1998; Wilder et al., 1982) and was deemed to be a worst case exposure.

Specimens were compressed (statically or cyclically depending on the group) and simultaneously flexed and extended to 6000 cycles. X-rays were taken after 4000, 5000, and 6000 cycles. Following the experimental protocol, specimens were loaded under 300N of static compression and subjected to an additional three passive test repeats.

7.2.3 Experiment 1 - Spinal Unit Mechanical Testing: Data Analysis

Loss in disc height was determined from the position data recorded from the actuator of the Instron. These data were sampled throughout the duration of the testing at a sampling rate of 20 Hz. Rotational stiffness within the neutral zone was determined by fitting a straight line between the extension end-point and the flexion end-point (see dotted and red lines in Figure 7.1)

from the torque-angle curves for each of the last three repeats of the passive test described in section 7.2.2. The mean of these three stiffness values was considered the pre-stiffness measure. Similar analyses were conducted on the post-test passive tests to obtain a post-stiffness measure. The percent change in these two stiffness values was determined using the following equation:

Eq. 7.1 $$\text{Percent Stiffness Change} = \frac{(\text{mean post stiffness} - \text{mean pre stiffness})}{\text{mean pre stiffness}} * 100$$

7.2.4 Experiment 2 - Post-collection Specimen Dissection

Following data collection, the posterior structures of the spinal unit were removed to expose the posterior surface of the intervertebral disc. This allowed for subsequent mechanical testing of the annulus. Discs that had intact posterior annulus layers post-collection were used for subsequent testing to examine the mechanical properties of single layers of the posterior annulus. From the 20 tested spinal units, six of the control specimens (four non-herniated; two partially herniated) and five of the vibrated specimens (two non-herniated; three partially herniated) were still intact posteriorly, yielding a total of 11 annular tissue samples. Tissue samples were dissected using a light microscope (Nikon SMZ 1000, Nikon Instruments Inc, Melville, NY, USA) in order to ensure that only one layer of the annulus had been isolated and that no damage had occurred during the dissection. A partial herniation was defined as posterior migration of the nucleus that had not reached the outer most posterior layer of the annulus. Single annular samples were further dissected such that the orientation of the collagen fibres ran parallel to the edges of the sample. Each sample was obtained from the posterior-lateral region of the annulus from the superficial layers (layers 1-4).

7.2.5 Experiment 2 - Annular Tissue Mechanical Testing: Data Collection

Each prepared tissue was mechanically tested using a custom biaxial tensile testing system (BioTester 5000, CellScale, Waterloo Instruments Inc, Waterloo, ON). Tissues were mounted in a similar fashion as described in Chapter 5 (section 5.2.2) such that tensile strain could be applied perpendicular to the orientation of the collagen fibres, and secured via five-pronged tungsten rakes (Figure 5.3 in Chapter 5). By mounting the tissues in this orientation, the intra-lamellar matrix (tissue between adjacent collagen fibres within the layer) could be isolated. Tissues were preloaded to no more than 5 mN in order to remove any residual slack as a result of mounting. A preconditioning test was subsequently conducted which consisted of three repeats of 10% strain at a rate of 1% strain/sec. Following preconditioning, each tissue was strained at a rate of 2% strain/sec until failure. Tissues were misted with saline (0.91% w/v of NaCl) in order to maintain tissue moisture. Force and displacement were recorded using custom software (LabJoy 5.80, CellScale, Waterloo Instruments Inc, Waterloo, ON) at a sampling rate of 10 Hz.

7.2.6 Experiment 2 - Annular Tissue Mechanical Testing: Data Analysis

Stress-strain curves for each failure test were created from the force and displacement data by normalizing by the cross-sectional area and length of the tissue sample, respectively. Cross-sectional area was measured using a measurement displacement sensor (ZX-LD40L, Omron Electronics, Toronto, ON). A number of variables were examined from these stress-strain analyses (previously shown in Chapter 5, Figure 5.4).

7.2.6.1 Toe Region

The stress and strain values at the end of the toe region (junction between toe region and subsequent linear region) were determined for each tissue.

7.2.6.2 Linear Region

The slope (modulus) of the linear region was determined for each tissue. Image detection software (LabJoy 5.80, CellScale, Waterloo Instruments Inc, Waterloo, ON) was also used to determine the deformation in the orthogonal axis (parallel to collagen fibre orientation) in order to determine Poisson's Ratio within the linear region. Poisson's ratio was calculated using the equation 5.1 in Chapter 5.

7.2.6.3 Initial Failure and Ultimate Strength

The stress and corresponding strain magnitude at the initial point of failure and ultimate failure were determined. Initial failure was defined as a sudden drop in stress or a transition into a non-linear region or plastic region. Ultimate strength and strain were defined as the maximum stress and corresponding strain magnitude.

7.2.6.4 Material Toughness

Material toughness was determined by integrating the stress-strain curve from zero strain to 12.5 % strain, using trapezoidal integration, and was considered the "usable toughness" region previously described in Chapter 5 (section 5.2.3.5).

Following mechanical testing, each disc was completely cut in the transverse plane in order to assess the annular damage (Figure 7.2). Damaged discs (herniation) were further analyzed using ImageJ version 1.42 (public domain image processing software distributed by the National Institutes of Health) software to determine the size of the damaged area. This damaged area was expressed as a percentage of the original size of the nucleus (pre mechanical testing) using the following equation:

Eq. 7.2 $$\text{Percent damage} = \left(\text{(damaged area) / (original area)} \right) * 100$$

Original nucleus size was determined by taking the mean between the measured nuclear area of the c2/c3 and c4/c5 discs (superior and inferior to the experimental disc) which were determined at the start of data collection.

7.2.7 Statistical Analysis

A chi-square analysis was conducted on the number of herniated specimens. An expected frequency of herniation of 40% was used based on previous literature (Marshall, 2008; Tampier, 2006).

A two-way Analysis of Variance was conducted with the following independent variables: condition (two levels: control versus vibration) and injury (two levels: herniation versus no herniation). Each of the variables described in sections 2.3 and 2.6 were statistically tested in order to determine the effect of condition and injury occurrence. An alpha level of 0.05 was used to determine significance.

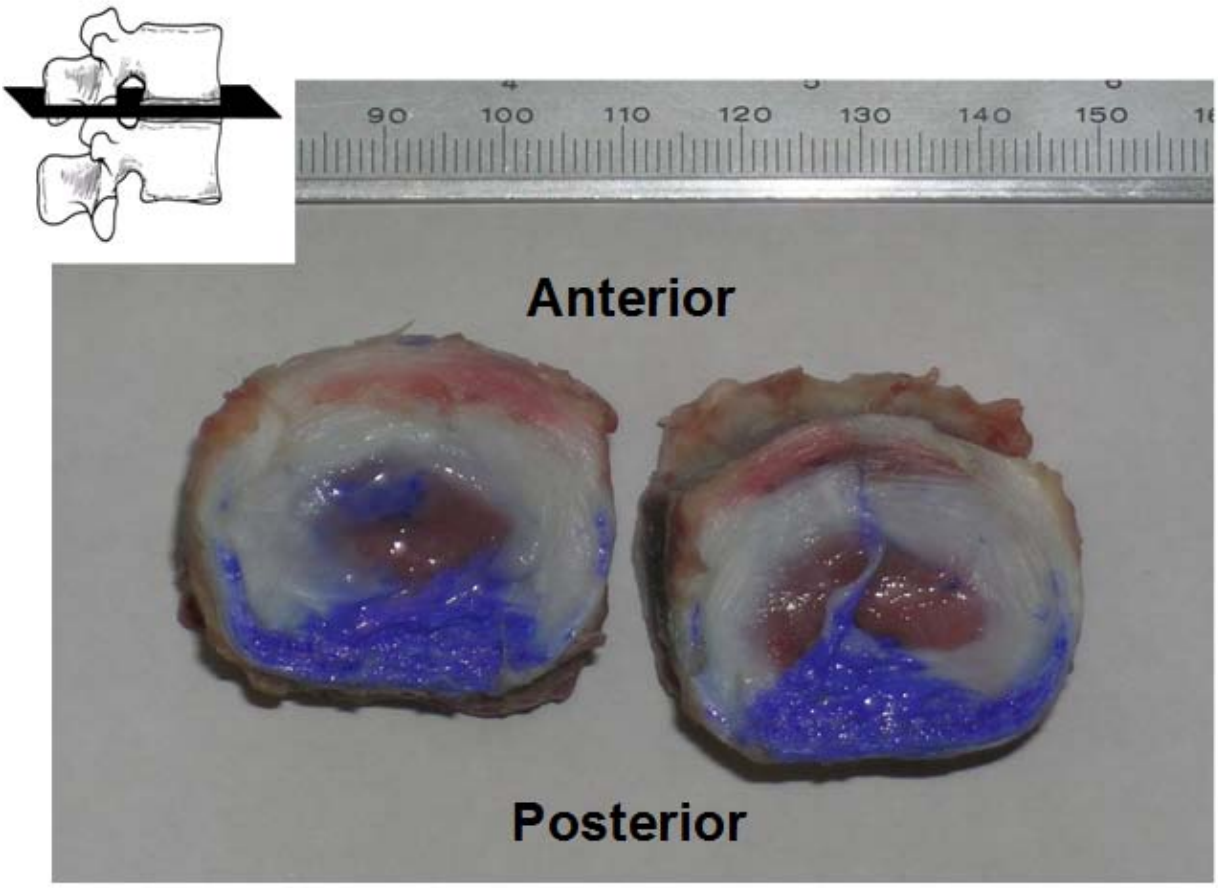

Figure 7.2: Example of a herniated disc. Upper left hand corner shows pictorial representation of how the disc was cut transversely in order to expose the inside of the disc and to assess the damage. Dye was injected into the nucleus prior to testing for visual tracking purposes. Scale is in cm.

7.3 Results

7.3.1 Number of Herniated Discs and Extent of Herniation

Twenty spinal units were tested; 10 control and 10 vibrated. Of the 10 control, four herniated (40%); while eight of the 10 vibrated spinal units herniated (80%) (chi square p-value = 0.01, Cohen's d effect size = 0.58). Of the four herniated control discs, three were partial herniations (herniation did not reach outer layer of annulus) and one was a full herniation (herniation reached outer layer of annulus). Of the eight herniated vibrated discs, six were partial herniations and two were full herniations. In terms of the percent damage, the four herniated discs in the control group had a mean percent damage of 269% (S.D. 116%) while the eight herniated discs in the vibration group had a mean percent damage of 169% (S.D. 186%); however, this was not significantly different (p = 0.35, statistical power = 30.7%).

7.3.2 Experiment 1 - Spinal Unit Mechanical Testing

Disc height loss was not significantly different between the control specimens (mean height loss of 3.56mm (S.D. 0.47)) and the vibrated specimens (mean height loss of 3.90mm (S.D. 0.72)); p = 0.75, statistical power = 34.7%. However, a significant interaction between condition (control versus vibration) and the presence of a disc herniation was observed (p = 0.046). Figure 7.3 depicts this interaction.

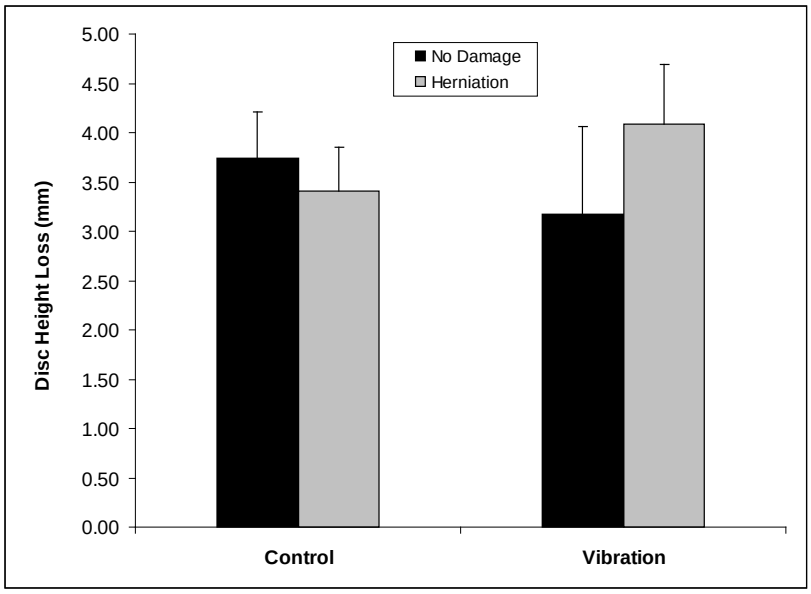

Figure 7.3: Significant interaction observed between condition (control/vibration) and injury (no herniation/herniation) for loss in disc height.

Percent stiffness change between pre and post cyclic (flexion/extension) mechanical testing was not significantly different between the control and vibration groups, with a mean stiffness increase of 23.0% (S.D 13.4) for the control specimens and 26.3% (S.D. 6.0) for the vibrated specimens ($p = 0.37$, statistical power = 17.5%). Further, no statistical difference in percent stiffness change was observed between the herniated and non-herniated discs ($p = 0.07$, statistical power = 38.2%), although, a trend towards a greater increase in stiffness was apparent in the non-damaged discs. Herniated discs had a mean percent increase in stiffness of 25.3% (S.D. 10.8) while the non-herniated discs had a mean percent increase in stiffness of 34.2% (S.D. 16.5).

7.3.3 Experiment 2 - Annular Tissue Mechanical Testing

No significant differences were observed between the vibrated and control specimens for any of the variables described in section 7.2.6. Further, no differences between herniated and non-herniated specimens were observed for these variables. However, a trend was observed for failure strain ($p = 0.07$, statistical power = 66.7%) with non-herniated discs failing at higher strains than herniated discs. Tables 7.1 and 7.2 summarize these findings.

7.3.4 X-ray Images

The original purpose of the X-rays was to identify when the disc had herniated; however, the X-rays were not able to provide enough visual information to accurately and consistently identify an injury. Therefore, the protocol was altered to subject each IVD to the same number of cycles (6000) rather than to rely on the X-rays to identify the point of injury. The second purpose of the X-rays was to obtain nuclear path information; however, the X-rays again were not able to provide sufficient detail to answer this question. Low concordance between sagittal plane X-rays and disc dissection (considered the gold standard) was seen by Yates (2009) and therefore

percent damage calculations were performed on each dissected disc to obtain a quantitative measure of damage. Sample X-ray images are in the Appendix (pages 147-150).

Table 7.1: Mean (standard deviation) values for tissue samples obtained from the control and vibrated discs.

	End of Toe Region Strain (%)	End of Toe Region Stress (MPa)	Elastic Modulus (MPa)	Poisson's Ratio
Control (n=6)	26. 2 (35.6)	0.14 (0.06)	3.07 (2.26)	0.50 (0.29)
Vibration (n=5)	16.6 (15.27)	0.17 (0.07)	1.90 (1.15)	0.44 (0.23)
p-value	0.73	0.55	0.21	0.85
statistical power (%)	9.2	11.7	19.9	6.7

	First Initial FailureStrain (%)	First Initial Failure Stress (MPa)	Failure Strain (%)	Tensile Strength (MPa)	Toughness (kPa)
Control (n=6)	65.1 (42.0)	1.15 (0.83)	76.5 (44.2)	1.30 (0.85)	4.40 (2.29)
Vibration (n=5)	56.2 (24.4)	0.83 (0.53)	94.1 (49.2)	1.04 (0.55)	8.86 (9.27)
p-value	0.99	0.32	0.26	0.40	0.38
statistical power (%)	7.2	12.1	9.5	9.4	18.3

Table 7.2: Mean (standard deviation) values for tissue samples obtained from the non-herniated and herniated discs.

	End of Toe Region Strain (%)	End of Toe Region Stress (MPa)	Elastic Modulus (MPa)	Poisson's Ratio
Non-herniated (n=6)	26.4 (39.7)	0.13 (0.09)	1.97 (0.74)	0.51 (0.18)
Herniated (n=5)	16.3 (12.6)	0.13 (0.04)	3.22 (1.94)	0.43 (0.33)
p-value	0.71	0.55	0.20	0.71
statistical power (%)	9.1	5.0	27.5	7.7

	First Initial FailureStrain (%)	First Initial Failure Stress (MPa)	Failure Strain (%)	Tensile Strength (MPa)	Toughness (kPa)
Non-herniated (n=6)	75.8 (37.9)	0.89 (0.48)	104.7 (47.0)	1.05 (0.58)	4.89 (2.23)
Herniated (n=5)	43.5 (11.6)	1.14 (0.94)	60.4 (20.9)	1.34 (0.87)	8.27 (9.66)
p-value	0.18	0.45	0.07	0.44	0.57
statistical power (%)	50.8	8.4	54.6	9.8	11.9

7.4 Discussion

Epidemiological studies have identified vibration as a risk factor for the development of intervertebral disc herniations (Viikari-Juntura, 1997; Virtanen et al., 2007); however, these studies could only comment on a relationship between long-term exposure to vibration and disc herniation, and have been unable to provide causation information. The current study was the first to examine the effect of a single dose exposure of vibration on the development of intervertebral disc herniation. It was discovered that a significantly greater number of intervertebral discs initiated the process of disc herniation when exposed to 5 Hz vibration in conjunction with repetitive flexion and extension and moderate compression.

Intervertebral disc herniation is a cumulative injury to the disc such that prolonged exposure is required to damage the annulus. Repetitive flexion/extension has been shown to induce herniation via repetitively stressing the annular layers (Aultman et al., 2005; Callaghan & McGill, 2001; Marshall, 2008; Tampier, 2006; Tampier et al., 2007). Vibration, similar to cyclic loading, appears to accelerate this cumulative injury, likely via a fatigue failure mechanism within the various components of the annulus. These components, namely the intra-lamellar matrix (connective tissue within each layer holding collagen bundles together), and the inter-lamellar matrix, (connective tissue between adjacent lamellae), are strongly associated with the initiation and progression of herniation. Specifically, research has shown that delamination often immediately precedes herniation (Adams & Hutton, 1985), and eventually progresses through clefts that have formed in the lamellae (Tampier et al., 2007). Delamination is averted by a strong intact inter-lamellar matrix, and clefts are less likely to occur when the intra-lamellar matrix is healthy and undamaged. Therefore, the integrity of both these matrices is essential for herniation prevention. Previous tissue work in this thesis has shown that exposure to 5 Hz

vibration, while in a neutral joint posture, altered the mechanical properties of both the intra and inter-lamellar matrices, resulting in increased extensibility of each component (Chapters 5 and 6). This was hypothesized to be due to damaged elastin in both matrices. It is likely that, in the current study, the added vibration had a similar damaging effect on elastin, thus compromising the annulus and accelerating herniation.

Interestingly, no differences in the extensibility of single annular tissues were observed from the outer posterior region, which is dissimilar to previous findings in neutral spines (Chapter 5). However, this is likely due to experimental differences with FSUs in the current study being subjected not only to vibration, but also repetitive flexion-extension which has been shown on its own to be injurious to the disc. This combination of exposures may have damaged additional structures such as collagen or proteoglycans, altering the mechanics of single layers. Further, the moduli, strain and stress values tended to be lower than reported in Chapter 5, when examined after only two hours of static or vibratory compression in neutral postures. This suggests that repetitive flexion-extension has a more damaging effect that compressive loading alone.

In the annular tissue samples, only failure strain was close to being significantly different between the damaged and non-damaged discs. A trend of lower failure strain in damaged tissue was observed. It is possible that collagen fibres and/or proteoglycans in the herniated discs were damaged as previously mentioned, which may have altered the mechanical properties differently (i.e. lower failure strain) than if only elastin were damaged.

It is interesting that vibration did not have an effect on disc height loss or change in stiffness when all specimens were collapsed, yet are comparable to reported disc height loss as a result of a similar loading protocol (mean disc height loss of 3.50mm reported by Drake &

Callaghan, 2009) however the significant interaction observed for loss in disc height is worth noting. Greater disc height loss was observed in the vibrated specimens that herniated as compared to the vibrated non-herniated discs, but this was not the case for the non-vibrated discs. In the non-vibrated discs, height loss was similar between the herniated and non-herniated discs. This suggests that discs that herniate following exposure to vibration in conjunction with repetitive flexion-extension will suffer from greater loss in disc height than herniated discs that have not been exposed to vibration. Therefore, vibration may indirectly cause greater height loss in the disc, which could lead to low back pain if nerve roots become impinged as a result of the disc height loss. It is important to note that the exposure to vibration in the current study was a single-dose exposure, which is likely different from the exposures examined in the epidemiological studies which were likely more long duration exposures.

In terms of mechanical differences between damaged and undamaged discs, herniated discs showed a reduced FSU rotational stiffness increase post collection. Although this finding was not statistically significant, the stiffness difference was likely due to the dispersion of the nuclear material in the herniated discs. Discs that have suffered from herniation tend to be less stiff than intact discs, but this has been attributed to loss in disc height and subsequent slack in the ligaments around the joint (Adams et al, 1987; Brown et al., 2002; Mimura et al., 1994). However, no difference in disc height loss was observed, which suggests that the mechanism of reduced stiffness in herniated discs is more complex than just loss in disc height.

The lack of differences in mechanical properties between damaged and undamaged tissue, other than failure strain, may have been due to the location of tissue extraction. Tissue samples were obtained from the superficial section of the posterior annulus, and unless a full

herniation had occurred, these tested tissue samples may not have actually been damaged. Future work should consider examining the mechanical properties of known damaged layers.

7.5 Conclusion

Exposure to vibration has been linked to intervertebral disc herniation via epidemiological studies; however these data are unable to provide causal information. This study examined the affect of vibration on herniation initiation via tissue experimentation. Specifically, 20 functional spine units were subjected to a known contributor to herniation; repetitive flexion and extension with moderate compression. Half of the spinal units were subjected to static compression (1400N) while the other ten were subjected to prolonged vibratory compression (1260-1540N) at a frequency of 5 Hz. There was a significant difference with an increase in the number of vibrated spinal units herniated as compared to the control spines after an equal number of flexion-extension cycles. This is the first study to document increased herniation with exposure to prolonged vibration. Continued work is needed to determine which specific structures in the disc become compromised as a result of both repetitive flexion-extension and exposure to axial vibration.

Chapter 8

Thesis Summary

8.1 Thesis Summary

The overriding focus of this thesis was to better our understanding of the mechanical properties, and their relationship to disc herniation, of single and multiple layered annular samples. Further, this thesis aimed to determine the mechanical effect of exposure to vibration on individual components of the annulus, including the intra-lamellar matrix and the inter-lamellar matrix. Each of these matrices is highly important in maintaining the integrity of the annulus, and each play a vital role in the prevention of intervertebral disc herniation.

Two-layered annular samples were examined in both uniaxial and biaxial tensile scenarios, and were also strained at various physiological rates. These studies investigated the effect of different loading states on the mechanical properties of the annulus and how it may alter the initiation and propagation of herniation. It was concluded that the annulus is subject to much higher stresses and is stiffer when strained biaxially, which is far more representative of how the annulus is strained *in vivo*. Furthermore, the majority of previously documented failure strengths and moduli values have been determined uniaxially, and do not reflect *in vivo* loads. These new findings will assist in creating more accurate models of the disc, and in particular the layers of the annulus, and allow for greater confidence in the loading scenarios that the annulus can tolerate and what scenarios can result in injury.

In terms of the effect of strain rate, if strained at rates likely induced by voluntary movements (up to 4% strain/sec), the annulus is strain rate independent. This is a dissimilar finding compared to many other documented soft tissues, which have been found to be strain rate dependent. This information is pertinent to the understanding of how the annulus is loaded *in vivo* and can assist in determining if the disc is at an elevated risk of injury during various loading scenarios, such as lifting, that may be performed at rates similar to those examined in the

current study. These two studies combined have shown that the annulus is subject to higher than previously documented stresses and is stiffer *in vivo* than previously reported, and these stresses and moduli remain constant through a range of physiological strain rates.

Another objective of this thesis was to determine the effect of vibration exposure on the mechanical properties of both the intra and inter-lamellar matrices, and further hypothesize how these changes affect initiation and progression of herniation. Unique, intricate dissection techniques were developed and used to assess these matrices following static and 5 Hz vibratory compressive load. It was discovered that tissues exposed to vibration were more extensible and strained to greater magnitudes but did not reach higher stresses before failing. This increased extensibility was evident in both the intra and inter-lamellar matrices. It was hypothesized that this increased extensibility was due to damage to elastin, as elastin assists in minimizing tissue deformation and helps tissues recover from tensile strain.

In the final study, functional spine units were subjected to a protocol shown to successfully induce herniation; repetitive flexion-extension under moderate compression (1400N). Half of the spinal units were further subjected to vibratory compression at a frequency of 5 Hz (ranging from 1260-1540N). Following 6000 flexion-extension cycles, a greater number of vibrated spines had initiated the herniation process, as compared to the non-vibrated spines. Although epidemiological studies had documented a correlation between exposure to vibration and herniation, this was the first study to conclude that exposure to vibration is in fact a mechanical risk factor for the development of herniation and increases the frequency of herniation.

8.2 Revisiting the Hypotheses

As stated in the Chapter 1, the overriding general hypothesis for this thesis was that exposure to vibration will alter the material properties of the lamella and accelerate *in vitro* induced IVD herniation. Specifically, it was hypothesized that:

1. Exposure to 5 Hz axial vibration will decrease the tensile strength and modulus of the intra-lamellar matrix due to material weakening often observed in materials following vibration (Hertzberg, 1980).
2. Exposure to 5 Hz axial vibration will also decrease the shear strength and modulus of the inter-lamellar matrix as it is hypothesized that vibration will accelerate delamination of the annulus.
3. A greater number of discs exposed to 5 Hz axial vibration in conjunction with repetitive flexion/extension will herniate as compared to control discs, which have not been exposed to vibration.

In terms of the effect of vibration on the intra-lamellar matrix, the only observed difference was an increase in the toe region strain in the vibrated samples, rejecting hypothesis #1. This difference in toe region strain magnitude was thought to be due to damage to the elastin. It was further speculated that collagen, a load bearing structure, was likely not damaged as there were no observed differences in the failure strength. A similar finding was observed in the inter-lamellar matrix following exposure to vibration, however the difference was in the failure strain, which was higher in the vibrated tissues, rejecting hypothesis #2.

It was confirmed that exposure to vibration increased the risk of herniation as a greater number of vibrated FSUs exhibited herniated intervertebral discs as compared to non-vibrated test specimens with an equal total loading exposure dosage, confirming hypothesis #3.

8.3 Herniation Initiation and Progression as a Result of Vibration

It has been hypothesized that a certain level of hydrostatic pressure is required within the disc to initiate herniation (Simunic et al., 2001). This pressure provides the necessary stresses on the inner layers of the annulus during repetitive flexion-extension to eventually weaken and damage these layers. During flexion, the posterior annular layers become strained, including the intra-lamellar matrix, which is responsible for keeping adjacent collagen bundles bound. When this matrix fails, clefts form in the lamellae providing a portal for the nuclear material to squeeze through. Exposure to vibration appears to affect this matrix by enabling increased strain between collagen fibres. Elastin is primarily responsible for preventing such accumulating strain, and therefore it is hypothesized that vibration damaged the elastin within the intra-lamellar matrix via a fatigue failure mechanism. It is further hypothesized that collagen was not damaged due to vibration, as collagen is the primary load bearing structure and no change in failure stress was observed. If elastin becomes damaged, the lamellae will not be able to recover from applied tensile strain such that clefts may form in the intra-lamellar matrix allowing nuclear material to squeeze through.

It has previously been suggested that delamination, or separation between the layers of the annulus, is necessary for disc herniation (Adams & Hutton, 1985). Specifically, once the nuclear material has squeezed through a cleft in the intra-lamellar matrix, the nuclear material will migrate into the space between adjacent lamellae where the inter-lamellar matrix has been

disrupted (Figure 8.1). After delamination has occurred, the nuclear material will be able to navigate and occupy more of this area. Further, once nuclear material has leached into the inter-lamellar matrix, more locations of the intra-lamellar matrix are now targeted for breaching. Therefore, it is easy to appreciate the need for strong healthy inter-lamellar connective tissue networks. However, vibration has a similar extensibility affect on this matrix as on the intra-lamellar matrix. Damaged elastin was again the hypothesized mechanism for this increased extensibility. If the inter-lamellar matrix is also more highly strained, the result could be residual tensile strain on other components such as collagen, which could eventually fail as a result of prolonged loading.

Intervertebral disc herniation continues this progression through clefts in the lamellae (specifically the intra-lamellar matrix), then navigates between adjacent layers (inter-lamellar matrix) until another weak bond is found and the nuclear material can squeeze through. It appears that vibration affects both of these matrices and therefore also would impact the initiation and propagation of intervertebral disc herniation.

The failure stresses observed in the intra-lamellar matrix (Chapter 5) were 15-20 times greater than those documented in the inter-lamellar matrix (Chapter 6). Given the difference in failure strengths, if loading demands on the annulus were high enough to cause failure to the intra-lamellar matrix, it is possible that the inter-lamellar matrix would be at an even greater risk of failure if subject to similar stresses. Strain also plays an important role in injury initiation and progression. In Chapter 5, the failure strains documented in the intra-lamellar matrix were as high at 115% strain. In the inter-lamellar matrix, failure deformations of approximately 2mm were observed, as reported in Chapter 6. Shear strains were not calculated for the inter-lamellar matrix in Chapter 6 as it was not possible to obtain an accurate measure of the thickness of this

matrix. An estimate of the thickness of the inter-lamellar matrix was determined from images of transverse slices of the disc documented by Tampier (2006). A mean thickness of 8μm was calculated, which is approximately $1/20^{th}$ the thickness of a single lamella. By dividing the measured deformation in the inter-lamellar matrix by this thickness, a failure shear strain of approximately 250% was estimated.

A substantially lower failure stress and higher failure strain would indicate that the inter-lamellar matrix is far more compliant than the intra-lamellar matrix. This would be expected given that a proposed important function of the inter-lamellar matrix is to allow a certain amount of relative motion between the layers. Therefore, if the function of the inter-lamellar matrix is to allow motion between the layers, fairly substantial shear strain between the layers must occur to result in failure, which are likely not reached during *in vivo* motions such as spinal flexion. However, repetitive motions may decrease the tolerance to this tissue such that there is an accumulation of deformation in the matrix which may result in failure, and in particular, delamination.

An alternative, and perhaps more likely, mechanism of herniation, would be that the localized stresses, and consequently strains, placed on the inner annular layers by the pressurized nucleus during repetitive flexion cause fatigue-failure of the intra-lamellar matrix. Once the first layer has been breached, the stress created by the nucleus continues to strain the inter-lamellar matrix until failure of this matrix has occurred. In this mode of failure, the localized stress of the nucleus would be similar on each matrix as herniation progresses through the annulus. Given the relative strength difference between the matrices, it can be assumed that the inter-lamellar matrix, and thus delamination, is the weakest link in the herniation pathway, similar to the theory

proposed by Adams and Hutton (1985) that delamination often occurs prior to herniation initiation.

This thesis has advanced our understanding of herniation by creating a more detailed theoretical model than previously established. By showing that vibration actually increased the occurrence of herniation, it was possible to associate the changes observed in the intra and inter-lamellar matrices to herniation initiation and progression, which in turn advanced our understanding of the involvement of these two matrices in herniation development. Figure 8.2 illustrations how structures such as type IV collagen and elastin assist in preventing cleft formation (within a lamella) and delamination (between adjacent lamellae).

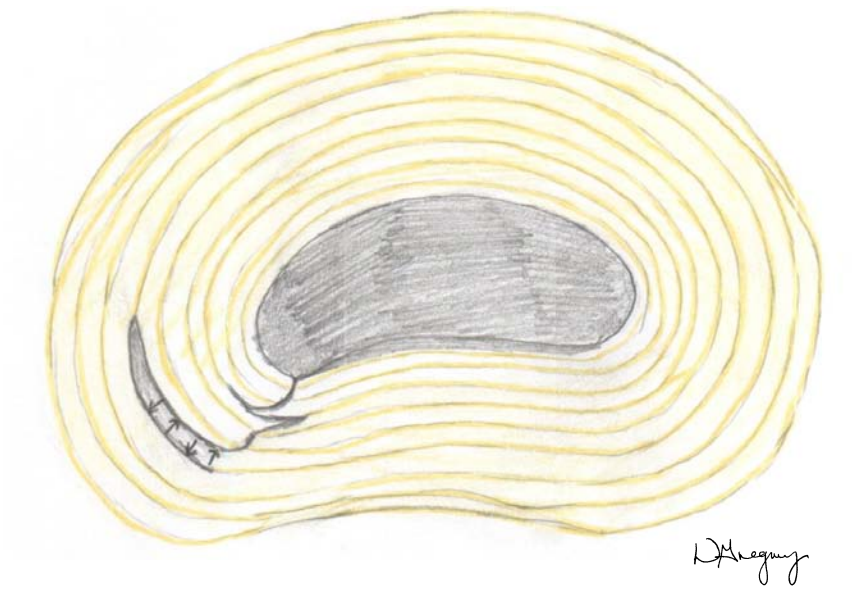

Figure 8.1: Pictorial representation of herniation progression through the annulus. Note the stress riser occurring between two lamellae (left side) resulting in a hydraulic fissure or delamination. Once delamination has occurred, nuclear material is free to occupy the newly open space.

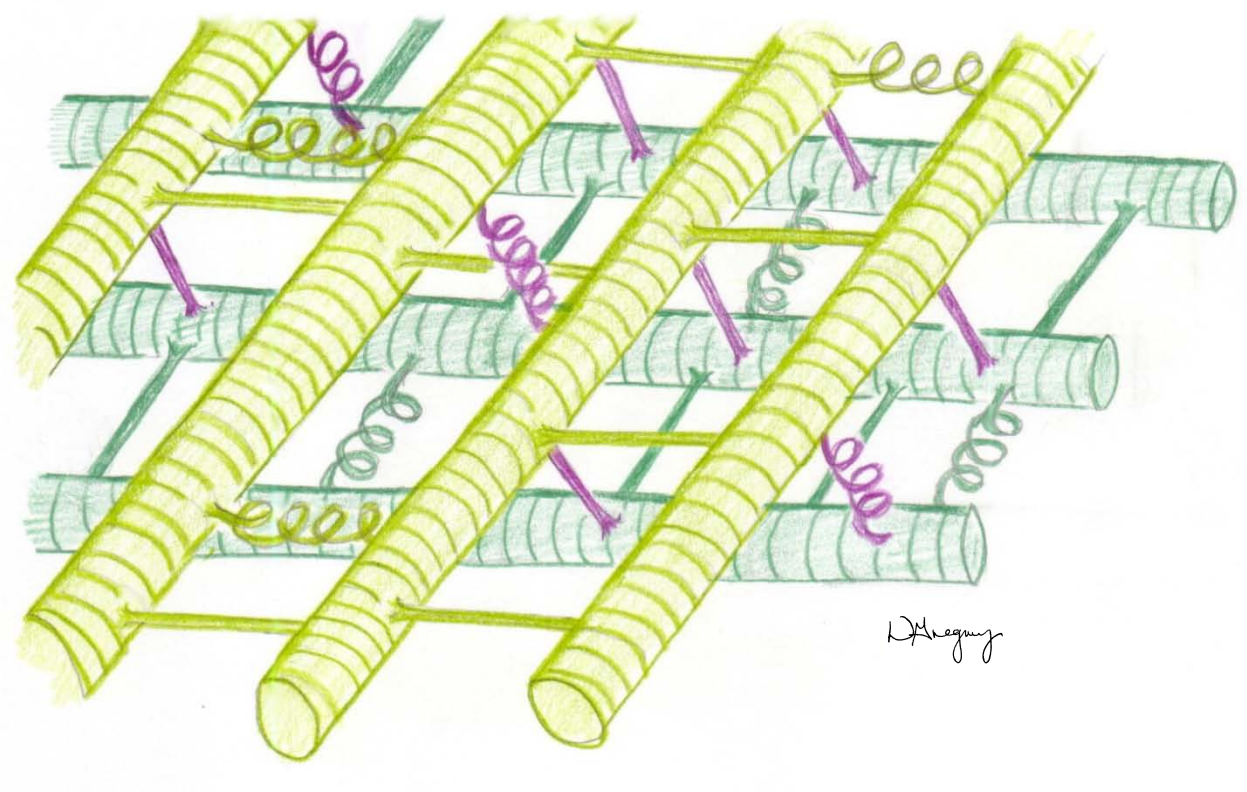

Figure 8.2: Artist representation of the annulus micro-structure. Light and dark green solid connections represent type IV collagen and light and dark green coils represent elastin in the intra-lamella matrix. Brown solid connections represent type IV collagen connecting adjacent lamellae, and brown coils represent elastin in the inter-lamellar matrix. The elastin (coils) assist in tensile recovery when either the intra or inter-lamellar matrix is strained.

8.4 Limitations

Each chapter addressed study-specific limitations, however limitations exist that pertain to the overall thesis findings. First, by using an animal model, care must be taken when applying these findings to human. However, given the documented similarities between the porcine cervical spine of the human lumbar spine in terms of anatomy, geometry and function (Oxland et al., 1991; Tampier, 2006, Yingling et al., 1999), it is acceptable to suggest that similar findings would have been observed if human tissue was used rather than animal tissue. Porcine cervical vertebrae and intervertebral discs are smaller than human counterparts (Tampier, 2006), and therefore it is likely would simply have to be scaled to humans.

Another important limitation to consider is that the vibration exposure in this thesis was a single dose exposure and is not directly comparable to the long term exposures that have been examined in epidemiological studies. However, by accelerating the injury mechanism, this thesis was successful at shedding new light on how exposure to vibration alters the components of the annulus as well as herniation initiation.

8.5 Future Directions

Damage to elastin is speculative based on the findings of this thesis. In order to determine which components of the disc become damaged as a result of vibration, biochemical analysis is necessary. Following exposure to vibration, histological staining can provide us with information about component concentrations and whether these components have suffered damage. Alternatively, by treating discs with enzymes known to breakdown structures such as collagen, proteoglycans or elastin, we can then determine the mechanical properties of the tissue deficient

of these components. This will provide additional information about the relative contribution of each component.

Last, it is vital to examine the effect of vibration exposure, as well as other risk factors that have been associated with herniation, in living tissue. Tissue has the ability to heal and remodel in response to applied physical stimuli such as vibration, and therefore it is likely that exposure to factors such as vibration will result in different mechanical changes in living tissue as compared to dead tissue.

Appendix

X-ray images were taken throughout data collection in Chapter 7. These X-rays were originally taken in order to determine when a herniation had occurred. However, in certain cases, identification of a herniation from the X-rays did not confirm the presence of a herniation when the specimen was dissected. Therefore, the protocol was changed to expose each specimen to the same number of flexion-extension cycles (6000) and then identify the occurrence of the initiation of herniation post-dissection. This appendix contains are two example specimens from Chapter 7. The first shows an example when the X-ray images (Figure A.1 A and B) and the dissection (Figure A.1 C) both confirmed herniation. In the second example, the X-ray images (Figure A.2 D and E) did not confirm the herniation that was ultimately observed during dissection (Figure A.2 F).

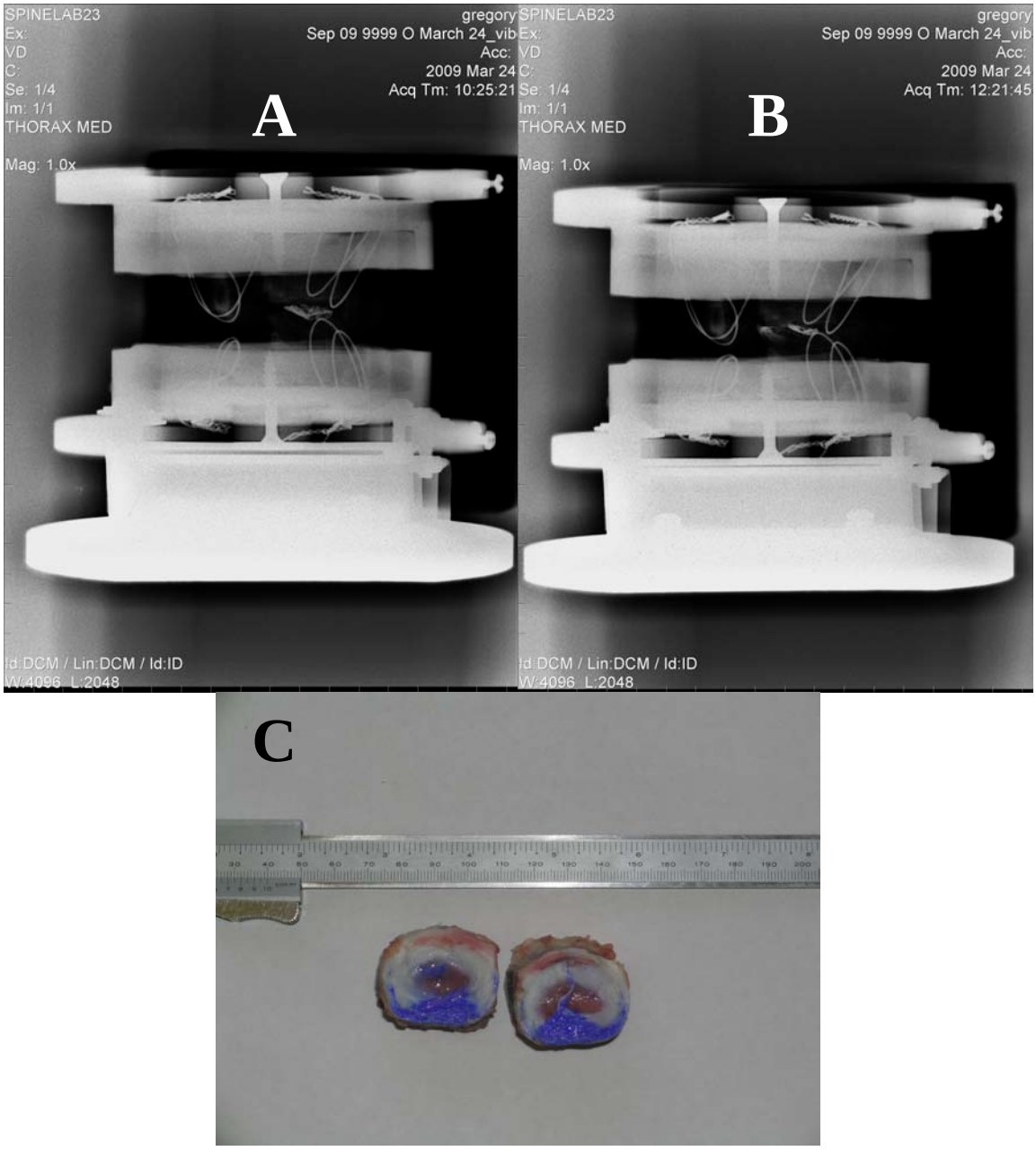

Figure A.1: Sample X-rays from Chapter 7. A) X-ray image at the start of collection before herniation protocol. B) X-ray taken after 6000 flexion/extension cycles. Radiopaque shows evidence of herniation. C) Dissection of segment confirms herniation.

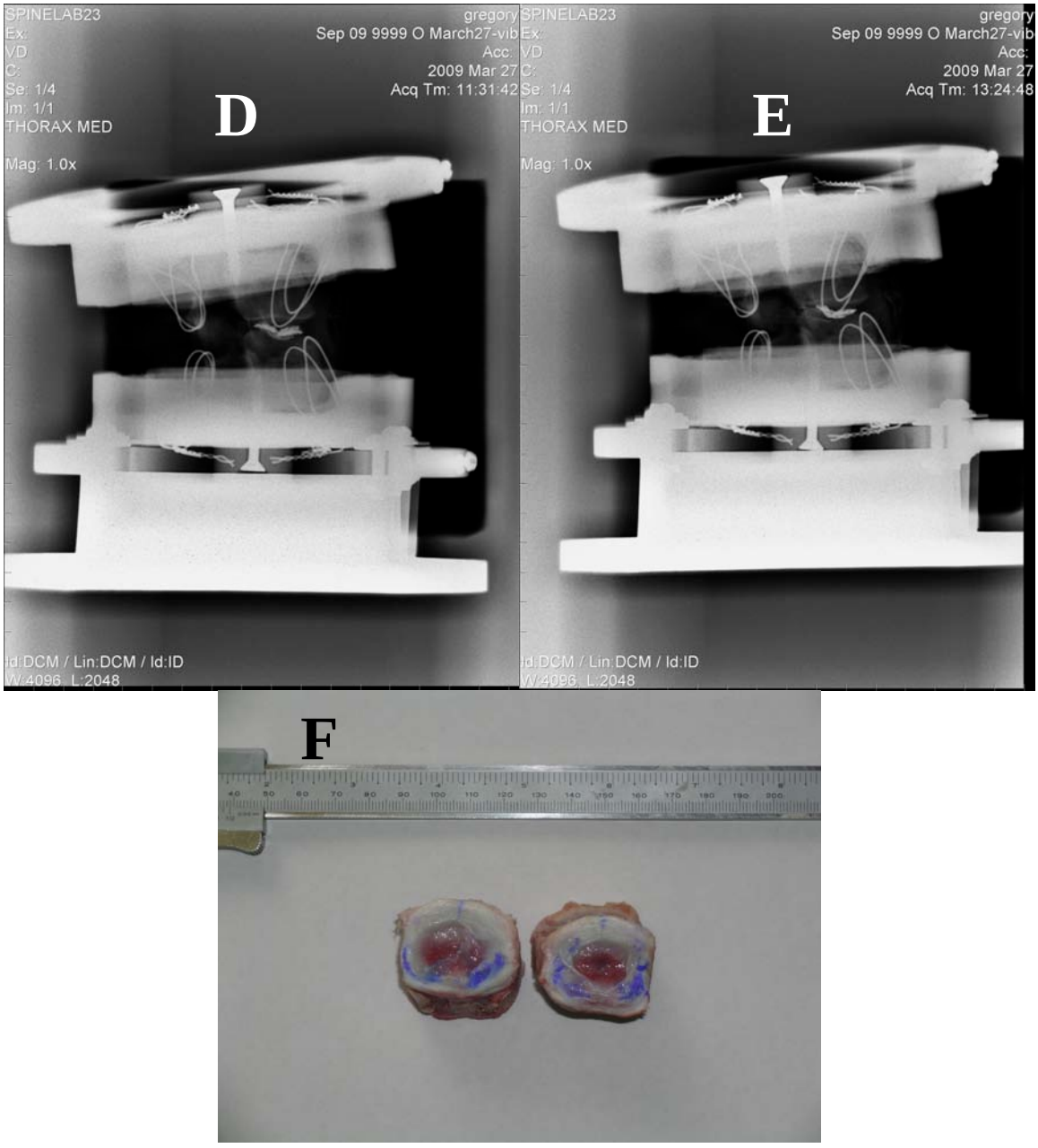

Figure A.2: Sample X-rays from Chapter 7. A) X-ray image at the start of collection before herniation protocol. B) X-ray taken after 6000 flexion/extension cycles. Radiopaque does not show sufficient evidence of herniation. C) Dissection of segment confirms herniation.

References

Adams, M. A. (1995). Mechanical testing of the spine. An appraisal of methodology, results, and conclusions. *Spine, 20*, 2151-2156.

Adams, M., Bogduk, N., Burton, K., & Dolan, P. (2006). *The biomechanics of back pain*. Toronto, ON, Canada: Elsevier Ltd.

Adams, M. A., & Dolan, P. (1996). Time-dependent changes in the lumbar spine's resistance to bending. *Clinical Biomechanics, 11*, 194-200.

Adams, M. A., Dolan, P. A., & Hutton, W. C. (1987). Diurnal variations in the stresses on the lumbar spine. *Spine, 12*, 130-137.

Adams, M. A., Freeman, B. J., Morrison, H. P., Nelson, I. W., & Dolan, P. (2000). Mechanical initiation of intervertebral disc degeneration. *Spine, 25*, 1625-1636.

Adams, M. A., & Green, T. P. (1993). Tensile properties of the annulus fibrosus I. The contribution of fibre-matrix interactions to tensile stiffness and strength. *European Spine Journal, 2*, 203-208.

Adams, M. A., & Hutton, W. C. (1982). Prolapsed intervertebral disc: A hyperflexion injury. *Spine, 7*, 184-191.

Adams, M. A., & Hutton, W. C. (1983). The effect of fatigue on the lumbar intervertebral-disk. *Journal of Bone and Joint Surgery British, 65*, 199-203.

Adams, M. A., & Hutton, W. C. (1985). Gradual disc prolapse. *Spine, 10*(6), 524-531.

Adams, M. A., McNally, D. S., Chinn, H., & Dolan, P. (1994). Posture and the compressive strength of the lumbar spine. *Clinical Biomechanics, 9*, 5-14.

Adams, M. A., McNally, D. S., Wagstaff, J., & Goodship, E. A. (1993). Abnormal stress concentrations in lumbar intervertebral discs following damage to the vertebral bodies: a cause of disc failure? *European Spine Journal, 1,* 214-221.

Aultman, C. D., Scannell, J., & McGill, S. M. (2005). The direction of progressive herniation in porcine spine motion segments is influenced by the orientation of the bending axis. *Clinical Biomechanics, 20,* 126-129.

Bailey, A. J., Robins, S. P., & Balian, G. (1974). Biological significance of the intermolecular crosslinks of collagen. *Nature, 251,* 105-109.

Bass, E. C., Ashford, F. A., Segal, M. R., & Lotz, J. C. (2004). Biaxial testing of human annulus fibrosus and its implications for a constitutive formulation. *Annals of Biomedical Engineering, 32,* 1231-1242.

Beadle, O. A. (1932). The intervertebral discs. Observations on their normal and morbid anatomy in relation to certain spinal deformities. *Journal of the American Medical Association, 98,* 1212.

Berthet-Colominas, C., Miller, A., Herbage, D., Ronziere, M. C., & Tocchetti, D. (1982). Structural studies of collagen-fibers from intervertebral-disk. *Biochimica et Biophysica Acta, 706,* 50-64.

Blevins, F. T., Hecker, A. T., Bigler, G. T., Boland, A. L., & Hayes, W.C. (1994). The effects of donor age and strain rate on the biomechanical properties of bon-patellar tendon-bone allographs. *American Journal of Sports Medicine, 22***,** 328-333.

Bovenzi, M., & Hulshof, C. T. J. (1999). An updated review of epidemiologic studies on the relationship between exposure to whole-body vibration and low back pain (1986-1997). *International Archives of Occupational and Environmental Health, 72,* 351-365.

Brown, S. H. M., Gregory, D. E., & McGill, S. M. (2008). Vertebral end-plate fractures as a result of high rate pressure loading in the nucleus of the young adult porcine spine. *Journal of Biomechanics, 41*, 122-127.

Brown, M. D., Holmes, D. C., & Heiner, A. D. (2002). Measurement of cadaver lumbar spine motion segment stiffness. *Spine, 27,* 918-922.

Bruehlmann, S. B., Hulme, P. A., & Duncan, N. A. (2004). In situ intercellular mechanics of the bovine outer annulus fibrosus subjected to biaxial strains. *Journal of Biomechanics, 37*, 223-231.

Bruehlmann, S. B., Rattner, J. B., Matyas, J. R., & Duncan, N. A. (2002). Regional variations in the cellular matrix of the annulus fibrosus of the intervertebral disc. *Journal of Anatomy, 201*, 159-171.

Callaghan, J. P., & McGill, S. M. (1995). Frozen storage increases the ultimate compressive load of porcine vertebrae. *Journal of Orthopaedic Research, 13*, 809-812.

Callaghan, J. P., & McGill, S. M. (2001). Intervertebral disc herniation: Studies on a porcine model exposed to highly repetitive flexion/extension motion with compressive force. *Clinical Biomechanics, 16*, 28-37.

Carter, D. R., & Caler, W. E. (1985). A cumulative damage model for bone fracture. *Journal of Orthopaedic Research, 3*, 84-90.

Cassidy, J. J., Hiltner, A., & Baer, E. (1989). Hierarchical structure of the intervertebral-disk. *Connective Tissue Research, 23*, 75-88.

Chuang, S. Y., Odono, R. M., & Hedman, T. P. (2007). Effects of exogenous crosslinking on in vitro tensile and compressive moduli of lumbar intervertebral discs. *Clinical Biomechanics, 22*, 14-20.

Crisco, J. J., Moore, D. C., & McGovern, R. D. (2002). Strain-rate sensitivity of the rabbit MCL diminishes at traumatic loading rates. *Journal of Biomechanics, 35,* 1379-1385.

Crownshield, R. D., & Pope, M. H. (1976). The strength and failure characteristics of rat medial collateral ligaments. *Journal of Trauma, 16,* 99-105.

Dammers, R., & Koehler, P. J. (2002). Lumbar disc herniation: level increases with age. *Surgical Neurology, 58,* 209-212.

Danto, M. I., & Woo, S. L. (1993). The mechanical properties of skeletally mature rabbit anterior cruciate ligament and patellar tendon over a range of strain rates. *Journal of Orthopaedic Research, 11,* 58-67.

Debes, J. C., & Fung, Y. C. (1992). Effect of temperature on the biaxial mechanics of excised lung parenchyma of the dog. *Journal of Applied Physiology, 73,* 1171-118.

Debes, J. C., & Fung, Y. C. (1995). Biaxial mechanics of excised canine pulmonary arteries. *American Journal of Physiology, 269,* H433-H442.

Dowling, N. E. (1993). *Mechanical behavior of materials*. Englewood Cliffs, NJ: Prentice Hall.

Drake, J. D. & Callaghan, J. P. (2009). Intervertebral neural foramina deformation due to two types of repetitive combined loading. *Clinical Biomechanics, 24,* 1-6.

Dupuis, H. (1989). Biodynamic behavior of the trunk and the abdomen during whole- body vibration. *Acta Anaesthesiologica Scandinavica, 33,* 34-38.

Ebara, S., Iatridis, J. C., Setton, L. A., Foster, R. J., Mow, V. C., & Weidenbaum, M. (1996). Tensile properties of nondegenerate human lumbar anulus fibrosus. *Spine, 21,* 452-461.

Edwards, W. T., Ordway, N. R., Zheng, Y., McCullen, G., Han, Z., & Yuan, H. A. (2001). Peak stresses observed in the posterior lateral annulus. *Spine, 26,* 1753-1759.

Elias, P. Z., Nuckley, D. J., & Ching, R. P. (2006). Effect of loading rate on the compressive mechanics of the immature baboon cervical spine. *Journal of Biomechanical Engineering, 128,* 18-23.

Elliot, D. M., & Setton, L. A. (2001). Anisotropic and inhomogeneous tensile behaviour of the human annulus fibrosus: Experimental measurement and material model predictions. *Journal of Biomechanical Engineering, 123,* 256-263.

Errington, R. J., Puustjarvi, K., White, I. R. F., Roberts, S., & Urban, J. P. (1998). Characterisation of cytoplasm-filled processes in cells of the intervertebral disc. *Journal of Anatomy, 192,* 369-378.

Eyre, D. R., & Muir, H. (1974). Collagen polymorphism: 2 molecular species in pig intervertebral-disk. *FEBS Letters, 42,* 192-196.

Eyre, D. R., & Muir, H. (1976). Type-1 and type-2 collagens in intervertebral-disk: Interchanging radial distributions in annulus fibrosus. *Biochemical Journal, 157,* 267-70.

Fujita, Y., Duncan, N. A., & Lotz, J. C. (1997). Radial tensile properties of the lumbar annulus fibrosus are site and degeneration dependent. *Journal of Orthopaedic Research, 15,* 814-819.

Fujita, Y., Wagner, D. R., Biviji, A. A., Duncan, N. A., & Lotz, J. C. (2000). Anisotropic shear behavior of the annulus fibrosus: Effect of harvest site and tissue prestrain. *Medical Engineering and Physics, 22,* 349-357.

Goel, V. K., Monroe, B. T., Gilbertson, L. G., Brinckmann, P., & Nat, R. (1995). Interlaminar shear stresses and laminae separation in a disc: Finite-element analysis of the L3-L4 motion segment subjected to axial compressive loads. *Spine, 20,* 689-698.

Gordon, S. J., Yang, K. H., Mayer, P. J., Mace, A. H., Kish, V. L., & Radin, E. L. (1991). Mechanism of disk rupture: A preliminary-report. *Spine, 16*, 450-456.

Grashow, J. S., Yoganathan, A. P., & Sacks, M. S. (2006). Biaxial stress-stretch behavior of the mitral valve anterior leaflet at physiologic strain rates. *Annals of Biomedical Engineering, 34*, 315-325.

Green, T. P., Adams, M. A., & Dolan, P. (1993). Tensile properties of the annulus fibrosus II. Ultimate tensile strength and fatigue life. *European Spine Journal, 2*, 209-214.

Guerin, H. A. L., & Elliott, D. M. (2006). Degeneration affects the fiber reorientation of human annulus fibrosus under tensile load. *Journal of Biomechanics, 39*, 1410-1418.

Gunning, J. L., Callaghan, J. P., & McGill, S. M. (2001). Spinal posture and prior loading history modulate compressive strength and type of failure in the spine: A biomechanical study using a porcine cervical spine model. *Clinical Biomechanics, 16*, 471-480.

Hastreiter, D., Ozuna, R. M., & Spector, M. (2001). Regional variations in certain cellular characteristics in human lumbar intervertebral discs, including the presence of alpha-smooth muscle actin. *Journal of Orthopaedic Research, 19*, 597-604.

Haughton, V. M. (1988). MR imaging of the spine. *Radiology, 166*, 297-301.

Haut, R. C. (1983). Age-dependent influence of strain rate on the tensile failure of rat-tail tendon. *Journal of Biomechanical Engineering, 105*, 296-299.

Haut, R. C., & Little, R. W. (1969). Rheological properties of canine anterior cruciate ligaments. *Journal of Biomechanics, 2*, 289-298.

Hayes A. J., Benjamin, M., & Ralphs, J. R. (2001). Extracellular matrix in development of the intervertebral disc. *Matrix Biology, 20*, 107-121.

Hertzberg, R. W. (1996). *Deformation and fracture mechanics of engineering materials*. New York: Wiley and Sons.

Hertzberg, R. W., & Manson, J. A. (1980). *Fatigue of Engineering Plastics*. New York: Academic Press, Inc.

Hickey, D. S., & Hukins, D. W. L. (1980). X-ray-diffraction studies of the arrangement of collagenous fibers in human-fetal intervertebral-disk. *Journal of Anatomy, 131*, 81-90.

Holzapfel, G. A., Schulze-Bauer, C. A. J., Feigl, G., & Regitnig, P. (2005). Single lamellar mechanics of the human lumbar anulus fibrosus. *Biomechanics and Modeling in Mechanobiology, 3*, 125-140.

Iatridis, J. C., Kumar, S., Foster, R. J., Weidenbaum, M., & Mow, V. C. (1999). Shear mechanical properties of human lumbar annulus fibrosus. *Journal of Orthopaedic Research, 17*, 732-737.

Inerot, S., & Axelsson, I. (1991). Structure and composition of proteoglycans from human annulus fibrosus. *Connective Tissue Research, 26*, 47-63.

Inoue, H. (1981). 3-dimensional architecture of lumbar intervertebral disks. *Spine, 6*, 139-146.

Ishihara, H., Tsuji, H., Hirano, N., Ohshima, H., & Terahata, N. (1992). Effects of continuous quantitative vibration on rheologic and biological behaviors of the intervertebral-disk. *Spine, 17*, S7-S12.

Johnson, E. F, Chetty, K., Moore, I. M., Stewart, A., & Jones, W. (1982). The distribution and arrangement of elastic fibers in the intervertebral-disk of the adult human. *Journal of Anatomy, 35*, 301-309.

Kasra, M., Parnianpour, M., Shirazi_Adl, A., Wang, J. L., & Grynpas, M. D. (2004). Effect of strain rate on tensile properties of sheep disc annulus fibrosus. *Technology and Health Care, 12*, 333-342.

Keaveny, T. M., & Hayes, W. C. (1993). A 20-year perspective on the mechanical properties of trabecular bone. *Journal of Biomechanical Engineering, 115*, 534-542.

Klein, J. A., & Hukins, D. W. L. (1982a). X-Ray-diffraction demonstrates reorientation of collagen-fibers in the annulus fibrosus during compression of the intervertebral-disk. *Biochimica et Biophysica Acta, 717*, 61-64.

Klein, J. A., & Hukins, D. W. L. (1982b). Collagen fiber orientation in the annulus fibrosus of intervertebral-disk during bending and torsion measured by x-ray-diffraction. *Biochimica et Biophysica Acta, 719*, 98-101.

Leavitt, S. S., Johnson, T. L., & Bayer, R. D. (1971). The process of recovery: Patterns in industrial back injury: 1. Costs and other quantitative measure of effort. *Industrial Medicine and Surgery, 40*, 7-14.

Lee, M. C., LeWinter, M. M., Freeman, G., Shabetai, R., & Fung, Y. C. (1985). Biaxial mechanical properties of the pericardium in normal and volume overload dogs. *American Journal of Physiology, 249*, H222-H230.

Lipson, S. J., & Muir, H. (1981). Proteoglycans in experimental intervertebral-disk degeneration. *Spine, 6*, 194-210.

Lis, A. M., Black, K. M., Korn, H., & Nordin, M. (2007). Association between sitting and occupational LBP. *European Spine Journal, 16*, 283-298.

Lo, I. K., Chi, S., Ivie, T., Frank, C. B., & Rattner, J. B. (2002). The cellular matrix: A feature of tensile bearing dense soft connective tissues. *Histology and Histopathology, 17*, 523-537.

Lundin, O., Ekstrom, L., Hellstrom, M., Holm, S., & Sward, L. (1998). Injuries in the adolescent porcine spine exposed to mechanics compression. *Spine, 23,* 2574-2579.

Lynch, H. A., Johannessen, W., Wu, J. P., & Elliott, D. M. (2003). Effect of fiber orientation and strain rate on the nonlinear uniaxial tensile material properties of tendon. *Journal of Biomechanical Engineering, 125,* 726-731.

Macfarlane, G. J., Thomas, E., Papageorgiou, A. C., Croft, P. R., Jayson, M. I. V., & Silman, A. J. (1997). Employment and physical work activities as predictors of future low back pain. *Spine, 22*(10), 1143-1149.

Magora, A. (1974). Investigation of the relations between low back pain and occupation. *Scandinavian Journal of Rehabilitation Medicine, 6,* 81-88.

Mansfield, N. J. (2005). *Human response to vibration*. Boca Raton, Fl: CRC Press.

Marchand, F., & Ahmed, A. M. (1990). Investigation of the laminate structure of lumbar- disk anulus fibrosus. *Spine, 15,* 402-410.

Marshall, L. (2008). *An investigation of the role of dynamic axial torque on the disc herniation mechanism*. Unpublished master's thesis, University of Waterloo, Waterloo, Ontario, Canada. May-Newman, K., & Yin, F. C. P. (1995). Biaxial mechanical behavior of excised porcine mitral valve leaflets. *American Journal of Physiology, 269,* H1319-H1327.

McNally, D. S., & Adams, M. A. (1992). Internal intervertebral disc mechanics as revealed by stress profilometry. *Spine, 17,* 66-73.

McNeilly, C. M., Banes, A. J., Benjamin, M., & Ralphs, J. R. (1996). Tendon cells in vivo form a three dimensional network of cell processes linked by gap junctions. *Journal of Anatomy, 189,* 593-600.

Melrose, J., Smith, S. M., Appleyard, R. C., & Little, C. B. (2008). Aggrecan, versican and type VI collagen are components of annulus translamellar crossbridges in the intervertebral disc. *European Spine Journal, 17*, 314-324.

Mimura, M., Panjabi, M. M., Oxland, T. R., Crisco, J. J., Yamamoto, I., & Vasavada, A. (1994). Disc degeneration affects the multidirectional flexibility of the lumbar spine. *Spine, 19,* 1371-1380.

Mobbs, R. J., & Steel, T. R. (2007). Migration of lumbar disc herniation: An unusual case. *Journal of Clinical Neuroscience, 14,* 581-584.

Moore, R. J., Vernon-Roberts, B., Fraser, R. D., & Schembri, M. (1996). The origin and fate of herniated lumbar intervertebral disc tissue. *Spine, 21*, 2149-2155.

Norman, R., Wells, R., Neumann, P., Frank, J., Shannon, H., & Kerr, M. (1998). A comparison of peak vs. cumulative physical work exposure risk factors for the reporting of low back pain in the automotive industry. *Clinical Biomechanics, 13,* 561-573.

Noyes, F. R., DeLucas, J. L., & Torvik, P. J. (1974). Biomechanics of anterior cruciate ligament failure: an analysis of strain-rate sensitivity and mechanisms of failure in primates. *Journal of Bone and Joint Surgery (Am), 56*, 236-253.

Nuckley, D. J., Hertsted, S. M., Eck, M. P., & Ching, R. P. (2005). Effect of displacement rate on the tensile mechanics of pediatric cervical functional spinal units. *Journal of Biomechanics, 38*, 2266-2275.

Oxland, T. R., Lin, R. M., & Panjabi, M. M. (1992). Three-dimensional mechanical properties of the thoracolumbar junction. *Journal of Orthopaedic Research, 10,* 573-580.

Oxland, T. R., Panjabi, M. M., Southern, E. P., & Duranceau, J. S. (1991). An anatomic basis for spinal instability: A porcine trauma model. *Journal of Orthopaedic Research, 9,* 452-462.

Panjabi, M. M., Andersson, G. B. J., Jorneus, L., Hult, E., & Mattsson, L. (1986). In vivo measurements of spinal column vibrations. *Journal of Bone and Joint Surgery American, 68A,* 695-702.

Panjabi, M. M., Krag, M. H., & Chung, T. Q. (1984). Effects of disc injury on mechanical behavior of the human spine. *Spine 9,* 707-713.

Panjabi, M. M., Krag, M., Summers, D., & Videman, T. (1985). Biomechanical time-tolerance of fresh cadaveric human spine specimens. *Journal of Orthopaedic Research, 3,* 292-300.

Parkinson, R. J. & Callaghan, J. P. (2007). Can periods of static loading be used to enhance the resistance of the spine to cumulative compression? *Journal of Biomechanics, 40*, 2944-2952.

Pezowicz, C. A., Robertson, P. A., & Broom, N. D. (2005). Intralamellar relationships within the collagenous architecture of the annulus fibrosus imaged in its fully hydrated state. *Journal of Anatomy, 207*, 299-312.

Pioletti, D. P., Rakotomanana, L. R., & Leyvraz, P.F. (1999). Strain rate effect on the mechanical behavior of the anterior cruiate ligament-bone complex. *Medical Engineering and Physics, 21*, 95-100.

Pope, M. H., Magnusson, M., & Wilder, D. G. (1998). Low back pain and whole body vibration. *Clinical Orthopaedics and Related Research, 354*, 241-248.

Postacchini, F., Bellocci, M., & Massobrio, M. (1984). Morphologic changes in annulus fibrosus during aging: An ultrastructural-study in rats. *Spine, 9*, 596-603.

Pritchard, S., Erickson, G. R., & Guilak, F. (2002). Hyperosmotically induced volume change and calcium signaling in intervertebral disk cells: The role of the actin cytoskeleton. *Biophysical Journal, 83,* 2502-2510.

Race, A., Broom, N. D., & Robertson, P. (2000). Effect of loading rate and hydration on the mechanical properties of the disc. *Spine, 25,* 662-669.

Riddell, N. M., Koo, G. P., & O'toole, J. L. (1966). Fatigue mechanisms of thermoplastics. *Polymer Engineering and Science, 6,* 363-368.

Robb, M. J. M., & Mansfield, N. J. (2007). Self-reported musculoskeletal problems amongst professional truck drivers. *Ergonomics, 50,* 814-827.

Sacks, M. S., & Chuong, C. J. (1998). Orthotropic mechanical properties of chemically treated bovine pericardium. *Annals of Biomedical Engineering, 26,* 892-902.

Schollum, M. L., Robertson, P. A., & Broom, N. D. (2008). ISSLS Prize Winner: Microstructure and mechanical disruption of the lumbar disc annulus. Part I: A microscopic investigation of the translamellar bridging network. *Spine, 33,* 2702-2710.

Shea, M., Edwards, W. T., Clothiaux, P. L., Crowell, R. R., Nachemson, A. L., White, A. A. 3rd, & Hayes, W. C. (1991). Three-dimensional load displacement properties of posterior lumbar fixation. *Journal of Orthopaedic Trauma, 5,* 420-427.

Shirazi-Adl, A., Shrivastava, S. C., & Ahmed, A. M. (1984). Stress analysis of the lumbar disc-body unit in compression. A three-dimensional nonlinear finite element study. *Spine, 9,* 120-134.

Simunic, D. I., Broom, N. D., & Robertson, P. A. (2001). Biomechanical factors influencing nuclear disruption of the intervertebral disc. *Spine, 26,* 1223-1230.

Skaggs, D. L., Weidenbaum, M., Iatridis, J. C., Ratcliffe, A., & Mow, V. C. (1994). Regional variation in tensile properties and biochemical-composition of the human lumbar anulus fibrosus. *Spine, 19,* 1310-1319.

Smith, L. J., Byers, S., Costi, J. J., & Fazzalari, N. L. (2008). Elastic fibers enhance the mechanical integrity of the human lumbar anulus fibrosus in the radial direction. *Annals of Biomedical Engineering, 36,* 214-223.

Smith, L. J., & Fazzalari, N. L. (2009). The elastic fibre network of the human lumbar anulus fibrosus: Architecture, mechanical function and potential role in the progression of intervertebral disc degeneration. *European Spine Journal, 18,* 439-448.

Solomonow, M. (2004). Ligaments: a source of work-related musculoskeletal disorders. *Journal of Electromyography and Kinesiology, 14,* 49-60.

Stokes, I. A. (1987). Surface strain on human intervertebral discs. *Journal of Orthopaedic Research, 5,* 348-355.

Tampier, C. (2006). *Progressive disc herniation: An investigation of the mechanism using histochemical and microscopic techniques*. Unpublished master's thesis, University of Waterloo, Waterloo, Ontario, Canada.

Tampier, C., Drake J. D., Callaghan, J. P., & McGill, S. M. (2007). Progressive disc herniation: An investigation of the mechanism using radiological, histochemical, and microscopic dissection techniques on a porcine model. *Spine, 32,* 2869-2874.

Ticker, J. B., Bigliani, L. U., & Soslowsky, L. J. (1996). Inferior glenohumeral ligament: Geometric and strain-rate dependent properties. *Journal of Shoulder and Elbow Surgery, 5,* 269-279.

Tsuji, H., Hirano, N., Ohshima, H., Ishihara, H., Terahata, N., & Motoe, T. (1993). Structural variation of the anterior and posterior anulus fibrosus in the development of human lumbar intervertebral-disk: A risk factor for intervertebral-disk rupture. *Spine, 18*, 204-210.

van Deursen, D. L., Snijders, C. J., Kingma, I., & van Dieen, J. H. (2001). In vitro torsion-induced stress distribution changes in porcine intervertebral discs. *Spine, 26*, 2582-2586.

Videman, T., Nurminen, M., & Troup, J. D. G. (1990). Lumbar spinal pathology in cadaveric material in relation to history of back pain, occupation, and physical loading. *Spine, 15*, 728-740.

Viikari-Juntura, E. (1997). The scientific basis for making guidelines and standards to prevent work-related musculoskeletal disorders. *Ergonomics, 40*, 1097-1117.

Virtanen, I. M., Karppinen, J., Taimela, S., Ott, J., Barral, S., Kaikkonen, K., Heikkila, O., Mutanen, P., Noponen, N., Mannikko, M., Tervonen, O., Natri, A., & Ala-Kokko, L. (2007). Occupational and genetic risk factors associated with intervertebral disc disease. *Spine, 32*, 1129-1134.

Weisman, G., Pope, M. H., & Johnson, R. J. (1980). Cyclic loading in knee ligament injuries. *American Journal of Sports Medicine, 8*, 24-30.

White, A. A., & Panjabi, M. M. (1990). *Clinical biomechanics of the spine*. Philadelphia: J. B. Lippincott Company.

Wilder, D. G. (1993). The biomechanics of vibration and low back pain. *American Journal of Industrial Medicine, 23*, 577-588.

Wilder, D. G., & Pope, M. H. (1996). Epidemiological and aetiological aspects of low back pain in vibration environments: An update. *Clinical Biomechanics, 11*, 61-73.

Wilder, D. G., Woodworth, B. B., Frymoyer, J. W., & Pope, M. H. (1982). Vibration and the human spine. *Spine, 7*, 243-254.

Woo, S. L., Debski, R. E., Zeminski, J., Abramowitch, S. D., Chan Shaw, S. S., & Fenwick, J. A. (2000). Injury and repair of ligaments and tendons. *Annual Review of Biomedical Engineering, 2*, 83-118.

Woo, S. L., Peterson, R. H., Ohland, K. J., Sites, T. J., & Danto, M. I. (1990). The effects of strain rate on the properties of the medial collateral ligament in skeletally immature and mature rabbits: a biomechanical and histological study. *Journal of Orthopaedic Research, 8*, 712-721.

Wren, T. A. L., Yerby, S. A., Beaupre, G. S., & Carter, D. R. (2001). Mechanical properties of the human achilles tendon. *Clinical Biomechanics, 16*, 245-251.

Yamamoto, N., & Hayashi, K. (1998). Mechanical properties of rabbit patellar tendon at high strain rate. *Biomedical Materials and Engineering, 8*, 83-90.

Yamazaki, S., Banes, A. J., Weinhold, P. S., Tsuzaki, M., Kawakami, M., & Minchew, J. T. (2002). Vibratory loading decreases extracellular matrix and matrix metalloproteinase gene expression in rabbit annulus cells. *The Spine Journal, 2*, 415-420.

Yates, J. P. (2009). Establishing the effect of vibration and postural constraint loading on the progression of intervertebral disc herniation. Unpublished master's thesis, University of Waterloo, Waterloo, Ontario, Canada.

Yasuma, T., Makino, E., Saito, S., & Inui, M. (1986). Histological development of intervertebral-disk herniation. *Journal of Bone and Joint Surgery American, 68A*, 1066-1072.

Yin, L. Z., & Elliott, D. M. (2005). A homogenization model of the annulus fibrosus. *Journal of Biomechanics, 38,* 1674-1684.

Yingling, V. R., Callaghan, J. P., & McGill, S. M. (1997). Dynamic loading affects the mechanical properties and failure site of porcine spines. *Clinical Biomechanics, 12,* 301-305.

Yingling, V. R., Callaghan, J. P., & McGill, S. M. (1999). The porcine cervical spine as a model of the human lumbar spine: an anatomical, geometric, and functional comparison. *Journal of Spinal Disorders, 12,* 415-423.

Yu, J., Fairbank, J. C. T., Roberts, S., & Urban, J. P. G. (2005). The elastic fiber network of the anulus fibrosus of the normal and scoliotic human intervertebral disc. *Spine, 30,* 1815-1820.

Yu, J., Perter, C., Roberts, S., & Urban, J. P. G. (2002). Elastic fibre organization in the intervertebral discs of the bovine tail. *Journal of Anatomy, 201,* 465-475.